NASA Contractor Report 3792

Scaling and Modeling of Three-Dimensional, End-Wall, Turbulent Boundary Layers

Uriel C. Goldberg and Eli Reshotko

GRANT NAG3-270
JUNE 1984

NASA

NASA Contractor Report 3792

Scaling and Modeling of Three-Dimensional, End-Wall, Turbulent Boundary Layers

Uriel C. Goldberg and Eli Reshotko
Case Western Reserve University
Cleveland, Ohio

Prepared for
Lewis Research Center
under Grant NAG3-270

National Aeronautics
and Space Administration

**Scientific and Technical
Information Branch**

1984

TABLE OF CONTENTS

LIST OF SYMBOLS

A	Parameter used in Johnston's triangular model
$A' = 2\kappa^{-1}\Pi$	Variable used in the Law-of-the- Wake
$B \simeq 5.0$	Constant used in the logarithmic overlap region
$C_f = 2\tau_w/\rho\tilde{U}_\infty^2$	Skin friction coefficient
$\hat{e}_i$	Unit vectors
F	Defect function used in the Law-of-the-Wake
l, L	Length scale ($=\lambda\delta$)
n	Exponent in power law growth
P	Pressure
Q	Outer variable (stands for U_i, P, T_{ij})
q	Middle-layer variable (stands for u_i, p, t_{ij}).
$\hat{q}$	Inner variable (stands for $\hat{u}_i, \hat{p}, \hat{t}_{ij}$)
R	Perpendicular distance of particle from axis of rotation
R_o	Perpendicular distance from axis of rotation to blade hub
$Re_l = \tilde{U}_e l/\nu$	Reynolds number based on l
$Re_\delta = \tilde{U}_e \delta/\nu$	Reynolds number based on δ

$Re_{\delta^*} = \tilde{U}_e \delta^* / \nu$	Reynolds number based on δ^*
$T_{ij} = -\overline{\tilde{u}_i' \tilde{u}_j'} / u_\tau^2$	Reynolds stress
U	Resultant velocity. Also streamwise velocity (clear from context).
U_x	Streamwise velocity component
U_p	U at apex in Johnston's triangle
U_y, V	Normal velocity component relative to endwall
U_z, W	Crossflow velocity component relative to endwall
u^*	velocity perturbation scale
$u_\tau = \left[\tau_w / \rho\right]^{1/2}$	Friction velocity
$u^+ = \tilde{U} / u_\tau$	Law-of-the-Wall velocity
X	Streamwise coordinate
Y	Normal coordinate relative to endwall
Z	Crosswise coordinate relative to endwall
$y = Y / \epsilon$	normal coordinate in middle layer of endwall
$\hat{y} = Y / \epsilon\hat{\epsilon}$	Normal coordinate in inner layer of endwall
$y^+ = \tilde{Y} u_\tau / \nu$	Law-of-the-Wall normal coordinate relative to endwall
z, $\hat{z}$	Normal coordinates in blade middle and inner layers, respectively

Greek Letters

α, β	Parameters appearing in Eq. (10)

β_e	External flow direction relative to direction at upstream position
γ	Angle appearing in polar plot of U_z vs U_x
γ_m	Value of γ at outer edge of defect layer
$\Gamma=\gamma/\gamma_m$	Wake variable
δ, Δ	Boundary layer thickness
δ^*	Displacement thickness
$\lambda = \left[2/C_f\right]^{1/2}$	
$\kappa \cong .41$	von Karman constant
$\epsilon=u_\tau/\tilde{U}_e$	Normal length scale of defect layer
$\epsilon\hat{\epsilon}=\epsilon^{-1}Re_l^{-1}$	Normal length scale of inner layer
$\sigma \equiv 1/(1-2n)$	
ρ	Density
ν	Kinematic viscosity
$\eta=\tilde{Y}/\delta$	Normalized normal coordinate
ϕ	Angle between U and U_x in polar plot of U_z vs U_x
ζ	Parameter in juncture flow equations
τ	Shear stress
$\xi \equiv X_{ref}/\lambda_w\Delta$	
Π	Wake parameter
Ω	Angular velocity of rotation

Superscripts

$\tilde{}$	Indicates a dimensional quantity
$\hat{}$	Indicates an inner layer variable

$\vec{\ }$	Indicates a vector quantity

Subscripts

0	Indicates a quantity evaluated at the point where the wall- and wake- velocity vectors are in the same direction
1	Indicates a quantity evaluated at the point of switching from the logarithmic overlap to the wake
m	Indicates maximum value
x	Indicates an X-wise quantity
z	Indicates a Z-wise quantity
w	Indicates a quantity evaluated at the endwall
e	Indicates a quantity evaluated at the local freestream
∞	Indicates a quantity evaluated at the upstream position
b	Indicates a quantity evaluated at the blade
c	Indicates a quantity evaluated at the corner
ref	Indicates a reference quantity
2D	Indicates two-dimensional flow

CHAPTER I

INTRODUCTION

Three-dimensional turbulent boundary layers occur in both external and internal flows. Examples are boundary layers on swept wings and boundary layers on turbomachinery endwalls between compressor blades or turbine blades. Gaining physical understanding of such flows is very important for both analysis and design purposes.

The present work treats turbomachinery endwall boundary layers, pointing out some basic physics of such flows and suggesting a model which attempts to describe parts of the flow-field analytically.

Figure 1 shows a schematic of a turbomachinery flow-field, indicating the regions treated by the present work. Region I is the part of the endwall flow which is not influenced by the blades and which is pressure-driven, the crosswise pressure gradient creating the secondary flows which give this part of the flow its three-dimensional character. Region II is the blade/endwall juncture region, where the three-dimensionality of the flow is created by secondary flows induced by interference effects due to the mutual interaction of the two boundary layers on each side of the juncture. There is another juncture region between Region I and the suction

side of the other blade, which is omitted from Fig. 1 for clarity. The cross-hatched plane depicts a typical streamwise station in which the present analysis is done.

Region I is treated much more extensively in the literature than Region II. Coles [1] was apparently the first to suggest the possibility of treating three-dimensional turbulent boundary layers in vector form, whereby the entire velocity profile is described by the sum of two vectors: a wall component and a wake component. Based on the experimental data available to him, he tentatively stated that if the wall component is in the direction of the surface shear stress, then the wake component would be very nearly parallel to the direction of the pressure gradient. Johnston [2] suggested the approach of treating the secondary (or crosswise) component of a three-dimensional turbulent boundary layer as a function of the main (or streamwise) component and of certain additional parameters. He was thus led through examination of data to the proposition of his well known triangular model to describe the form of the velocity hodograph. Based on his own experiments and those of others, he suggested two explicit relationships to describe the triangular model: one for the region adjacent to the wall and the other for that near the freestream. His model is successful enough in the regions away from the vertex of the triangle but fails to match the data adequately in the vicinity of the vertex. As will be shown later, this region corresponds to the transitional region from the wall- to the wake-sublayer. In spite of its relative success, Johnston's model

suffers from being a product of data-correlation without the benefit of a supporting analysis.

The main phenomenon in juncture flows is the corner vortex [3-6], which is composed of two sources: the "horseshoe" vortex, created by the wrapping of the oncoming vorticity around the blades, and the "passage" vortex, which rolls up from the skewed boundary layer-induced crossflow. The blade leading edge region is predominantly inviscid and rotational. Shabaka's [5] experiments indicate the existence of a Reynolds stress-induced "boundary jet" outflow from the juncture over the endwall. It is important to realize that, since the eddy viscosity scales are different for the blade and endwall, a single eddy viscosity model cannot work for juncture flows.

In order to gain further insight into the physics of three-dimensional, endwall turbulent boundary layers, it became clear that more analysis would be helpful. To this end, Mellor's [7] two-dimensional asymptotic analysis for large Reynolds number turbulent boundary layers has been extended to three dimensions in the present work. The results of this analysis provide the scaling of three-dimensional boundary layers of both juncture - and pressure-driven - types, including rotational effects. The analysis of the former type includes both symmetric and asymmetric cases. The analysis of the latter type leads to the proposition of a composite three-dimensional Law-of-the-Wall and Law-of-the-Wake model, utilizing a vector approach in the wake sub-layer. This model is com-

pared with van den Berg and Elsenaar's [8] infinite swept-wing flow data and Mueller's [10] forced turning flow data with good agreement. It should be mentioned that Johnston's triangle emerges as a particular limit of this model.

The analysis presented here does not include solutions of the equations of motion found for the various sub-regions, and therefore it comes short of predicting forces and moments acting on the blades of a turbomachinery component.

CHAPTER II

ASYMPTOTIC ANALYSIS

II.1. The Pressure-Driven Case (Region I)

A typical skewed boundary layer and basic nomenclature are shown in Fig. 2. For incompressible, steady flow, with no curvatures, the mean part of a turbulent flow is described by the following equations:

Mass conservation:

$$\partial U_i/\partial X_i=0 \tag{1}$$

Momentum:

$$U_j\left[\partial U_i/\partial X_j\right] = -\partial P/\partial X_i+$$

$$\partial/\partial X_j\ \left[\epsilon^2 T_{ij}+\epsilon^2\hat{\epsilon}\partial U_i/\partial X_j\right] \tag{2}$$

where

$$U_i=\tilde{U}_i/\tilde{U}_e,\quad P=\tilde{P}/\rho\tilde{U}_e^2,\quad T_{ij}=-\overline{\tilde{u}_i'\tilde{u}_j'}/u^{*2}.$$

$$X_l = \tilde{X}_l / l \,,\quad \epsilon = u^* / \tilde{U}_e \,,\quad \epsilon^2 \hat{\epsilon} = \nu / (\tilde{U}_e l) = R_{e_l}^{-1}$$

In the above equations, ϵ^2 is the scale for the Reynolds stresses, with u^* being an as of yet undetermined perturbation velocity scale. $\epsilon^2 \hat{\epsilon}$ is the scale for the viscous stresses, which is also given by $R_{e_l}^{-1}$. Thus $\hat{\epsilon}$ is the relative magnitude of viscous- to Reynolds-stresses.

In addition, the following boundary conditions are required:

$$U_l(X, 0, Z) = 0$$

and, assuming a uniform external flow,

$$\begin{Bmatrix} U_x \\ U_z \end{Bmatrix} \begin{bmatrix} X, \infty, Z \end{bmatrix} = \begin{Bmatrix} 1 \\ 0 \end{Bmatrix}$$

(for a fixed (X,Z) location)

Next, an asymptotic analysis is carried out (following Mellor [7]) for the above equations, using the following expansions:

A. Outer Expansion

$$Q = Q_1 + \epsilon Q_2 + \epsilon^2 Q_3 + \cdots$$

$T_{ij} = 0$ (*This assumes no free-stream turbulence*)

where Q stands for the three velocity components and pressure:

$$Q=(U_x(X,Y,Z),U_y,U_z,\ P) \quad (1)$$

B. Middle Expansion

$$y=Y/\epsilon$$

$$U_x = u_{x_1}\ (X,y,Z) + \epsilon u_{x_2} + \epsilon^2 u_{x_3} + \cdots$$

$$U_y=\epsilon\left[u_{y_1}+\epsilon u_{y_2}+\epsilon^2 u_{y_3}+\cdots\right]$$

$$U_z = u_{z_1} + \epsilon u_{z_2} + \epsilon^2 u_{z_3} + \cdots$$

$$P = p_1 + \epsilon p_2 + \epsilon^2 p_3 + \cdots$$

$$T_{ij} = t_{1_{ij}} + \epsilon t_{2_{ij}} + \epsilon^2 t_{3_{ij}} + \cdots$$

C. Inner Expansion

$$\hat{y}=y/\hat{\epsilon}=Y/\epsilon\hat{\epsilon}$$

$$U_x = \hat{u}_{x_1}\ (X,\hat{y},Z) + \epsilon\hat{u}_{x_2} + \epsilon^2\hat{u}_{x_3} + \cdots$$

---

(1)NOTE: In the present analysis an expression of the form U(X,Y,Z) should be interpreted as U(Y) at a given (X,Z) location.

$$U_y = \epsilon\hat{\epsilon}\left[\hat{u}_{y_1} + \epsilon\hat{u}_{y_2} + \epsilon^2\hat{u}_{y_3} + \cdots\right]$$

$$U_z = \hat{u}_{z_1} + \epsilon\hat{u}_{z_2} + \epsilon^2\hat{u}_{z_3} + \cdots$$

$$P = \hat{p}_1 + \epsilon\hat{p}_2 + \epsilon^2\hat{p}_3 + \cdots$$

$$T_{ij} = \hat{t}_{1_{ij}} + \epsilon\hat{t}_{2_{ij}} + \epsilon^2\hat{t}_{3_{ij}} + \cdots$$

These expansions are substituted into Eqs. (1) and (2) and the analysis proceeds in the manner of matched asymptotic expansions, the details of which are described in Appendices A, B and C. It should be noted that this analysis assumes that both ϵ and $\hat{\epsilon}$ are much smaller than unity. The features of the resulting equations in the three regions are summarized in Table 1 to the first three orders. The main features of the flow, as indicated in the table, are the following: the outer layer is inviscid; the middle layer is influenced by Reynolds stresses to orders 2 and 3, where the 2nd order equations are of the boundary layer type while the 3rd order ones are Re averaged Navier Stokes equations; the inner layer is dominated by constant total shear (viscous- plus Reynolds-stresses) across it, with no pressure gradient or inertia effects through order 3. The important information for the subsequent analysis is contained in the 1st order outer region equations and in the 2nd order middle- and inner- region equations.

As a result of the asymptotic analysis and the matching procedure, the following conclusions emerge:

1. The flow possesses a 3-layer structure;

2. The inner and middle layers have a common logarithmic overlap;

3. The inner layer is exponentially thin compared to the middle layer: $\hat{\epsilon} = O\left[e^{-\frac{1}{\epsilon}}\right]$ as $\epsilon \to 0$;

4. The pressure gradient does not influence the inner layer, hence the wall shear stress is the only driving force there. It is reasonable to assume that the shear field maintains its two-dimensionality within this sub-layer. Thus the flow is two-dimensional in the inner layer and the velocity vectors are co-planar in the τ_w-direction.

5. Since the outer flow is in the freestream direction, all the turning from the τ_w - direction to the $\tilde{U}_e$ - direction must take place in the middle layer.

While the first three conclusions apply also to two-dimensional boundary layerss, the last two are special to the three-dimensional case.

See Appendix G for the effects of rotation on the equations of motion in the pressure-driven case.

II.2. The Case of Juncture Flow (Region II)

Figure 3 describes the main features of the flow field in a juncture. An oncoming endwall boundary layer interacts with a blade situated normal to the endwall. This interaction gives rise to several phenomena: the vorticity carried by the oncoming b.l. wraps around the blade, thereby creating a "horseshoe" vortex; the stagnation line at the blade leading edge creates a pressure gradient that induces skewing of the oncoming b.l. and the formation of an endwall crossflow, which later rolls up into a so-called "passage vortex"; this and the "horseshoe" vortex augment each other and create the corner vortex which stretches downstream without diminishing its strength for quite a distance downstream of the blade leading edge; if the latter is blunt, the oncoming flow may separate upstream of it, creating one of several possible three-dimensional separation patterns, such as a saddle-point or a node.

As the oncoming flow hits the blade, a boundary layer develops over it. This b.l. interacts with the one which has been developing over the endwall, resulting in a corner (or juncture) flow which is investigated in this section.

II.2.1. Scaling and normalized equations

The flow variables in the juncture are normalized as follows:

$$U_i = \tilde{U}_i/\tilde{U}_e, \quad P = \tilde{P}/\rho\,\tilde{U}_e^2, \quad T_{ij} = \overline{-\tilde{u}_i'\tilde{u}_j'}/u_{\tau_{ij}}^2$$

$$x = \bar{x}/\bar{x}_{ref}, \quad Y = \bar{Y}/\lambda_w\Delta, \quad Z = \bar{Z}/\lambda_b\delta \qquad (\lambda = \sqrt{2/C_f})$$

where $(\bar{x}, \bar{Y}, \bar{Z})$ is a locally cartesian coordinate system.

The scaling of $\bar{Y}$ and $\bar{Z}$ is based on the results of the analysis of the three-dimensional boundary layer outside the juncture region (Region I), which is performed in Section 2.1. (See also Appendix D). When the equations of motion are written in terms of these variables, the factors $X_{ref}/(\lambda_w\Delta) = \xi$ and $\lambda_b\,\delta/(\lambda_w\Delta) = \zeta$ appear in them (see Appendix F1) and these require additional consideration. By using the (1/n)th power law for turbulent flat plate flow as a model, it can be shown (Appendix F1) that the equations of motion for the juncture flow become

$$\frac{\partial U}{\partial X} + \xi\frac{\partial V}{\partial Y} + \frac{\xi}{\zeta}\frac{\partial W}{\partial Z} = 0$$

$$U\frac{\partial U}{\partial X} + \xi V\frac{\partial U}{\partial Y} + \frac{\xi}{\zeta}W\frac{\partial U}{\partial Z} = -\frac{\partial P}{\partial X} + \frac{\partial}{\partial X}\left[\xi^{-1}\epsilon_w^2\hat{\epsilon}_w\frac{\partial U}{\partial X} + \epsilon_w^2 T_{xx}\right] +$$

$$+ \xi\frac{\partial}{\partial Y}\left[\epsilon_w^2\hat{\epsilon}_w\frac{\partial U}{\partial Y} + \epsilon_w^2 T_{yx}\right] + \frac{\xi}{\zeta}\frac{\partial}{\partial Z}\left[\zeta^{-1}\epsilon_w^2\hat{\epsilon}_w\frac{\partial U}{\partial Z} + \epsilon_w^2 T_{zx}\right]$$

$$U\frac{\partial V}{\partial X} + \xi V\frac{\partial V}{\partial Y} + \frac{\xi}{\zeta}W\frac{\partial V}{\partial Z} = -\xi\frac{\partial P}{\partial Y} + \frac{\partial}{\partial X}\left[\xi^{-1}\epsilon_w^2\hat{\epsilon}_w\frac{\partial V}{\partial X} + \epsilon_w^2 T_{xy}\right] + \qquad (3)$$

$$+ \xi \frac{\partial}{\partial Y}\left[\epsilon_w^2 \hat{\epsilon}_w \frac{\partial V}{\partial Y} + \epsilon_w^2 T_{yy}\right] + \frac{\xi}{\zeta}\frac{\partial}{\partial Z}\left[\zeta^{-1} \epsilon_w^2 \hat{\epsilon}_w \frac{\partial V}{\partial Z} + \epsilon_w^2 T_{zy}\right]$$

$$U \frac{\partial W}{\partial X} + \xi V \frac{\partial W}{\partial Y} + \frac{\xi}{\zeta} W \frac{\partial W}{\partial Z} = -\frac{\xi}{\zeta}\frac{\partial P}{\partial Z} + \frac{\partial}{\partial X}\left[\xi^{-1} \epsilon_w^2 \hat{\epsilon}_w \frac{\partial W}{\partial X}\right.$$

$$\left. + \zeta^{2\sigma} \epsilon_w^2 T_{xz}\right] +$$

$$+ \xi \frac{\partial}{\partial Y}\left[\epsilon_w^2 \hat{\epsilon}_w \frac{\partial W}{\partial Y} + \zeta^{2\sigma} \epsilon_w^2 T_{yz}\right] + \frac{\xi}{\zeta}\frac{\partial}{\partial Z}\left[\zeta^{-1} \epsilon_w^2 \hat{\epsilon}_w \frac{\partial W}{\partial Z}\right.$$

$$\left. + \zeta^{2\sigma} \epsilon_w^2 T_{zz}\right]$$

where, in analogy with the treatment of Region I,

$$\epsilon_w^2 \hat{\epsilon}_w \equiv \nu/(\tilde{U}_e \lambda_w \Delta), \epsilon_w \equiv u_{T_w}/\tilde{U}_e$$

and the additional notation is

$$\zeta \equiv (\epsilon_b/\epsilon_w)^{1-2n}, \sigma \equiv 1/(1-2n), \xi \equiv x_{ref}/(\lambda_w \Delta)$$

The boundary conditions are:

$$U = V = W = 0 \text{ @ } \begin{cases} Y = 0, Z \geq 0 \\ Z = 0, Y \geq 0 \end{cases}$$

II.2.2. Asymptotic treatment

Two independent parameters appear in Eqn. (3), namely ϵ_w and ζ (the 3rd parameter, $\hat{\epsilon}_w$, is related to ϵ_w as shown in Appendix B). While ϵ_w is a small parameter everywhere along the juncture, ζ increases from 0 at the blade leading edge to O(1) at the trailing edge, and may thus be viewed as a measure of both streamwise location and extent of asymmetry. For the purpose of

asymptotic analysis of Eqn. (3), a new parameter, ϵ_c, is used as a basic perturbation paramoter, to be determined (along with $\hat{\epsilon}_c$) from matching conditions (Appendix F2). In order to avoid double expansions in terms of ϵ_w and ζ, it is intended to stretch the juncture coordinates Y_c and Z_c in such a manner that the juncture equations derived from Eqn. (3) are symmetric w.r.t. these coordinates as well as w.r.t. V_c and W_c regardless of whether the flow itself is symmetric or not. Such a coordinate transformation leaves ϵ_c as the only perturbation parameter, enabling single expansions as for the Region I treatment. The details of the coordinate stretchings are given in Appendix F1, resulting in the following expansions, valid for an arbitrary (non-zero) ζ:

Middle region

$$y = Y/(\xi\epsilon_c),\quad z = \zeta\, Z/(\xi\epsilon_c),\quad \xi = \epsilon_w^2\hat{\epsilon}_w/(\epsilon_c^2\hat{\epsilon}_c)$$

$$U = u_1 + \epsilon_c u_2 + \epsilon_c^2 u_3 + \cdots$$

$$V = \epsilon_c\left[v_1 + \epsilon_c v_2 + \epsilon_c^2 v_3 + \cdots\right]$$

$$W = \epsilon_c\left[w_1 + \epsilon_c w_2 + \epsilon_c^2 w_3 + \cdots\right]$$

$$P = p_1 + \epsilon_c p_2 + \epsilon_c^2 p_3 + \cdots$$

$$T_{ij} = \left[\epsilon_c/\epsilon_w\right]^2 \left[1 + \left[\zeta^{-2\sigma} - 1\right]\delta_{jz}\right] \cdot$$

$$\left[t_{1_{ij}} + \epsilon_c t_{2_{ij}} + \epsilon_c^2 t_{3_{ij}} + \cdots\right], \delta_{jz} = \begin{cases} 0, j \neq z \\ 1, j = z \end{cases}$$

Inner region

$$\hat{y} = Y/(\xi \epsilon_c \hat{\epsilon}_c), \quad \hat{z} = \zeta Z/(\xi \epsilon_c \hat{\epsilon}_c)$$

$$U = \hat{u}_1 + \epsilon_c \hat{u}_2 + \epsilon_c^2 \hat{u}_3 + \cdots$$

$$V = \epsilon_c \hat{\epsilon}_c \left[\hat{v}_1 + \epsilon_c \hat{v}_2 + \epsilon_c^2 \hat{v}_3 + \cdots\right]$$

$$W = \epsilon_c \hat{\epsilon}_c \left[\hat{w}_1 + \epsilon_c \hat{w}_2 + \epsilon_c^2 \hat{w}_3 + \cdots\right]$$

$$P = \hat{p}_1 + \epsilon_c \hat{p}_2 + \epsilon_c^2 \hat{p}_3 + \cdots$$

$$T_{ij} = \left[\epsilon_c/\epsilon_w\right]^2 \left[1 + \left[\zeta^{-2\sigma} - 1\right]\delta_{jz}\right] \cdot$$

$$\left[\hat{t}_{1_{ij}} + \epsilon_c \hat{t}_{2_{ij}} + \epsilon_c^2 \hat{t}_{3_{ij}} + \cdots\right]$$

As shown in Appendix F2.

$$\lim_{z_c \to \infty} \epsilon_c = \epsilon_w, \quad \lim_{y_c \to \infty} \epsilon_c = \epsilon_b, \quad \lim_{\hat{z}_c \to \infty} \hat{\epsilon}_c = \hat{\epsilon}_w, \quad \lim_{\hat{y}_c \to \infty} \hat{\epsilon}_c = \hat{\epsilon}_b$$

These expansions are inserted into Eqn. (3) and the resulting equations are sorted out to orders 1, ϵ_c and ϵ_c^2 for the middle and inner regions, as shown in Appendix F1. It is important to realize

that the Reynolds stresses scale differently in the endwall- and blade- boundary layers (Regions I). Thus, in the endwall b.l.:

$$T_{w_{ij}} = t_{1_{ij}} + \epsilon_w t_{2_{ij}} + \cdots$$

with related expansion for the inner layer. In the blade b.l.:

$$T_{b_{ij}} = t'_{1_{ij}} + \epsilon_b t'_{2_{ij}} + \cdots$$

and similarly for the inner layer. The juncture region contains Reynolds stress contributions from both boundary layers adjacent to it, and this is taken into account by the series expansion representation of $T_{c_{ij}}$ as demonstrated below:

$$\lim_{z_c \to \infty} T_{c_{ij}} = \begin{cases} t_{1_{ij}} + \epsilon_w t_{2_{ij}} + \cdots, & j \neq z \\ \zeta^{-2\sigma}\left[t'_{1_{ij}} + \epsilon_w t'_{2_{ij}} + \cdots\right], & j = z \end{cases}$$

$$\lim_{y_c \to \infty} T_{c_{ij}} = \begin{cases} \zeta^{2\sigma}\left[t_{1_{ij}} + \epsilon_b t_{2_{ij}} + \cdots\right], & j \neq z \\ t'_{1_{ij}} + \epsilon_b t'_{2_{ij}} + \cdots, & j = z \end{cases}$$

Thus, the factors $\zeta^{\pm 2\sigma}$ compensate for the two different scales for T_{ij} on endwall and blade, enabling smooth matching of the juncture region Reynolds stresses with those on the two Region I boundary layers.

The equations of motion are derived in Appendix F1, while Appendix F2 includes a detailed description of the procedure to match the corner region with the boundary layers outside the corner. Since the equations are symmetric, it suffices to perform the matching to half of the corner, say the sector between the Z-axis and the bisector of the right angle between this and the Y-axis. The resulting matching lines are indicated in Fig. 4 by the numbers 1, 2 and 3. Important results from the matching procedure are given in Appendix F2 and summarized below:

1. The pressure in the corner region is imposed by the external flow; the gradients of the external pressure normal to the solid boundaries vanish along the corner.

2. The streamwise velocity has a common logarithmic overlap between the corner middle region and the inner layers on both endwall and blade.

3. The streamwise velocity component in the inner region vanishes to O(1).

The final version of the equations of motion is given in Table 2. These equations indicate the following main features of turbulent corner flows:

1. The pressure field in the corner region is imposed by the outer flow.

2. In the middle region, the flow is inviscid and without Reynolds stresses to O(1), and is described by an Euler-type equation for the streamwise momentum. This same

momentum equation becomes of a parabolized Navier-Stokes type with Reynolds stresses only, to $O(\epsilon)$. The $O(\epsilon^2)$ flow is described by a Re-averaged N-S-type equation for the streamwise momentum and by parabolized N-S equations for the two crosswise momenta. Again, these equations include Reynolds stresses only.

3. The inner region is characterized by the fact that the crosswise derivatives of the total shear (viscous + Reynolds stresses) on each wall are equal in magnitude and opposite in sign. Also, the $O(\epsilon^2)$ flow includes pressure gradients normal to both walls, which are balanced by crosswise Reynolds stress gradients. There are no inertia effects in the inner region through $O(\epsilon^2)$ at least.

It is noted that, unlike the Region I equations, those of Region II cannot be solved starting at the lowest order and continuing to higher orders based on previous solutions. Rather, one has to use symultaneously equations belonging to different orders, to have enough non-trivial equations for the number of unknowns [15,16]. Specifically, in the middle region the continuity and streamwise momentum equations of $O(\epsilon^m)$ have to be coupled with the two crossflow momentum equations of $O(\epsilon^{m+2})$ to solve for the $O(\epsilon^m)$ velocity components and $O(\epsilon^{m+2})$ pressure; in the inner region the continuity and streamwise mometum equations of $O(\epsilon^m)$ must be

solved symultaneously with the crosswise momentum equations of $O(\epsilon^{m+2}\hat{\epsilon}^2)$ to get a complete flow picture. This means that considerably more terms of the asymptotic series must be retained in Region II than in Region I, especially in the inner region. Note also that a "composite profile" does not exist for the juncture flow, since the outer, middle and inner regions do not share common surfaces and thus do not have common asymptotes (see Fig. 4).

Finally, the extent of the juncture region for an arbitrary δ/Δ ratio is of interest. This is determined by letting the coordinates of the various subregions be of the order of their scales. Thus

$$y_c = O(1) \rightarrow Y = O(\xi\epsilon_c) \rightarrow \tilde{Y} = 0\left[\epsilon_w^{-1}\,\epsilon_c\xi\Delta\right] = 0\left[\xi\Delta u_{\tau_c}/u_{\tau_w}\right]$$

$$\hat{y}_c = O(1) \rightarrow Y = 0\left[\xi\,\epsilon_c\hat{\epsilon}_c\right] \rightarrow \tilde{Y} = 0\left[\epsilon_w^{-1}\,\epsilon_c\hat{\epsilon}_c\xi\Delta\right] = 0\left[\xi\,\frac{\Delta\nu}{\Delta_c u_{\tau_w}}\right]$$

$$z_c = O(1) \rightarrow Z = 0\left[\epsilon_c\xi/\zeta\right] \rightarrow \tilde{Z} = 0\left[\epsilon_b^{-1}\epsilon_c\delta\xi/\zeta\right] = 0\left[\frac{u_{\tau_c}}{u_{\tau_b}}\,\frac{\xi}{\zeta}\,\delta\right]$$

$$\hat{z}_c = O(1) \rightarrow Z = 0\left[\epsilon_c\hat{\epsilon}_c\xi/\zeta\right] \rightarrow \tilde{Z} = 0\left[\epsilon_b^{-1}\epsilon_c\hat{\epsilon}_c\delta\xi/\zeta\right]$$

$$= 0\left[\frac{\xi}{\zeta}\,\frac{\delta}{\Delta_c}\,\frac{\nu}{u_{\tau_b}}\right]$$

Figure 4 shows the various sub-regions for a juncture flow with

nonzero but otherwise arbitrary δ/Δ ratio. The corner vortex, discussed earlier in this Chapter, is situated in the juncture middle region.

For rotational effects on the equations of motion in the juncture, consult Appendix G.

CHAPTER III

PROFILE RELATIONS FOR PRESSURE-DRIVEN BOUNDARY LAYERS

III.1. General Discussion

Based on the results of the pressure-driven 3D analysis, the general forms for the Law-of-the-Wall and Law-of-the-Wake are the following:

Law-of-the-Wall

$$u^+ \left[y^+\right] = \frac{\tilde{U}\left[\tilde{X},\tilde{Y},\tilde{Z}\right]}{u_\tau\left[\tilde{X},\tilde{Z}\right]}$$

where

$$y^+ = \frac{\tilde{Y}u_\tau}{\nu},\quad u_\tau = \left[\frac{\tau_w}{\rho}\right]^{1/2}$$

Law-of-the-Wake

$$\vec{F}\left[\tilde{X},\eta,\tilde{Z}\right] = \frac{\vec{\tilde{U}}_e\left[\tilde{X},\tilde{Z}\right] - \vec{\tilde{U}}\left[\tilde{X},\tilde{Y},\tilde{Z}\right]}{u_\tau\left[\tilde{X},\tilde{Z}\right]}$$

where

$$\eta = \frac{\tilde{Y}}{\delta}$$

Matching these two laws yields the logarithmic overlap (see Appendix D):

$$F\left[\tilde{X}, \eta, \tilde{Z}\right] \sim -\kappa^{-1} \ln \eta + A', \eta \to 0$$

$$u^{+}\left[y^{+}\right] \sim \kappa^{-1} \ln y^{+} + B, y^{+} \to \infty$$

where

$$\kappa \cong .41, B \cong 5.0, A' = 2\kappa^{-1} \Pi$$

which are Coles' parameters.

If u^{*} is now chosen as u_{τ} then the relationships between F and u^{+} on the one hand and the 2nd order middle- and inner-variables on the other, become (see Appendix D):

$$F = -\left[u_{x_2}^2 + u_{z_2}^2\right]^{1/2}, \eta = y$$

$$u^{+} = \left[\hat{u}_{x_2}^2 + \hat{u}_{z_2}^2\right]^{1/2}, y^{+} = \hat{y}$$

This enables the construction of the composite velocity profile, following the general scheme

$$\left\{\begin{matrix}\text{composite} \\ \text{profile}\end{matrix}\right\} = (\text{outer profile}) - (\text{common outer-middle asymptote}) + (\text{middle profile}) - (\text{common middle-inner asymptote}) + (\text{inner profile})$$

Written out explicitly, the composite profile, to order ϵ, has the form (see Appendices C and D):

$$\begin{Bmatrix} U_x \\ U_z \end{Bmatrix} = \left[\begin{Bmatrix} U_{x_1} \\ U_{z_1} \end{Bmatrix} (X,Y,Z) \right] -$$

$$\left[\begin{Bmatrix} U_{x_1} \\ U_{z_1} \end{Bmatrix} (X,0,Z) + \epsilon\, \eta\, \frac{\partial}{\partial Y} \begin{Bmatrix} U_{x_1} \\ U_{z_1} \end{Bmatrix} (X,0,Z) \right] +$$

$$\left[\begin{Bmatrix} U_{x_1} \\ U_{z_1} \end{Bmatrix} (X,\eta,Z) - \epsilon \begin{Bmatrix} \cos\gamma \\ -\sin\gamma \end{Bmatrix} F(X,\eta,Z) \right]$$

$$- \left[\epsilon \begin{Bmatrix} \cos\phi_w \\ \sin\phi_w \end{Bmatrix} \left[\kappa^{-1} \ln y^+ + B \right] \right]$$

$$+ \left[\epsilon \begin{Bmatrix} \cos\phi_w \\ \sin\phi_w \end{Bmatrix} u^+ (y^+) \right]$$

where

$$U = \left[U_x^2 + U_z^2 \right]^{1/2}, \quad \phi = \tan^{-1} \left[\frac{U_z}{U_x} \right]$$

and γ is the angle between $\vec{F}$ and $\vec{U}_e$. In order to be able to use this profile in actual calculations, it is necessary to provide explicit models for the Wall- and Wake-Laws.

III.2. LAW-OF-THE WALL

Based on the results of the asymptotic analysis, the Wall-Law is written in the form:

$$u^+ = f\left[y^+\right] . \phi = \phi_w \qquad (4)$$

with components

$$u_x^+ = u^+ \cos\phi_w . \quad u_z^+ = u^+ \sin\phi_w .$$

For f Musker's [12] explicit expression is chosen:

$$f(y^+) = 5.424 \tan^{-1}\left\{\frac{2y^+ - 8.15}{16.7}\right\}$$

$$+ \log_{10}\left\{\frac{\left[y^+ + 10.6\right]^{9.6}}{\left[y^{+2} - 8.15y^+ + 86\right]^2}\right\} - 3.52$$

III.3. LAW-OF-THE-WAKE

In view of the conclusions from the asymptotic analysis, the wake function is defined in the form:

$$\vec{F} = \frac{\vec{U}_e - \vec{U}}{u_\tau}$$

with streamwise component

$$F_x = F\cos\gamma = \frac{\tilde{U}_e - \tilde{U}_x}{u_\tau}$$

and crossflow component

$$F_z = -F\sin\gamma = -\frac{\tilde{U}_z}{u_\tau}$$

See Fig. 5 for basic nomenclature.

The two-dimensional defect function may be expressed by Musker's [12] formula

$$F_{2D} = \kappa^{-1}\left[2\Pi\left[1-3\eta^2+2\eta^3\right] - \ln\eta - \eta^2\left[1-\eta\right]\right] \qquad (5)$$

where the Wake Parameter, Π, is determinable from[1] (see Appendix E1).

$$2\Pi - \ln\left[\kappa\frac{1+\Pi}{Re_{\delta_x^*}}\right] + \kappa\left[B-\lambda_x\right] = 0$$

with

$$\delta_x^* \equiv \int_0^{\delta}\left[1-U_x\right]\,d\tilde{Y}$$

and

$$\lambda_x = \left[\frac{2}{C_{f_x}}\right]^{1/2} = \frac{\lambda}{\left[\cos\phi_w\right]^{1/2}}$$

There is not an unique generalization of F_{2D} to three dimensions. Possibilities for F_{2D} include:

1. $\left|\vec{U}_e - \vec{U}\right| / u_\tau$:

2. $\left[\left|\vec{U}_e\right| - \left|\vec{U}\right|\right] / u_\tau$: 3. $\left[U_e - U_x\right] / u_\tau$.

The first possibility was rejected since it led to poor data - correlation; the second is difficult to test or use; the third possibility is the simplest and is the one used henceforth. Thus

$$F = \frac{F_{2D}}{\cos\gamma} \tag{6}$$

The geometry of Fig. 5 provides the Wake-Law formulation:

$$\begin{cases} U = \left[1 - 2\lambda^{-1} F\cos\gamma + \left[\lambda^{-1} F\right]^2\right]^{1/2} \\ \phi = \tan^{-1}\left\{\dfrac{\lambda^{-1} F \sin\gamma}{1 - \lambda^{-1} F\cos\gamma}\right\} \end{cases} \tag{7}$$

or, equivalently,

$$\tan\gamma = \left\{\frac{\lambda}{F\cos\gamma} - 1\right\}\tan\phi \tag{8}$$

In order to complete the formulation of the Law-of-the-Wake, it is necessary to determine the function $\gamma(\eta)$. Figure 6 shows a plot of experimental values of $\Gamma \equiv \frac{\gamma}{\gamma_m}$, where γ_m is the maximum value of γ. The data are from Refs. 8 and 10. It is observed that

the lower portion of the plot is different for different stations and that these individual branches merge into a single curve further up. This suggests that Γ could be describable by a combination of two parts, one of which is a function of η and of some physical parameters peculiar to each measurement station, while the other is a function of η only. Pursuing this direction, one arrives at the formulation described below, the details of which are worked out in Appendix E2. In the logarithmic overlap region, γ is determined from the solution of

$$\frac{d\gamma}{d\eta} = \frac{\lambda\cos^2\gamma}{F_{2D}^2\,\tan\gamma}\left[\frac{U}{\kappa\eta} - \left[\frac{F_{2D}}{\lambda\cos^2\gamma} - 1\right]\frac{dF_{2D}}{d\eta}\right] \tag{9}$$

where U is given by Eq. (7) and F_{2D} by Eq. (5).

The initial condition is

$$\gamma = \gamma_0 \ @ \ \eta = \eta_0 \tag{9a}$$

where η_0 is the point where the Wake-Law crosses ϕ_w (see Appendix E2, and Figs. 7 and 8).

In the defect layer, γ is chosen in the form

$$\Gamma \equiv \frac{\gamma}{\gamma_m} = 1-\beta\left[1-\eta\right]^{\alpha} \tag{10}$$

as shown in Appendix E2, where

$$\alpha = \left[1-\eta_1\right] \frac{\left[\frac{d\Gamma}{d\eta}\right]_{\eta_1}}{\left[1-\Gamma_1\right]}, \quad \beta = \frac{\left[1-\Gamma_1\right]}{\left[1-\eta_1\right]^{\alpha}} \tag{10a}$$

with subscripts 1 denoting the point of switching from the portion of the curve described by Eq. (9) to the one described by Eq. (10). (see Appendix E2). The dimensionless distance η_1 is a function of Reynolds number and pressure gradient. A typical value is 0.035. Figure 8 depicts the relation of η_1 to η_0, and Appendix E3 outlines the procedure to determine η_1.

At the upper edge of the defect layer γ attains its maximum value, γ_m, which is calculable from [2]

$$\gamma_m = \tan^{-1}\left\{2U_e^2 \int_0^{\beta_e} \frac{d\Psi}{U_e^2}\right\} \tag{11}$$

where β_e is the local freestream direction relative to the direction at the upstream position. Eqn. (11) is a result of integrating a shearless version of the boundary-layer equations along main-flow streamlines. This approach is based on the assumption that a shearless analysis can yield valid results in the outer part of boundary-layers which are well developed before being perturbed by a main-flow turning. Under such circumstances crossflows develop mainly as a result of the reorientation of vorticity in the layer, while frictional effects are felt only near the wall. The determination of γ_m thus requires knowledge of the external flow field only. Figure 9

depicts a typical comparison between the above model for γ and experimental data.

It should be noted that the entire analysis described above did not involve the actual solution of the equations of motion. Therefore, four parameters are required as input in order to enable calculations. These are:

1. C_f
2. ϕ_w
3. Re_δ
4. β_e

In addition, the determination of γ_m requires knowledge of the external flow field. In a real situation these would be unknowns, and the equations of motion would have to be solved, subject to a prescribed pressure distribution and initial velocity profile. However, regardless of the method of solution, the above model could then be incorporated into the solution scheme, since it does not introduce any additional unknowns of its own.

III.4. Comparison with Experimental Data

The data of Refs. 8 and 10 have been used to check the validity of the proposed models for the Wall- and Wake-Laws. Both sources of data use flow geometries which lead to a build-up of adverse pressure gradient with eventual three-dimensional separation. The measurement stations chosen for comparison between theory and

data were all fully attached. Results of two stations from Ref. 8 and three from Ref. 10 are reported here: in station C4 of Ref. 10 an 8% crossflow is present; in station D5 the crossflow is about 12% and in station F7 it reaches about 25% of the streamwise flow component. In station 7 of Ref. 8 the crossflow is about 22% and in station 8 it reaches 27%. Figures 10A through 10E show comparisons between the present model and the data of the representative measurement stations. The figures include comparisons for both the hodograph and the resultant velocity profile (in terms of magnitude and direction). The agreement is good for all stations. In particular, it is noted that the model is able to predict the smooth transition from the wall- to the wake-region. The discrepancy between the model and the data of Ref. 10 involving the magnitude of the velocity (most pronounced in station F7) may be due to the fact that the experiment of Mueller has a curvature effect, which is not accounted for in the model.

III.5. Comparison with Johnston's Triangular Model

Johnston [2] assumed the following model for the U_z-U_x hodograph:

$$U_z = \begin{cases} U_x \tan\phi_w, & U_x \leq U_p \\ A\left[1-U_x\right], & U_x > U_p \end{cases}$$

In contrast, the present model assumes no geometric relationship.

Rather, the hodograph results on the basis of the fundamental assumption that the wake function is a vector quantity. In comparing the two models, it is observed that the first leg of Johnston's triangle corresponds to the Wall-Law of the present model, while the second leg corresponds to a special limit of the present model's Wake-Law, namely, $\Gamma = 1$ with $A = \tan\gamma_m$. However, this is an inadequate choice since it fails to correctly describe either the transition from the wall- to the wake-region or the magnitude and location of the maximum crossflow (see Fig. 7). These shortcomings are apparent from Johnston's own polar plots (see Ref. 2). The other basic difference between the two models stems from the fact that whereas Johnston regards the vertex of his triangle as the edge of the wall sublayer, the present model locates this point at η_0, corresponding to γ_0 (see Fig. 7).

CHAPTER IV

CONCLUSIONS

An asymptotic analysis has been carried out for three-dimensional, endwall turbulent boundary layers. This analysis indicates that, as in the two-dimensional case, the flow is multi-structured, possessing an inner (or wall) layer; a middle (or defect) layer; and an outer layer, and the pressure in the b.l. is imposed by the outer flow.

In the blade/endwall juncture, the defect region is describable by parabolized Navier-Stokes equations through $O(\epsilon^2)$ except for the streamwise momentum of $O(\epsilon^2)$ which is a Re-averaged N-S-type equation. Rotational effects appear in the form of centrifugal terms to $O(1)$, Coriolis terms to $O(\epsilon^2)$ and there is no influence on the $O(\epsilon)$ momentum components. Viscous stresses are absent from the defect region. The inner region is characterized by the crosswise total shear gradients on each wall being equal in magnitude and opposite in sign, and no inertia effects, except for centrifugal accelerations in the case of a rotor.

It is also found that the streamwise velocity has a common logarithmic overlap between the corner middle region and the inner layers on both endwall and blade.

The same equations which describe the non-symmetrical juncture flow also describe the symmetrical case, but the coordinates and Reynolds stresses scale differently in the two cases.

In the pressure-driven part of the endwall boundary layer outside the juncture, the inner layer is dominated by constant total shear across it, inertia and pressure gradients having no significant influence there. The middle layer is driven by both pressure gradients and Reynolds stresses, and may be described by boundary layer-type equations to $O(\epsilon)$ and Re-averaged N-S equations to $O(\epsilon^2)$. These two sub-layers share a common logarithmic overlap region. The outer layer is inviscid and generally rotational, describable by the Euler equations.

The results of the analysis indicate that the wall sub-layer is two-dimensional, flowing in the local wall shear direction, and all the turning from this to the freestream direction takes place in the defect sub-layer.

Based on the results of the analysis for the pressure-driven part of the b.l., a model is proposed for the three-dimensional counterpart of the Law-of-the-Wall and Law-of-the-Wake, which agrees quite well with experimental data.

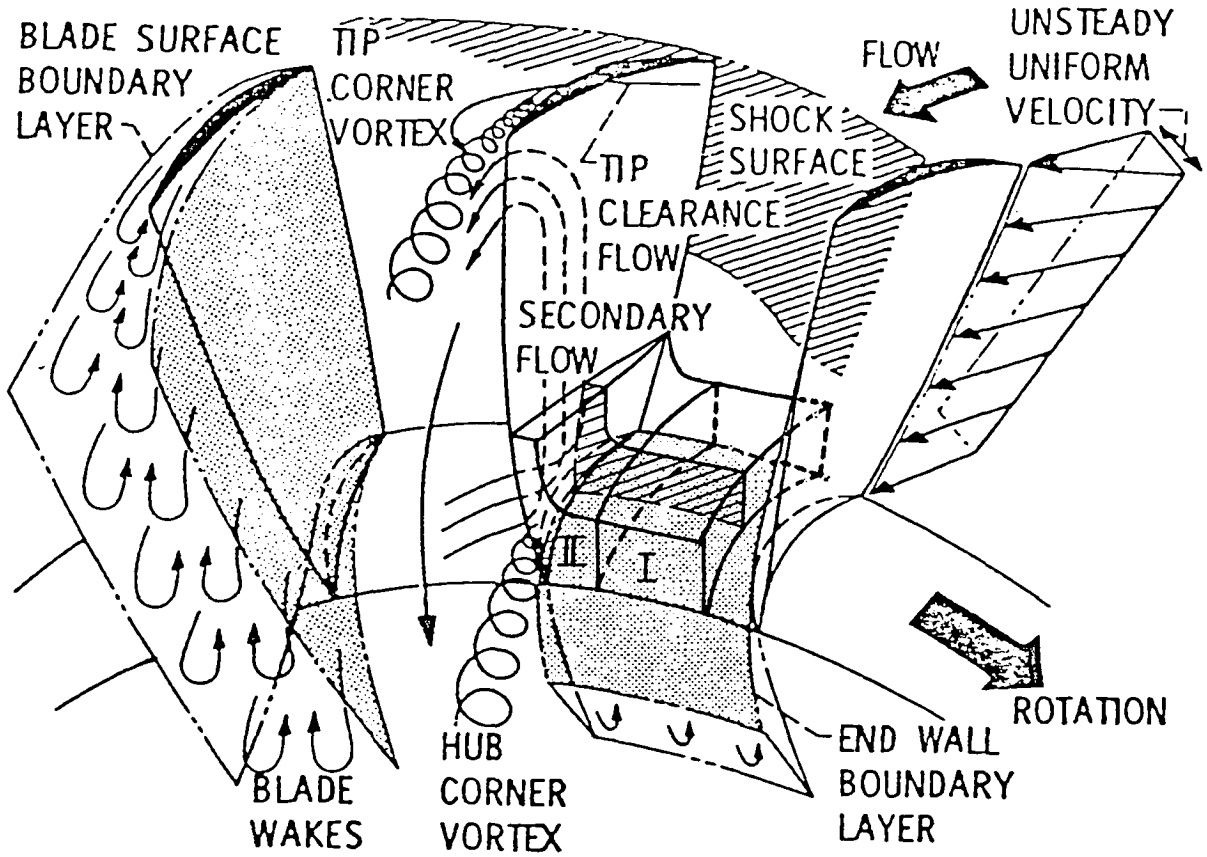

FIG. 1 SCHEMATIC OF FLOW-FIELD, SHOWING REGIONS TREATED BY PRESENT ANALYSIS

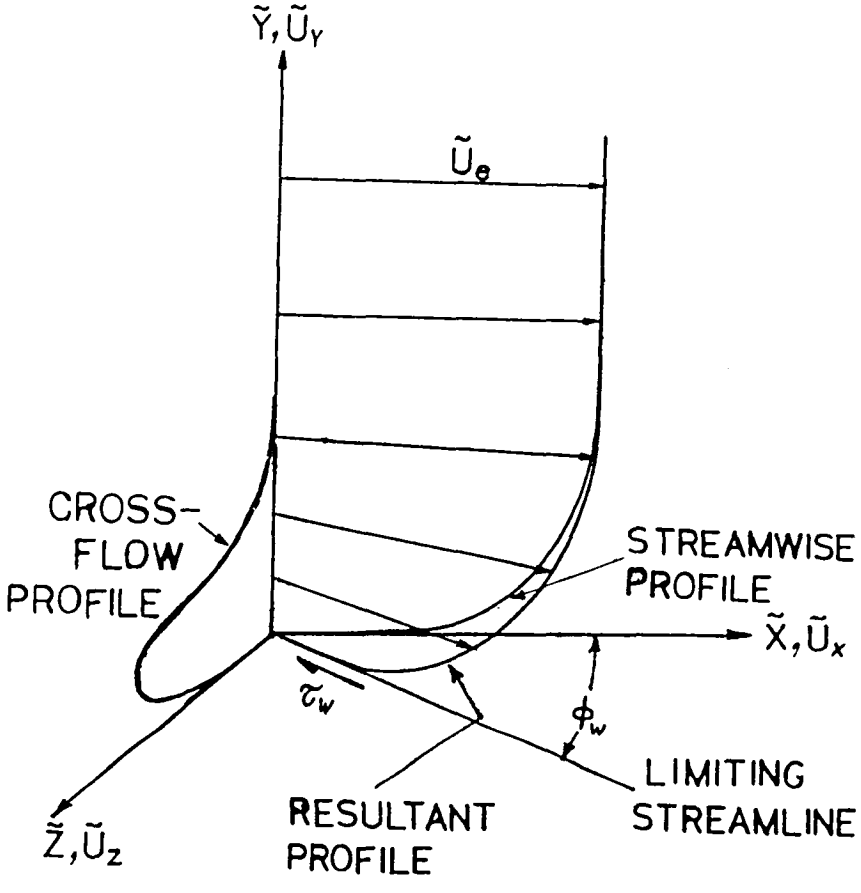

FIG. 2 SKEWED BOUNDARY LAYER AND BASIC TERMINOLOGY

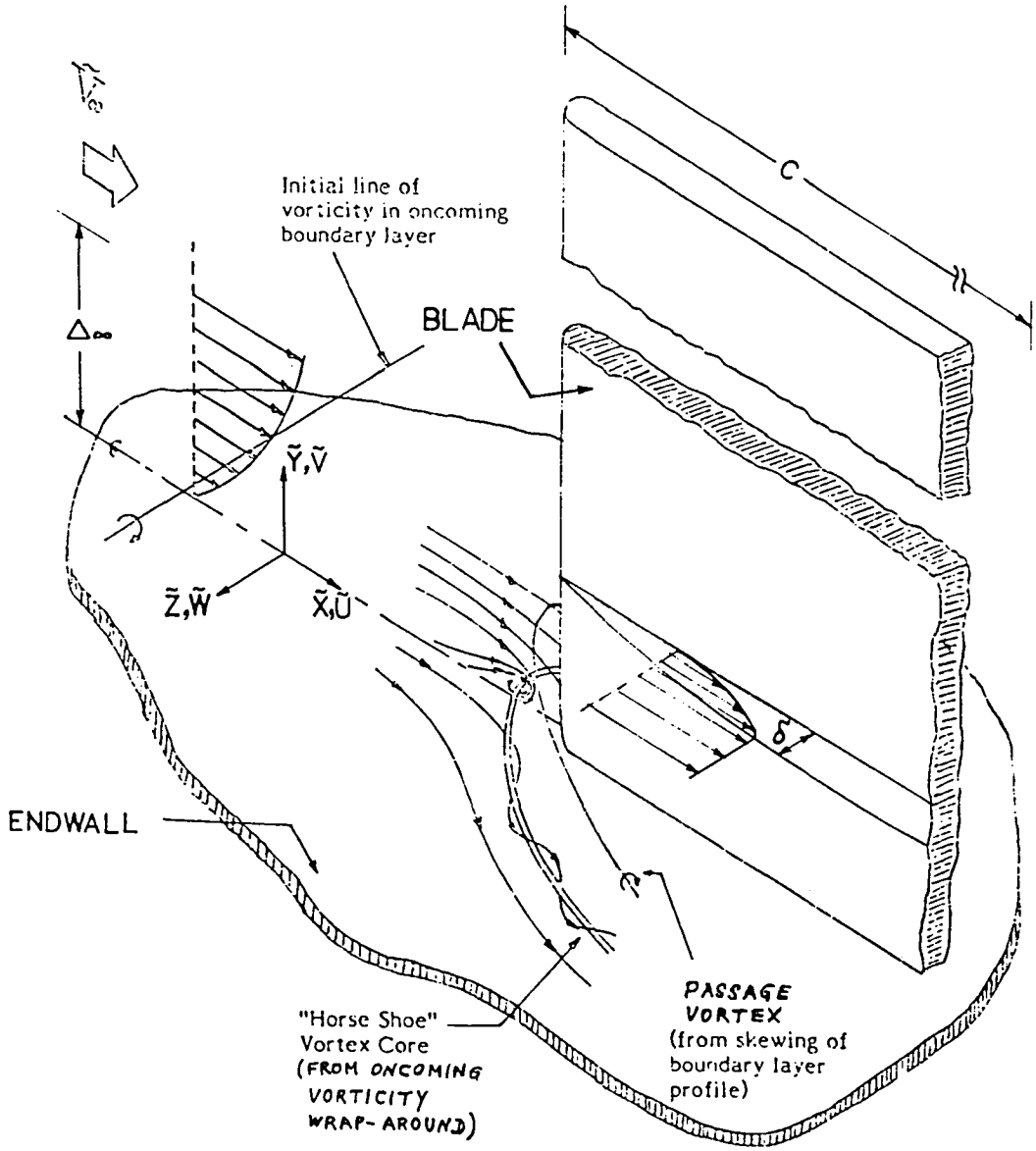

FIG. 3 SCHEMATIC OF THE FLOW IN A JUNCTURE[6]

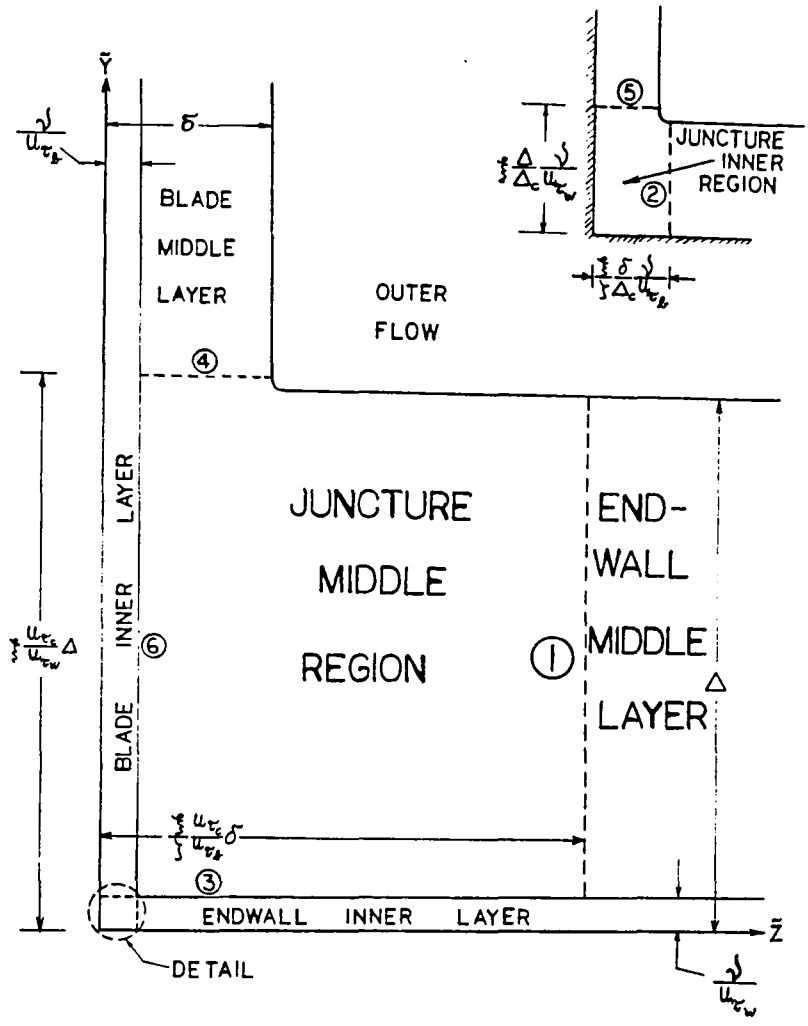

FIG. 4 ASYMPTOTIC SUB-REGIONS IN A TURBULENT JUNCTURE FLOW

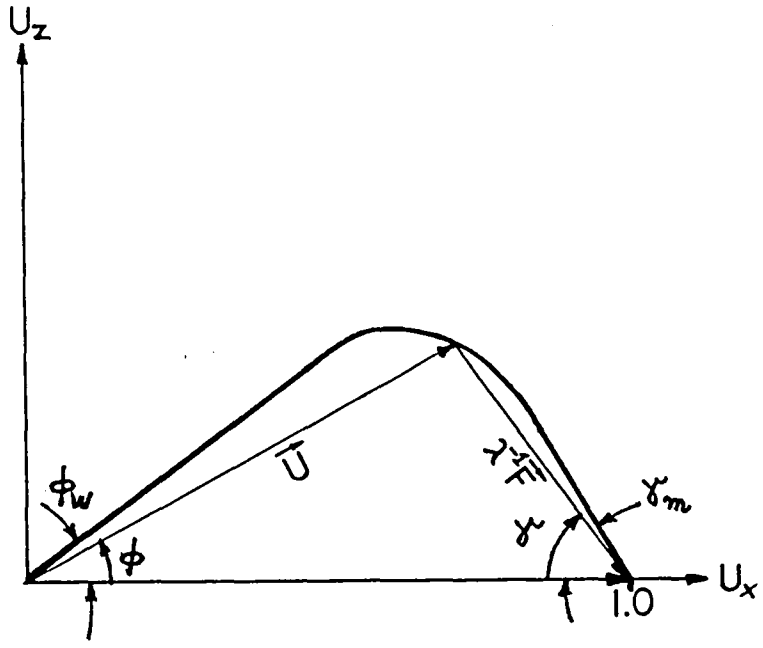

FIG. 5 HODOGRAPH WITH VECTOR TRIANGLE AND BASIC TERMINOLOGY

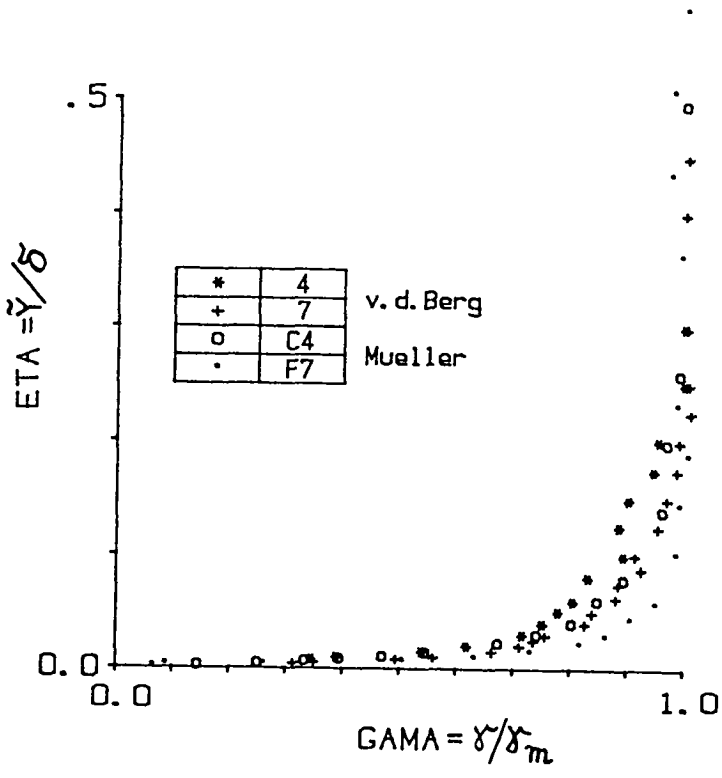

FIG. 6 TYPICAL EXPERIMENTAL DATA OF Γ VS. η FROM REFS. 8 AND 10

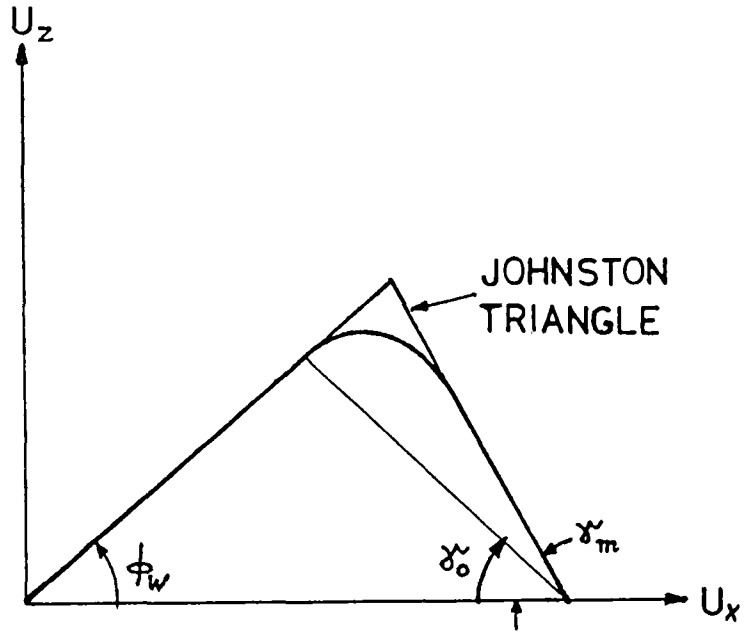

FIG. 7 HODOGRAPH WITH JOHNSTON'S TRIANGLE SUPERIMPOSED. ALSO INDICATES THE GEOMETRICAL SIGNIFICANCE OF γ_o

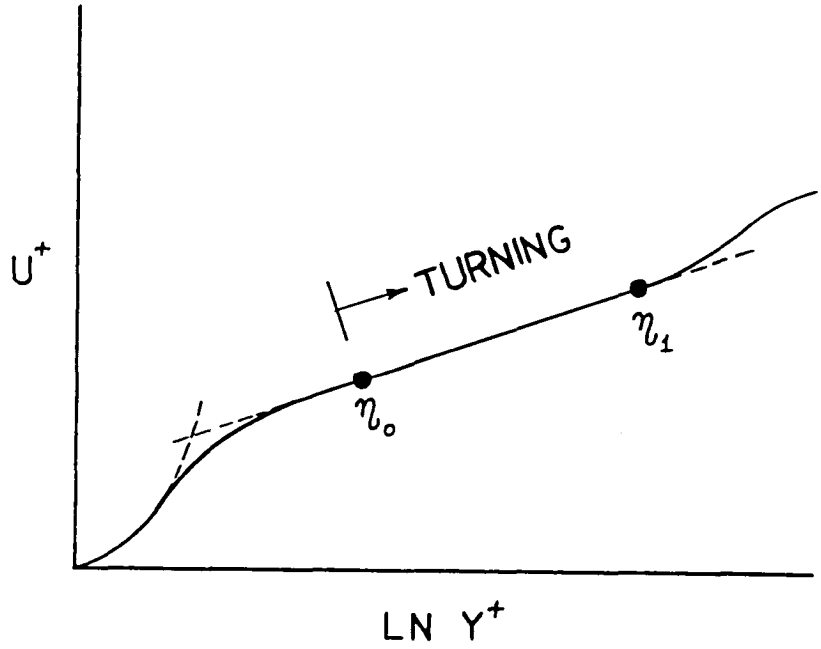

FIG.8 SCHEMATIC OF A VELOCITY PLOT, SHOWING THE RELATION OF η_1 TO η_o

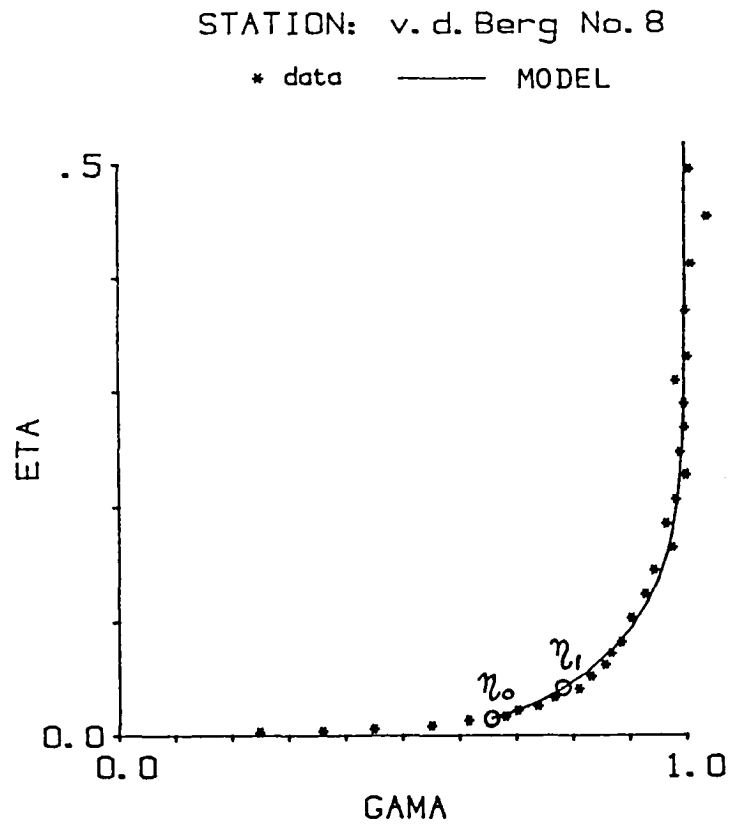

FIG. 9 COMPARISON BETWEEN THE MODEL FOR $\Gamma(\eta)$ AND EXPERIMENTAL DATA OF REF.8 , STATION No. 8. (THE FIVE LOWEST POINTS BELONG TO THE WALL SUB-LAYER)

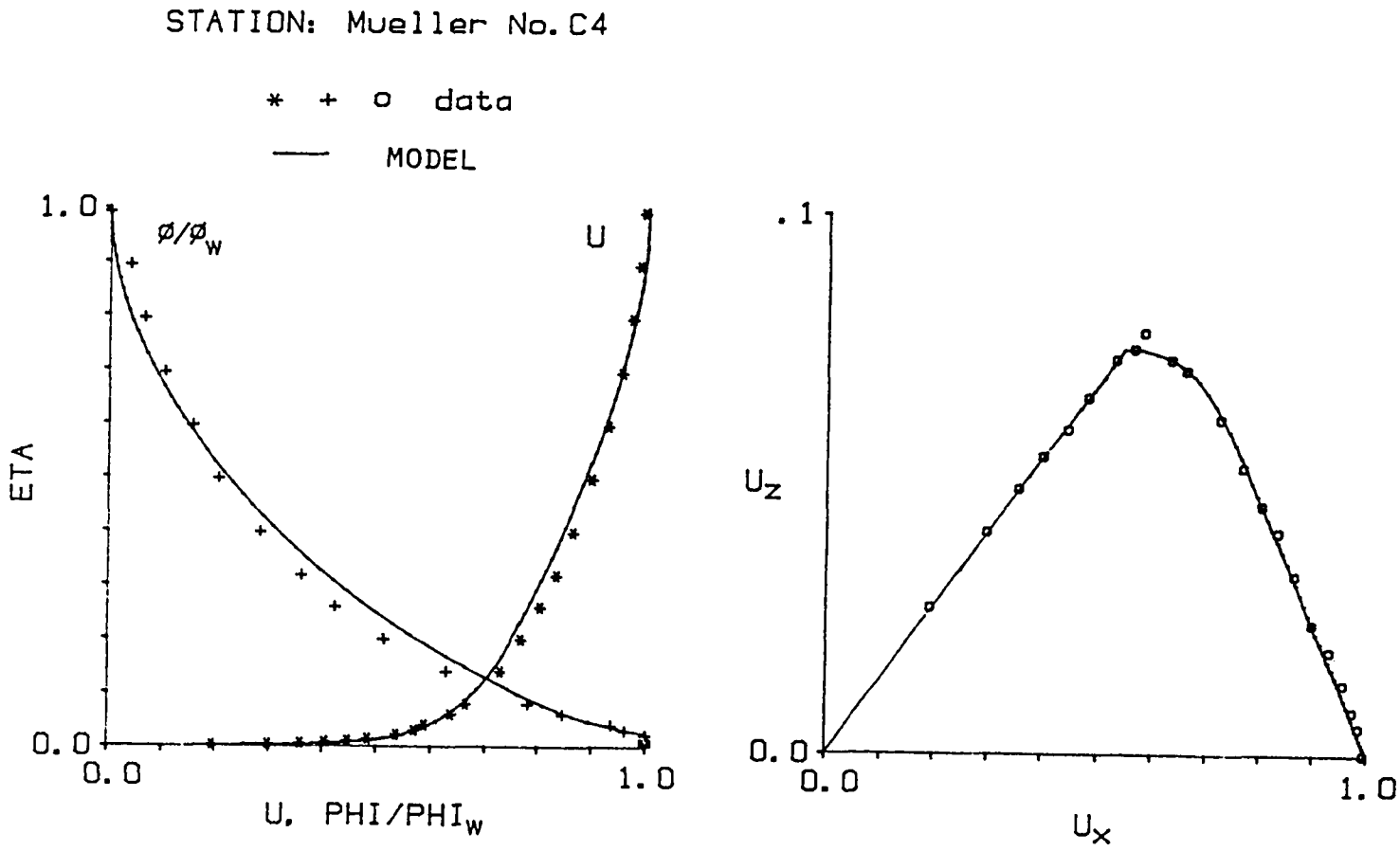

A

FIG. 10 COMPARISON BETWEEN MODEL AND EXPERIMENTAL DATA OF SELECTED MEASUREMENT STATIONS FROM REFS. 8 AND 10. (SHOWN ARE RESULTANT VELOCITY IN MAGNITUDE AND DIRECTION, AND THE VELOCITY HODOGRAPH)

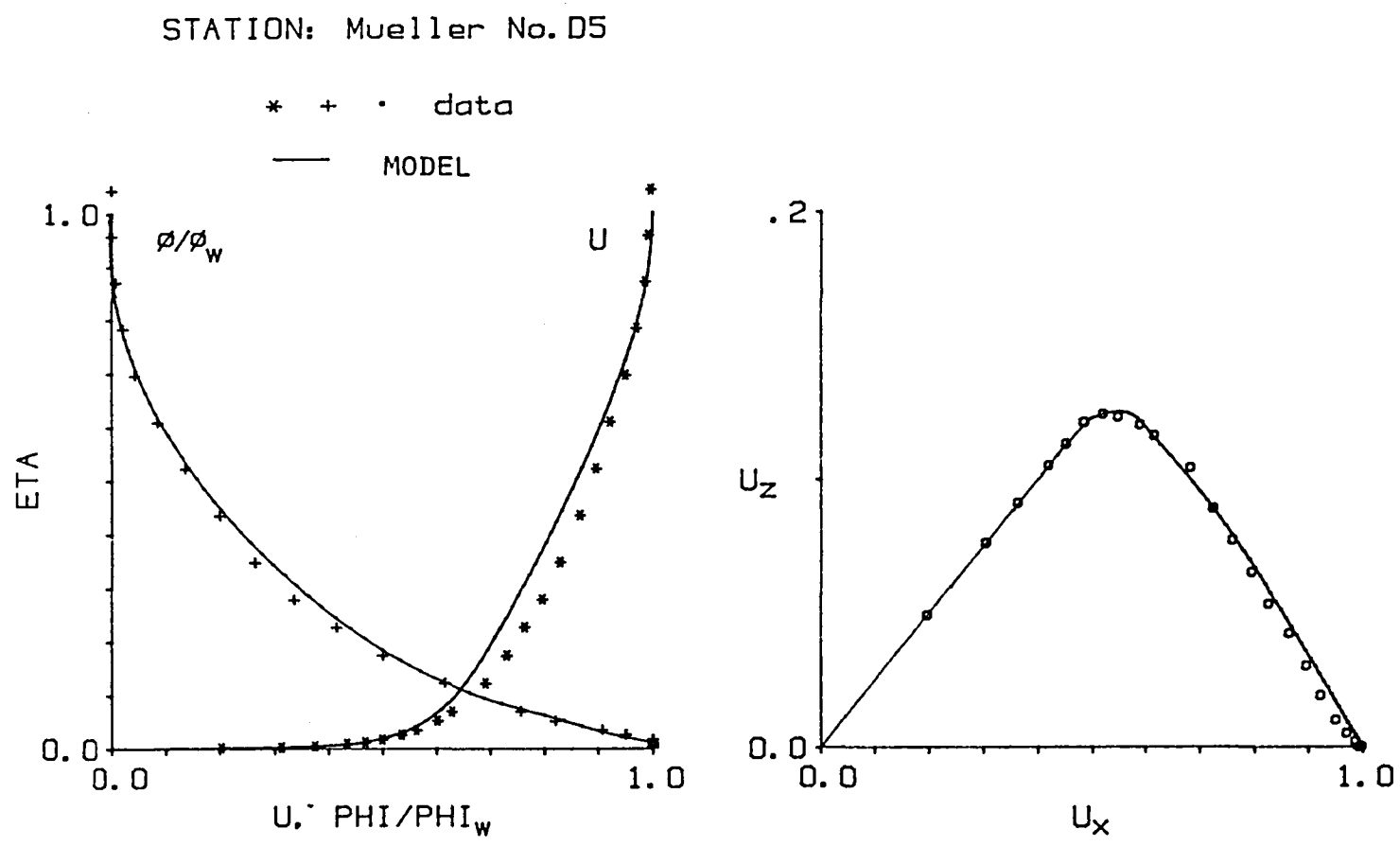
STATION: Mueller No. D5
* + · data
MODEL
1.0
ø/ø_w
U
ETA
0.0
0.0
1.0
U,˙ PHI/PHI_w
.2
U_Z
0.0
0.0
1.0
U_X

B

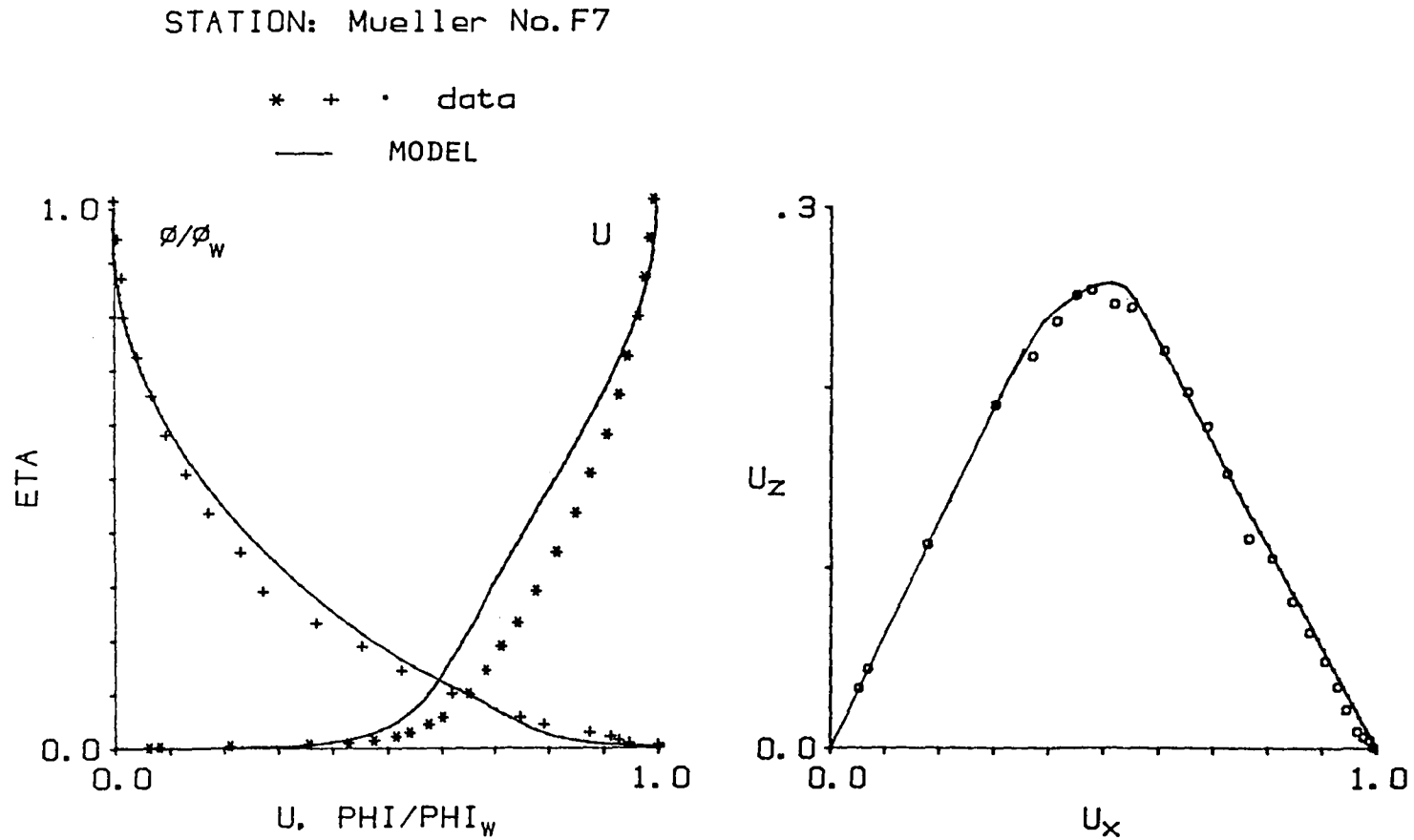
STATION: Mueller No. F7
* + · data
—— MODEL
1.0
ø/ø_w
U
ETA
0.0
0.0
1.0
U, PHI/PHI_w
.3
U_Z
0.0
0.0
1.0
U_X

c

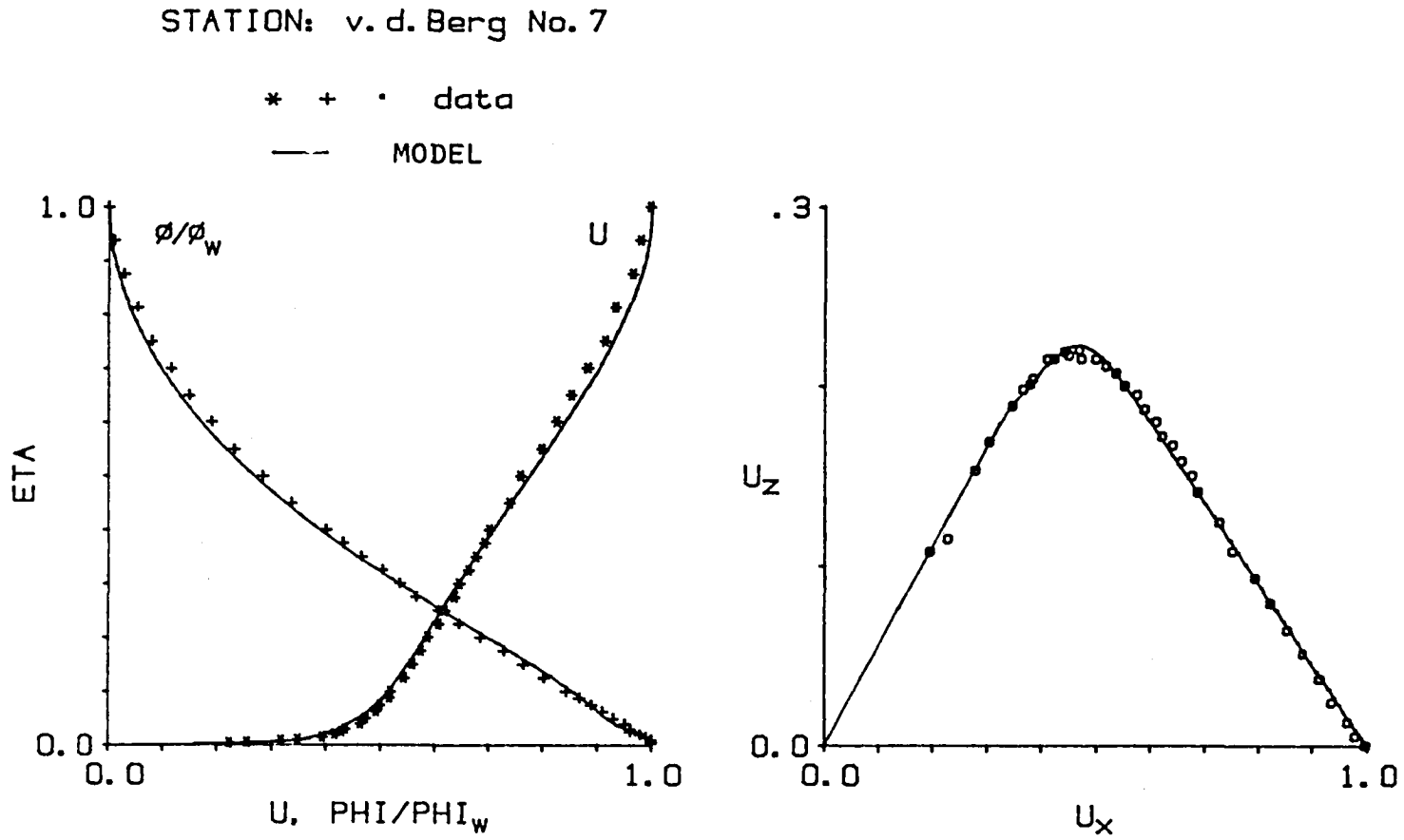
STATION: v. d. Berg No. 7
* + · data
—— MODEL
1.0
ø/ø_w
U
ETA
0.0
0.0
1.0
U, PHI/PHI_w
.3
U_Z
0.0
0.0
1.0
U_X

D

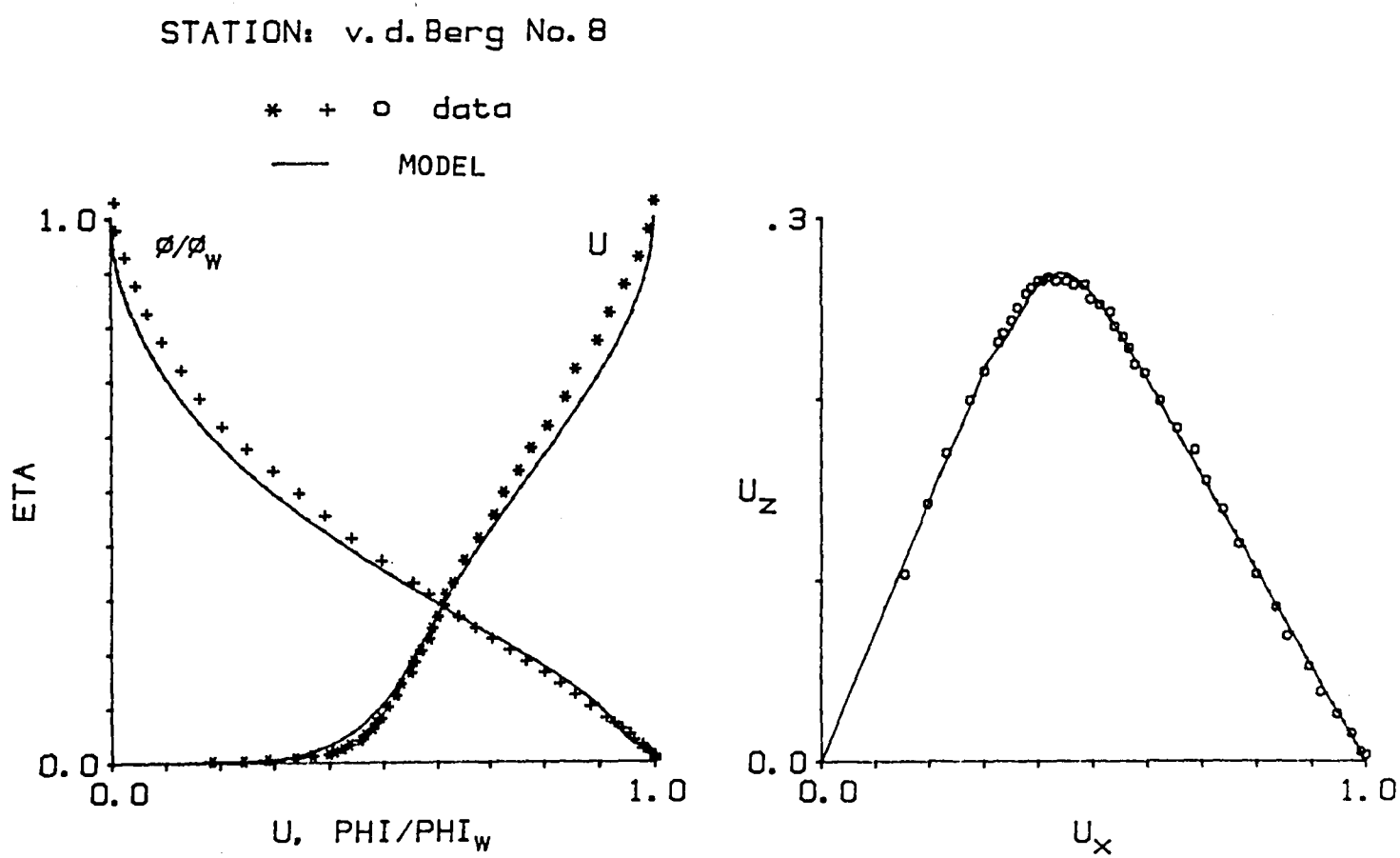
STATION: v. d. Berg No. 8
* + o data
MODEL
1.0
0.0
ETA
ø/ø_w
U
0.0
1.0
U, PHI/PHI_w
.3
0.0
U_Z
0.0
1.0
U_X

E

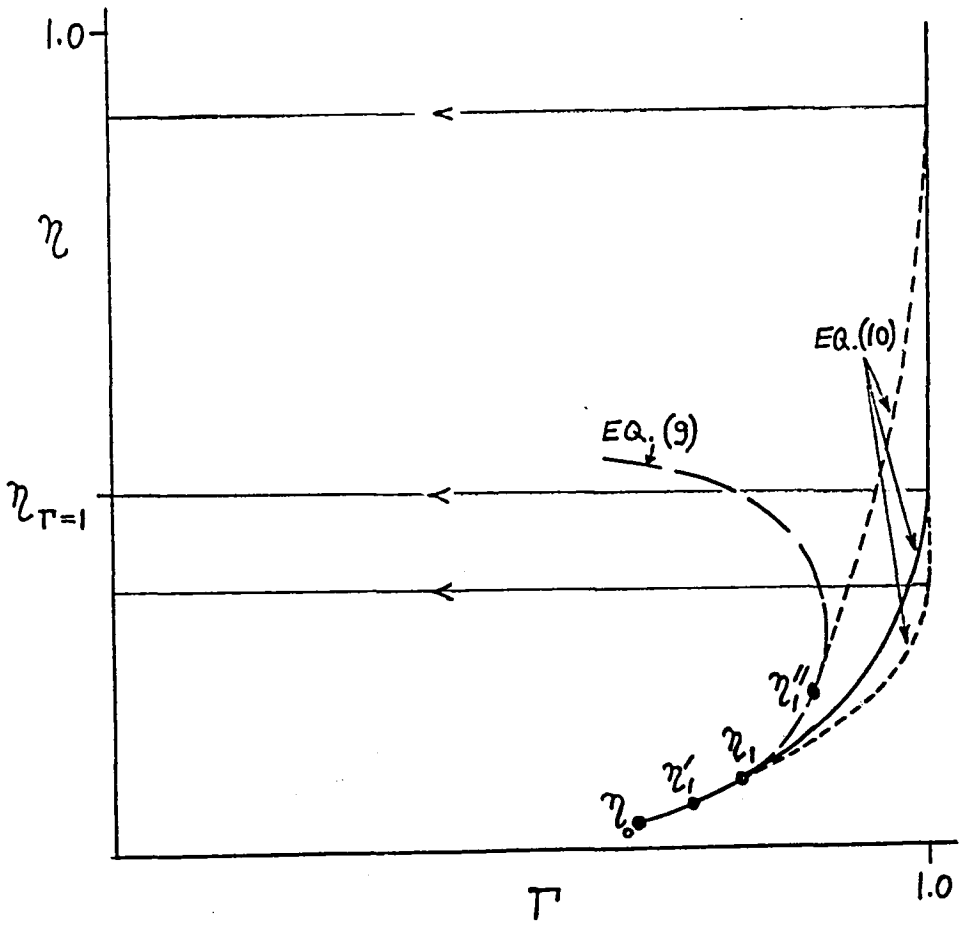

FIG. 11 DETERMINATION OF η_1

Table 1 - Momentum equation in the three sub-layers, to orders 1, ϵ, and ϵ^2.

	OUTER REGION	MIDDLE REGION	INNER REGION
O R D 1	Euler equations (No Reynolds stresses)	$p_1 =$ $P_1(X,0,Z)$ Euler equations	$\hat{p}_1 = P_1(X,0,Z)$ $\hat{u}_{x_1} = \hat{u}_{y_1} = \hat{u}_{z_1} = 0$
O R D ϵ	$U_{x_2} = U_{y_2} = U_{z_2} = 0$ $P_2 \equiv 0$	$p_2 = 0$ Boundary-Layer equations. Reynolds stresses only	$\hat{p}_2 = 0$ Constant total shear across sub-layer
O R D ϵ^2	Euler equations	Re-averaged Navier-Stokes equations for X- and Z-momenta Reynolds stresses only	$\hat{p}_3 = P_3(X,0,Z) + \hat{t}_{1_{yy}}$ Constant total shear across sub-layer

Table 2: Juncture equations for an arbitrary (non-zero) δ/Δ ratio. (See text for definitions of coordinates).

Middle region	Inner region
O(1)	
$\frac{\partial u_1}{\partial x} + \frac{\partial v_1}{\partial y} + \frac{\partial w_1}{\partial z} = 0$	$\frac{\partial \hat{v}_1}{\partial \hat{y}} + \frac{\partial \hat{w}_1}{\partial \hat{z}} = 0$
$u_1 \frac{\partial u_1}{\partial x} + v_1 \frac{\partial u_1}{\partial y} + w_1 \frac{\partial u_1}{\partial z} = -\frac{dP_1}{dx}(x,0,0)$	$\hat{p}_1 = P_1(x,0,0)$
$O(\epsilon)$	
$\frac{\partial u_2}{\partial x} + \frac{\partial v_2}{\partial y} + \frac{\partial w_2}{\partial z} = 0$	$\frac{\partial \hat{u}_2}{\partial x} + \frac{\partial \hat{v}_2}{\partial \hat{y}} + \frac{\partial \hat{w}_2}{\partial \hat{z}} = 0$
$\frac{\partial}{\partial x}(u_1 u_2) + v_1 \frac{\partial u_2}{\partial y} + v_2 \frac{\partial u_1}{\partial y} + w_1 \frac{\partial u_2}{\partial z} + w_2 \frac{\partial u_1}{\partial z} = \frac{\partial t_{1_{yx}}}{\partial y} + \frac{\partial t_{1_{zx}}}{\partial z}$	$0 = \frac{\partial}{\partial \hat{y}}\left[\frac{\partial \hat{u}_2}{\partial \hat{y}} + \hat{t}_{1_{yx}}\right] + \frac{\partial}{\partial \hat{z}}\left[\frac{\partial \hat{u}_2}{\partial \hat{z}} + \hat{t}_{1_{zx}}\right]$
$p_2 \equiv 0$	$\hat{p}_2 \equiv 0$

Middle Region	Inner Region
$O(\epsilon^2)$	
$\frac{\partial u_3}{\partial x} + \frac{\partial u_3}{\partial y} + \frac{\partial w_3}{\partial z} = 0$	$\frac{\partial \hat{u}_3}{\partial x} + \frac{\partial \hat{v}_3}{\partial \hat{y}} + \frac{\partial \hat{w}_3}{\partial \hat{z}} = 0$
$\frac{\partial}{\partial x}(u_1 u_3) + u_2 \frac{\partial u_2}{\partial x} +$	$0 = \frac{\partial}{\partial \hat{y}}\left[\frac{\partial \hat{u}_3}{\partial \hat{y}} + \hat{t}_{2_{yx}}\right] +$
$v_1 \frac{\partial u_3}{\partial y} + v_2 \frac{\partial u_2}{\partial y} +$	
$+ v_3 \frac{\partial u_1}{\partial y} + w_1 \frac{\partial u_3}{\partial z} +$	$\frac{\partial}{\partial \hat{z}}\left[\frac{\partial \hat{u}_3}{\partial \hat{z}} + \hat{t}_{2_{zx}}\right]$
$w_2 \frac{\partial u_2}{\partial z} + w_3 \frac{\partial u_1}{\partial z} =$	$0 =$
$-\frac{\partial p_3}{\partial x} +$	$-\frac{\partial \hat{p}_3}{\partial \hat{y}} + \frac{\partial \hat{t}_{1_{yy}}}{\partial \hat{y}} + \frac{\partial \hat{t}_{1_{zy}}}{\partial \hat{z}}$
$+ \frac{\partial t_{1_{xx}}}{\partial x} + \frac{\partial t_{2_{yx}}}{\partial y} + \frac{\partial t_{2_{zx}}}{\partial z}$	
$u_1 \frac{\partial v_1}{\partial x} + v_1 \frac{\partial v_1}{\partial y} + w_1 \frac{\partial v_1}{\partial z} =$	$0 =$
$-\frac{\partial p_3}{\partial y} + \frac{\partial t_{1_{yy}}}{\partial y} + \frac{\partial t_{1_{zy}}}{\partial z}$	$-\frac{\partial \hat{p}_3}{\partial \hat{z}} + \frac{\partial \hat{t}_{1_{yz}}}{\partial \hat{y}} + \frac{\partial \hat{t}_{1_{zz}}}{\partial \hat{z}}$
$u_1 \frac{\partial w_1}{\partial x} + v_1 \frac{\partial w_1}{\partial y} + w_1 \frac{\partial w_1}{\partial z} =$	
$-\frac{\partial p_3}{\partial z} + \frac{\partial t_{1_{yz}}}{\partial y} + \frac{\partial t_{1_{zz}}}{\partial z}$	

REFERENCES

1. Coles, D.E., "The Law of the Wake in the Turbulent Boundary Layer", JFM vol. 1, pt. 2, 1956, pp. 191-226.

2. Johnston, J.P., "On the Three-Dimensional Turbulent Boundary Layer Generated by Secondary Flow", J. Basic Eng., March 1960, pp. 233-248.

3. "Aerodynamics Design of Axial-Flow Compressors", NASA SP-36, 1965, pp. 385-410.

4. Salvage, J.W., "A Review of the Current Concept of Cascade Secondary Flow Effects", von Karman Institute for Fluid Dynamics, TN 95, 3/1974.

5. Shabaka, I.M.M.A., "Turbulent Flow in a Simulated Wing-Body Junction", Ph.D. Thesis, Aeronautics Department, Imperial College, London 1979.

6. McMahon, H., Hubbartt, J., and Kubendan, L., "Measurements of Mean Velocities and Reynolds Stresses in a Juncture Flow", In Theoretical Aerodynamics Contractor/Grantee Review, NASA-Langley Research Center, September 1981, pp. 98-119.

7. Mellor, G.L., "The Large Reynolds Number, Asymptotic Theory of Turbulent Boundary Layers", Int. J. Eng. Sci., vol. 10, 1972, pp. 851-873.

8. Berg, B. van den and Elsenaar, A., 1972 NLR Tech. Rep. No. 72092 U.

9. Berg, B. van den, Elsenaar, A., Lindhout, J.P.F., and Wesseling, P., "Measurements in an Incompressible Three-Dimensional Turbulent Boundary Layer, under Infinite Swept-Wing Conditions, and Comparison with Theory", JFM vol. 70, pt. 1, 1975, pp. 127-148.

10. Mueller, U.R., "Mean Velocities and Reynolds Stresses Measured in a Three-Dimensional Boundary Layer", In proc. Viscous and Interacting Flow Field Effects, 5th U.S. Air Force and the Federal Republic of Germany Data Exchange Agreement Meeting, AFFDL Tech. Rep. No. 80-3088, p. 359, 1980.

11. Mueller, U.R., "Measurement of the Reynolds Stresses and the Mean flow Field in a Three-Dimensional Pressure-Driven Boundary Layer", JFM vol. 119, pp. 121-153, 1982.

12. Musker, A.J., "Explicit Expression for the Smooth Wall Velocity Distribution in a Turbulent Boundary Layer", AIAA Journal, vol. 17, June 1979.

13. Dowell, M., and Jarratt, P., "The 'Pegasus' Method for Computing the Root of an Equation", BIT vol. 12, 1972, pp. 503-508.

14. Mager, A., "Generalization of Boundary-Layer Momentum-Integral Equations to Three-Dimensional Flows Including those of Rotating System", NACA Rep. 1067, 1952.

15. Rubin, S.G., "Incompressible Flow Along a Corner", JFM 26, pt. 1, September 1966, pp. 97-110.

16. Rubin, S.G., private communication.

Appendix A: Preliminary form of the equations of motion in the various layers to orders 1, ϵ and ϵ^2

After substituting the asymptotic expansions for the three layers into Eqns. (1) and (2) and collecting terms of the same order, the following equations are obtained:

1. Outer layer

O(1)

$$\frac{\partial U_1}{\partial x} + \frac{\partial V_1}{\partial Y} + \frac{\partial W_1}{\partial Z} = 0$$

$$\left[U_1 \frac{\partial}{\partial x} + V_1 \frac{\partial}{\partial Y} + W_1 \frac{\partial}{\partial Z}\right] \left\{U_1, V_1, W_1\right\}^T =$$

$$- \left\{\frac{\partial}{\partial x}, \frac{\partial}{\partial Y}, \frac{\partial}{\partial Z}\right\}^T \left[P_1\right] \qquad \text{(A1)}$$

O(ϵ)

$$\frac{\partial U_2}{\partial x} + \frac{\partial V_2}{\partial Y} + \frac{\partial W_2}{\partial Z} = 0$$

$$\left[U_1 \frac{\partial}{\partial x} + V_1 \frac{\partial}{\partial Y} + W_1 \frac{\partial}{\partial Z}\right] \left\{U_2, V_2, W_2\right\}^T +$$

$$\left[U_2 \frac{\partial}{\partial x} + V_2 \frac{\partial}{\partial Y} + W_2 \frac{\partial}{\partial Z}\right] \left\{U_1 \cdot V_2 \cdot W_1\right\}^T =$$

$$= - \left\{\frac{\partial}{\partial x} \cdot \frac{\partial}{\partial Y} \cdot \frac{\partial}{\partial Z}\right\}^T [P_2] \qquad \text{(A2)}$$

$O(\epsilon^2)$

$$\frac{\partial U_3}{\partial x} + \frac{\partial V_3}{\partial Y} + \frac{\partial W_3}{\partial Z} = 0$$

$$\left[U_1 \frac{\partial}{\partial x} + V_1 \frac{\partial}{\partial Y} + W_1 \frac{\partial}{\partial Z}\right] \left\{U_3 \cdot V_3 \cdot W_3\right\}^T +$$

$$\left[U_2 \frac{\partial}{\partial x} + V_2 \frac{\partial}{\partial Y} + W_2 \frac{\partial}{\partial Z}\right] \left\{U_2 \cdot V_2 \cdot W_2\right\}^T +$$

$$\left[U_3 \frac{\partial}{\partial x} + V_3 \frac{\partial}{\partial Y} + W_3 \frac{\partial}{\partial Z}\right] \left\{U_1 \cdot V_1 \cdot W_1\right\}^T =$$

$$- \left\{\frac{\partial}{\partial x} \cdot \frac{\partial}{\partial Y} \cdot \frac{\partial}{\partial Z}\right\}^T [P_3] \qquad \text{(A3)}$$

2. Middle layer

$O(1)$

$$\frac{\partial u_1}{\partial x} + \frac{\partial v_1}{\partial y} + \frac{\partial w_1}{\partial Z} = 0$$

$$u_1 \frac{\partial u_1}{\partial x} + v_1 \frac{\partial u_1}{\partial y} + w_1 \frac{\partial u_1}{\partial Z} = - \frac{\partial p_1}{\partial x}$$

$$0 = \frac{\partial p_1}{\partial y}$$

$$u_1 \frac{\partial w_1}{\partial x} + v_1 \frac{\partial w_1}{\partial y} + w_1 \frac{\partial w_1}{\partial Z} = - \frac{\partial p_1}{\partial Z} \qquad \text{(A4)}$$

$O(\epsilon)$

$$\frac{\partial u_2}{\partial x} + \frac{\partial v_2}{\partial y} + \frac{\partial w_2}{\partial Z} = 0$$

$$\frac{\partial}{\partial x} \left[u_1 \; u_2 \right] + v_1 \frac{\partial u_2}{\partial y} + v_2 \frac{\partial u_1}{\partial y} + w_1 \frac{\partial u_2}{\partial Z} + w_2 \frac{\partial u_1}{\partial Z} =$$

$$- \frac{\partial p_2}{\partial x} + \frac{\partial t_{1xy}}{\partial y}$$

$$0 = \frac{\partial p_2}{\partial y}$$

$$u_1 \frac{\partial w_2}{\partial x} + u_2 \frac{\partial w_1}{\partial x} + v_1 \frac{\partial w_2}{\partial y} + v_2 \frac{\partial w_1}{\partial y} + \frac{\partial}{\partial Z} \left[w_1 w_2 \right]$$

$$= - \frac{\partial p_2}{\partial Z} + \frac{\partial t_{1_{yz}}}{\partial y} \qquad \text{(A5)}$$

$O(\epsilon^2)$

$$\frac{\partial u_3}{\partial x} + \frac{\partial v_3}{\partial y} + \frac{\partial w_3}{\partial Z} = 0$$

$$\frac{\partial}{\partial x}\left[u_1 u_3\right] + u_2 \frac{\partial u_2}{\partial x} + v_1 \frac{\partial u_3}{\partial y} + v_2 \frac{\partial u_2}{\partial y} + v_3 \frac{\partial u_1}{\partial y} + w_1 \frac{\partial u_3}{\partial z} +$$

$$w_2 \frac{\partial u_2}{\partial z} + w_3 \frac{\partial u_1}{\partial z} =$$

$$-\frac{\partial p_3}{\partial x} + \frac{\partial t_{1xx}}{\partial x} + \frac{\partial t_{2yx}}{\partial y} + \frac{\partial t_{1xz}}{\partial z}$$

$$u_1 \frac{\partial v_1}{\partial x} + v_1 \frac{\partial v_1}{\partial y} + w_1 \frac{\partial v_1}{\partial z} = -\frac{\partial p_3}{\partial y} + \frac{\partial t_{1yy}}{\partial y}$$

$$u_1 \frac{\partial w_3}{\partial x} + u_2 \frac{\partial w_2}{\partial x} + u_3 \frac{\partial w_1}{\partial x} + v_1 \frac{\partial w_3}{\partial y} + v_2 \frac{\partial w_2}{\partial y} +$$

$$v_3 \frac{\partial w_1}{\partial y} + \frac{\partial}{\partial z}\left[w_1 w_3\right] + w_2 \frac{\partial w_2}{\partial z} =$$

$$-\frac{\partial p_3}{\partial z} + \frac{\partial t_{1xz}}{\partial x} + \frac{\partial t_{2yz}}{\partial y} + \frac{\partial t_{1zz}}{\partial z} \qquad \text{(A6)}$$

3. Inner layer

O(1)

$$\frac{\partial \hat{u}_1}{\partial x} + \frac{\partial \hat{v}_1}{\partial \hat{y}} + \frac{\partial \hat{w}_1}{\partial z} = 0$$

$$0 = \frac{\partial^2 \hat{u}_1}{\partial \hat{y}^2}$$

$$0 = \frac{\partial \hat{p}_1}{\partial \hat{y}}$$

$$0 = \frac{\partial^2 \hat{w}_1}{\partial \hat{y}^2} \qquad \text{(A7)}$$

$O(\epsilon)$

$$\frac{\partial \hat{u}_2}{\partial x} + \frac{\partial \hat{v}_2}{\partial \hat{y}} + \frac{\partial \hat{w}_2}{\partial Z} = 0$$

$$0 = \frac{\partial}{\partial \hat{y}} \left[\hat{t}_{1_{xy}} + \frac{\partial \hat{u}_2}{\partial \hat{y}} \right]$$

$$0 = \frac{\partial \hat{p}_2}{\partial \hat{y}}$$

$$0 = \frac{\partial}{\partial \hat{y}} \left[\hat{t}_{1_{yz}} + \frac{\partial \hat{w}_2}{\partial \hat{y}} \right] \qquad \text{(A8)}$$

$O(\epsilon^2)$

$$\frac{\partial \hat{u}_3}{\partial x} + \frac{\partial \hat{v}_3}{\partial \hat{y}} + \frac{\partial \hat{w}_3}{\partial Z} = 0$$

$$0 = \frac{\partial}{\partial \hat{y}} \left[\hat{t}_{2_{xy}} + \frac{\partial \hat{u}_3}{\partial \hat{y}} \right]$$

$$0 = \frac{\partial}{\partial \hat{y}} \left[-\hat{p}_3 + \hat{t}_{1_{yy}} \right]$$

$$0 = \frac{\partial}{\partial \hat{y}} \left[\hat{t}_{2_{yz}} + \frac{\partial \hat{w}_3}{\partial \hat{y}} \right] \qquad \text{(A9)}$$

Appendix B: Matching procedure

1. Formal matching of outer and middle layers

U(x,Y,Z) is expanded by a Taylor series around Y = 0:

$$U(x,Y,Z) = U_1\ (x,0,Z) = \epsilon\ y\ \frac{\partial U_1}{\partial Y}\ (x,0,Z) + \epsilon^2\ \frac{y^2}{2}\ \frac{\partial^2 U_1}{\partial Y^2}\ (x,0,Z)$$

$$+\ \ldots + \epsilon\ U_2\ (x,0,Z) + \epsilon^2\ y\ \frac{\partial U_2}{\partial Y}\ (x,0,Z) + \ldots +$$

$$\epsilon^2\ U_3\ (x,0,Z) + \ldots =$$

$$= u_1\ (x,y,Z) + \epsilon\ u_2\ (x,y,Z) + \epsilon^2\ u_3\ (x,y,Z) + \ldots;\ y \to \infty$$

Thus

$$u_1\ (x,y,Z) \sim U_1(x,0,Z):\ y \to \infty \qquad \text{(B1)}$$

$$u_2\ (x,y,Z) \sim y\ \frac{\partial U_1}{\partial Y}\ (x,0,Z) + U_2\ (x,0,Z):\ y \to \infty$$

$$u_3\ (x,y,Z) \sim \frac{y^2}{2}\ \frac{\partial^2 U_1}{\partial Y^2}\ (x,0,Z) + y\ \frac{\partial U_2}{\partial Y}\ (x,0,Z) +$$

$$U_3\ (x,0,Z):\ y \to \infty$$

$$\vdots$$

and similar relationships hold for the crossflow component, w.

Following the same procedure as above, yields:

$$V_1(x,0,Z) = 0 \tag{B2}$$

$$V_2(x,0,Z) = \lim_{y \to \infty} \left[v_1(x,y,Z) - y \frac{\partial V_1}{\partial Y}(x,0,Z) \right] \tag{B3}$$

$$V_3(x,0,Z) = \lim_{y \to \infty} \left[v_2(x,y,Z) - y \frac{\partial V_2}{\partial Y}(x,0,Z) - \frac{y^2}{2} \frac{\partial^2 V_1}{\partial Y^2}(x,0,Z) \right]$$

$$\vdots$$

$$p_1(x,Z) = P_1(x,0,Z) \quad (\textit{since } \partial p_1/\partial y = 0) \tag{B4}$$

$$p_2(x,Z) \sim y \frac{\partial P_1}{\partial Y}(x,0,Z) + P_2(x,0,Z): \; y \to \infty \tag{B5}$$

$$p_3(x,y,Z) \sim \frac{y^2}{2} \frac{\partial^2 P_1}{\partial Y^2}(x,0,Z) + y \frac{\partial P_2}{\partial Y}(x,0,Z) + P_3(x,0,Z): \; y \to \infty$$

$$\vdots$$

$$t_{n_{ij}}(x,y,Z) \sim 0: \; y \to \infty, \text{ for } n = 1,2,3,\cdots$$

(since no freestream turbulence was assumed to exist)

2. Formal matching of middle and inner layers

Again, variables are expanded in Taylor series around y = 0:

$$V(x,y,Z) = \epsilon v_1(x,0,Z) + \epsilon \hat{\epsilon} \hat{y} \frac{\partial v_1}{\partial y}(x,0,Z) + \ldots +$$

$$\epsilon^2 v_2 (x,0,Z) +$$

$$+ \epsilon^2 \hat{\epsilon} \hat{y} \frac{\partial v_2}{\partial y} (x,0,Z) + \ldots + \epsilon^3 v_3 (x,0,Z) +$$

$$\epsilon^3 \hat{\epsilon} \hat{y} \frac{\partial v_3}{\partial y} (x,0,Z) + \ldots =$$

$$= \epsilon \hat{\epsilon} \hat{v}_1 (x, \hat{y}, Z) +$$

$$\epsilon^2 \hat{\epsilon} \hat{v}_2 (x, \hat{y}, Z) + \epsilon^3 \hat{\epsilon} \hat{v}_3 (x, \hat{y}, z) + \ldots ;$$

$$\hat{y} \to \infty$$

Hence

$$v_1 (x,0,Z) = v_2 (x,0,Z) = v_3 (x,0,Z) = \cdots = 0 \quad \text{(B6)}$$

$$\hat{v}_l (x,\hat{y},Z) \sim \hat{y} \frac{\partial v_l}{\partial y} (x,0,Z); \ \hat{y} \to \infty, \ l = 1,2,3,\cdots$$

$$P = p_1(x,Z) + \epsilon p_2 (x,Z) + \epsilon^2 p_3(x,0,Z) + \epsilon^2\hat{\epsilon} \frac{\partial p_3}{\partial y} (x,0,Z) + \cdots =$$

$$= \hat{p}_1 (x,Z) + \epsilon \hat{p}_2 (x,Z) + \epsilon^2 p_3 (x,\hat{y},Z) + \cdots$$

Thus

$$\hat{p}_1(x,Z) = p_1 (x,Z) = P_1 (x,0,Z)$$

$$\hat{p}_2 (x,Z) = p_2 (x,Z) \quad \text{(B7)}$$

$$\hat{p}_3 \ (x,\hat{y},Z) \sim p_3 \ (x,0,Z); \hat{y} \to \infty$$

$$\vdots$$

and similarly

$$\hat{t}_{n_{ij}} \ (x,\hat{y},Z) \sim t_{n_{ij}} \ (x,0,Z); \ \hat{y} \to \infty, \ n = 1,2,3,\cdots$$

The U and W components require a special treatment.

$$U \ (x,y,Z) = u_1 \ (x,0,Z) + \hat{\epsilon} \ \hat{y} \ \frac{\partial u_1}{\partial y} \ (x,0,Z) + \cdots +$$

$$\epsilon \ u_2 \ (x,0,Z) + \cdots +$$

$$+ \epsilon^2 \ u_3 \ (x,0,Z) + \cdots = \hat{u}_1 \ (x,\hat{y},Z) + \epsilon \ \hat{u}_2 \ (x,\hat{y},Z) +$$

$$\epsilon^2 \ \hat{u}_3 \ (x,\hat{y},Z) + \cdots; \ \hat{y} \to \infty \qquad \text{(B8)}$$

From Eqn. (A7) and the boundary condition $\hat{u}_1 \ (x,0,Z) = 0$, it follows that $\hat{u}_1$ must be of the form

$$\hat{u}_1 \ (x,\hat{y},Z) = f(x,Z)\hat{y}$$

which is unbounded as $\hat{y} \to \infty$. Thus the first order terms in Eqn. (B8) cannot be matched directly. Therefore Eqn. (B8) is differentiated w.r.t. y, yielding:

$$\frac{1}{\hat{\epsilon}}\left[f(x,Z) + \epsilon\frac{\partial\hat{u}_2}{\partial\hat{y}}(x,\hat{y},Z) + \epsilon^2\frac{\partial\hat{u}_3}{\partial\hat{y}}(x,\hat{y},Z) + \cdots\right]_{\hat{y}\to\infty} =$$

$$= \frac{\partial u_1}{\partial y}(x,0,Z) + \epsilon\frac{\partial u_2}{\partial y}(x,0,Z) + \epsilon^2\frac{\partial u_3}{\partial y}(x,0,Z) + \cdots \quad (B9)$$

Since the leading term in the inner expansion is of $0\left[\hat{\epsilon}^{-1}\right]$ and that in the middle expansion is of $0(1)$, the only possibility for a match is that both vanish identically. A similar argument holds for the W-component. Thus

$$\hat{u}_1 = \hat{w}_1 \equiv 0,$$

and from the continuity Eq. and B.C. $\hat{v}_1 = 0$ @ $\hat{y} = 0$ it also follows that $\hat{v}_1 \equiv 0$. Also

$$\frac{\partial}{\partial y}\begin{Bmatrix} u_1 \\ w_1 \end{Bmatrix}_{(x,0,Z)} = 0$$

and this combined with the B.C. $\begin{Bmatrix} U \\ W \end{Bmatrix}_{\hat{y}=0} = 0$ uniquely determines u_1 and w_1 at y = 0:

$$\begin{Bmatrix} u_1 \\ w_1 \end{Bmatrix}_{y=0} = \begin{Bmatrix} \cos\phi_w \\ \sin\phi_w \end{Bmatrix} \textit{ at a given } (x,Z) \textit{ location.}$$

Since $\hat{y} = y/\hat{\epsilon}$, the only possibility for a match in the remaining part of Eqn. (B9) is

$$\begin{cases} \partial u_2/\partial y \sim b_2/y,\ \partial u_3/\partial y \sim b_3/y, \cdots;\ y \to 0 \\ \partial \hat{u}_2/\partial \hat{y} \sim b_2/\hat{y},\ \partial \hat{u}_3/\partial \hat{y} \sim b_3/\hat{y},\ \cdots;\ \hat{y} \to \infty \end{cases}$$

which, after integrating gives

$$u_2 \sim b_2 \ln y + C_2,\ u_3 \sim b_3 \ln y + C_3, \cdots;\ y \to 0 \quad \text{(B10)}$$

$$\hat{u}_2 \sim b_2 \ln \hat{y} + \hat{C}_2, \hat{u}_3 \sim b_3 \ln \hat{y} + \hat{C}_3, \cdots;\ \hat{y} \to \infty \quad \text{(B11)}$$

where the b's and C's are functions of x and Z. Similar expressions hold for the w and $\hat{w}$ components. This establishes the existence of a logarithmic overlap between the inner and middle layers. Inserting these results into (B8) yields

$$\left[\epsilon b_2 + \epsilon^2 b_3 + \cdots\right] \ln \hat{y} = u_1\ (x, 0, Z) + \left[\epsilon b_2 + \epsilon^2 b_3 + \cdots\right] \ln y +$$

$$+ \epsilon \left[C_2 - \hat{C}_2\right] + \epsilon^2 \left[C_3 - \hat{C}_3\right] + \cdots$$

or

$$\left[\epsilon b_2 + \epsilon^2 b_3 + \cdots\right] \ln \frac{1}{\hat{\epsilon}} = u_1\ (x, 0, Z) + \epsilon \left[C_2 - \hat{C}_2\right] + \epsilon^2 \left[C_3 - \hat{C}_3\right] + \cdots$$

whence it follows that

$$-\epsilon \ln \hat{\epsilon} = O(1) \to \hat{\epsilon} = O\left[e^{-1/\epsilon}\right] \text{ as } \epsilon \to 0$$

This confirms the assumption that $\hat{\epsilon} = O(\epsilon^n)$ which allowed a single parameter asymptotic expansion approach.

3. Results from the matching procedure

A. From the continuity Eqn. of (A4):

$$v_1 = -\int \left[\frac{\partial u_1}{\partial x} + \frac{\partial w_1}{\partial Z}\right] dy + \cancel{v_1}\Big]_{y=0} \to 0 \quad [Eq.\ (B6)]$$

and using Eq. (B1),

$$\lim_{y \to \infty} v_1 = -\int \left[\lim_{y \to \infty} \left[\frac{\partial u_1}{\partial x} + \frac{\partial w_1}{\partial Z}\right]\right] dy =$$

$$-\int \left[\frac{\partial U_1}{\partial x} + \frac{\partial W_1}{\partial Z}\right]_{(x,0,Z)} dy =$$

$$= -y \left[\frac{\partial U_1}{\partial x} + \frac{\partial W_1}{\partial Z}\right]_{(x,0,Z)} \qquad (B12)$$

Also, from the cont. eqn. of (A1),

$$\frac{\partial V_1}{\partial Y}(x,0,Z) = -\left[\frac{\partial U_1}{\partial x} + \frac{\partial W_1}{\partial Z}\right]_{(x,0,Z)}$$

Substituting this and (B12) into Eqn. (B3) yields

$$V_2(x,0,Z) = 0$$

This, together with the fact that the 1st order outer solution satisfies all the B.C.'s at $Y \to \infty$, so that the 2nd order equations must satisfy homogeneous B.C.'s there as well as at Y = 0, dictate that the solution to Eqn. (A2) be the trivial one:

$$U_2 = V_2 = W_2 = P_2 \equiv 0$$

B. From Eqn. (B2) and the fact that $\frac{\partial V_1}{\partial Y}(x,0,Z)$ does not necessarily vanish, it follows that V_1 has the form $V_1 = Yf(x,Y,Z)$, so that $\begin{Bmatrix} \partial/\partial x \\ \partial/\partial Z \end{Bmatrix} V_1 (x,0,Z) = 0$. The Y-mom. part of Eqn. (A1) thus dictates that $\frac{\partial P_1}{\partial Y}(x,0,Z) = 0$. Combined with the previous result $P_2 = 0$, Eq. (B5) yields

$$P_2 \equiv 0$$

It then follows from Eqn. (B7) that

$$\hat{P}_2 \equiv 0$$

Appendix C: Final form of the equations of motion and their matching- and boundary- conditions

1. Outer layer

O(1)

$$\frac{\partial U_1}{\partial x} + \frac{\partial V_1}{\partial Y} + \frac{\partial W_1}{\partial Z} = 0$$

$$\left[U_1 \frac{\partial}{\partial x} + V_1 \frac{\partial}{\partial Y} + W_1 \frac{\partial}{\partial Z}\right] \left\{U_1 . V_1 . W_1\right\}^T =$$

$$- \left\{\frac{\partial}{\partial x}, \frac{\partial}{\partial Y}, \frac{\partial}{\partial Z}\right\}^T \left[P_1\right]$$

O(ϵ)

$$U_2 = V_2 = W_2 = P_2 \equiv 0$$

O(ϵ^2)

$$\frac{\partial U_3}{\partial x} + \frac{\partial V_3}{\partial Y} + \frac{\partial W_3}{\partial Z} = 0$$

$$\left[U_1 \frac{\partial}{\partial x} + V_1 \frac{\partial}{\partial Y} + W_1 \frac{\partial}{\partial Z}\right] \left\{U_3 . V_3 . W_3\right\}^T +$$

$$\left[U_3 \frac{\partial}{\partial x} + V_3 \frac{\partial}{\partial Y} + W_3 \frac{\partial}{\partial Z}\right] \left\{U_1 . V_1 . W_1\right\}^T =$$

$$= - \left[\frac{\partial}{\partial x}, \frac{\partial}{\partial Y}, \frac{\partial}{\partial Z}\right]^T [P_3]$$

2. Middle layer

O(1)

$$\frac{\partial u_1}{\partial x} + \frac{\partial v_1}{\partial y} + \frac{\partial w_1}{\partial Z} = 0$$

$$u_1 \frac{\partial u_1}{\partial x} + v_1 \frac{\partial u_1}{\partial y} + w_1 \frac{\partial u_1}{\partial Z} = - \frac{\partial p_1}{\partial x}$$

$$0 = \frac{\partial p_1}{\partial y}$$

$$u_1 \frac{\partial w_1}{\partial x} + v_1 \frac{\partial w_1}{\partial y} + w_1 \frac{\partial w_1}{\partial Z} = - \frac{\partial p_1}{\partial Z}$$

O(ϵ)

$$\frac{\partial u_2}{\partial x} + \frac{\partial v_2}{\partial y} + \frac{\partial w_2}{\partial Z} = 0$$

$$\frac{\partial}{\partial x}\left[u_1 \; u_2\right] + v_1 \frac{\partial u_2}{\partial y} + v_2 \frac{\partial u_1}{\partial y} + w_1 \frac{\partial u_2}{\partial Z} + w_2 \frac{\partial u_1}{\partial Z} = \frac{\partial t_{1_{xy}}}{\partial y}$$

$$u_1 \frac{\partial w_2}{\partial x} + u_2 \frac{\partial w_1}{\partial x} + v_1 \frac{\partial w_2}{\partial y} + v_2 \frac{\partial w_1}{\partial y} + \frac{\partial}{\partial Z}\left[w_1 w_2\right] = \frac{\partial t_{1_{yz}}}{\partial y}$$

O(ϵ^2)

$$\frac{\partial u_3}{\partial x} + \frac{\partial v_3}{\partial y} + \frac{\partial w_3}{\partial Z} = 0$$

$$\frac{\partial}{\partial x}\left[u_1 u_3\right] + u_2 \frac{\partial u_2}{\partial x} + v_1 \frac{\partial u_3}{\partial y} + v_2 \frac{\partial u_2}{\partial y} + v_3 \frac{\partial u_1}{\partial y} + w_1 \frac{\partial u_3}{\partial Z} +$$

$$w_2 \frac{\partial u_2}{\partial Z} + w_3 \frac{\partial u_1}{\partial Z} = -\frac{\partial p_3}{\partial x} + \frac{\partial t_{1_{xx}}}{\partial x} + \frac{\partial t_{2_{xy}}}{\partial y} + \frac{\partial t_{1_{xz}}}{\partial Z}$$

$$u_1 \frac{\partial v_1}{\partial x} + v_1 \frac{\partial v_1}{\partial y} + w_1 \frac{\partial v_1}{\partial Z} = -\frac{\partial p_3}{\partial y} + \frac{\partial t_{1_{yy}}}{\partial y}$$

$$u_1 \frac{\partial w_3}{\partial x} + u_2 \frac{\partial w_2}{\partial x} + u_3 \frac{\partial w_1}{\partial x} + v_1 \frac{\partial w_3}{\partial y} + v_2 \frac{\partial w_2}{\partial y} + v_3 \frac{\partial w_1}{\partial y} +$$

$$\frac{\partial}{\partial Z}\left[w_1 w_3\right] + w_2 \frac{\partial w_2}{\partial Z} =$$

$$= -\frac{\partial p_3}{\partial Z} + \frac{\partial t_{1_{xz}}}{\partial x} + \frac{\partial t_{2_{yz}}}{\partial y} + \frac{\partial t_{1_{zz}}}{\partial Z}$$

3. Inner layer

O(1)

$$\hat{u}_1 = \hat{v}_1 = \hat{w}_1 \equiv 0$$

$$\hat{p}_1 = P_1(x, 0, Z)$$

O(ε)

$$\frac{\partial \hat{u}_2}{\partial x} + \frac{\partial \hat{v}_2}{\partial \hat{y}} + \frac{\partial \hat{w}_2}{\partial Z} = 0$$

$$0 = \frac{\partial}{\partial \hat{y}}\left[\hat{t}_{1_{xy}} + \frac{\partial \hat{u}_2}{\partial \hat{y}}\right]$$

$$0 = \frac{\partial}{\partial \hat{y}}\left[\hat{t}_{1_{yz}} + \frac{\partial \hat{w}_2}{\partial \hat{y}}\right]$$

$O(\epsilon^2)$

$$\frac{\partial \hat{u}_3}{\partial x} + \frac{\partial \hat{v}_3}{\partial \hat{y}} + \frac{\partial \hat{w}_3}{\partial Z} = 0$$

$$0 = \frac{\partial}{\partial \hat{y}}\left[\hat{t}_{2_{xy}} + \frac{\partial \hat{u}_3}{\partial \hat{y}}\right]$$

$$0 = \frac{\partial}{\partial \hat{y}}\left[-\hat{p}_3 + \hat{t}_{1_{yy}}\right]$$

$$0 = \frac{\partial}{\partial \hat{y}}\left[\hat{t}_{2_{yz}} + \frac{\partial \hat{w}_3}{\partial \hat{y}}\right]$$

4. Outer– middle matching conditions

$$u_1(x,y,Z) \sim U_1(x,0,Z); y \to \infty$$

$$u_2(x,y,Z) \sim y\,\frac{\partial U_1}{\partial Y}(x,0,Z);\ y \to \infty$$

$$u_3(x,y,Z) \sim \frac{y^2}{2}\,\frac{\partial^2 U_1}{\partial Y^2}(x,0,Z) + U_3(x,0,Z);\ y \to \infty$$

with similar relationships for w.

$$V_1(x,0,Z) = 0$$

$$v_1(x,y,Z) \sim -y\left[\frac{\partial U_1}{\partial x} + \frac{\partial W_1}{\partial Z}\right]_{(x,0,Z)} ; \; y \to \infty$$

$$v_2(x,y,Z) \sim V_3(x,0,Z) + \frac{y^2}{2}\frac{\partial^2 V_1}{\partial Y^2}(x,0,Z); \; y \to \infty$$

$$p_1(x,Z) = P_1(x,0,Z)$$

$$0 = \frac{\partial P_1}{\partial Y}(x,0,Z)$$

$$p_3(x,y,Z) \sim \frac{y^2}{2}\frac{\partial^2 P_1}{\partial Y^2}(x,0,Z) + P_3(x,y,Z); \; y \to \infty$$

$$t_{n_{ij}}(x,y,Z) \sim 0; y \to \infty, \text{ for } n = 1,2,3,\cdots$$

5. Middle – Inner matching conditions

$$v_1(x,0,Z) = v_2(x,0,Z) = v_3(x,0,Z) = 0$$

$$0 = \frac{\partial}{\partial y}\begin{bmatrix} u_1 \\ v_1 \\ w_1 \end{bmatrix}_{(x,0,Z)}$$

$$\hat{v}_2(X,\hat{y},Z) \sim \hat{y}\frac{\partial v_2}{\partial y}(x,0,Z); \; \hat{y} \to \infty$$

$$\hat{v}_3 \ (x,\hat{y},Z) \sim \hat{y} \ \frac{\partial v_3}{\partial y} \ (x,0,Z); \hat{y} \to \infty$$

$$\hat{p}_1 \ (x,Z) = p_1 \ (x,0,Z)$$

$$\hat{p}_3 \ (x,\hat{y},Z) \sim p_3 \ (x,0,Z) \ \hat{y} \to \infty$$

$$\hat{t}_{n_{ij}} \ (x,\hat{y},Z) \sim t_{n_{ij}} \ (x,0,Z); \ \hat{y} \to \infty, \ n = 1,2,3,\cdots$$

$$u_2 \sim b_2 \ln y + C_2, \ u_3 \sim b_3 \ln y + C_3; \ y \to 0$$

$$\hat{u}_2 \sim b_2 \ln \hat{y} + \hat{C}_2, \ \hat{u}_3 \sim b_3 \ln \hat{y} + \hat{C}_3; \ \hat{y} \to \infty$$

with similar relationships for w and $\hat{w}$.

B.C.'s: $\hat{u}_n \ (x,0,Z) = \hat{v}_n \ (x,0,Z) = \hat{w}_n \ (x,0,Z) = 0, \ n = 2,3,$ $\cdots$

Appendix D: Determination of the 3D logarithmic overlap

In vector form, we have

$$\textit{Law-of-the-Wall}: \quad \frac{\vec{\tilde{U}}}{u_\tau} = \vec{f}\,(y^+) \tag{D1}$$

$$\textit{Law-of-the-Wake}: \quad \left[\vec{\tilde{U}}_e - \vec{\tilde{U}}\right]/u_\tau = \vec{F}(\eta) \tag{D2}$$

$$\textit{From Eqn. (D1)}: \quad \frac{d\vec{\tilde{U}}}{d\tilde{Y}} = \frac{u_\tau^2}{\nu}\frac{d\vec{f}}{dy^+} \tag{D3}$$

$$\text{and from Eqn. (D2)}: \quad \frac{d\vec{\tilde{U}}}{d\tilde{Y}} = -\frac{u_\tau}{\delta}\frac{d\vec{F}}{d\eta} \tag{D4}$$

Multiplying Eqns. (D3) and (D4) by $\tilde{Y}/u_\tau$ and equating, yields

$$\underbrace{y^+ \frac{d\vec{f}}{dy^+}}_{f(y^+)} = \underbrace{-\eta \frac{d\vec{F}}{d\eta}}_{f(\eta)} = \vec{C} \tag{D5}$$

where $\vec{C}$ is a constant vector.

Rewriting Eqn. (D5) in component form,

$$y^+ \left[\frac{df_x}{dy^+}\hat{e}_x + \frac{df_z}{dy^+}\hat{e}_z\right] = -\eta\left[\frac{dF_x}{d\eta}\hat{e}_x + \frac{dF_z}{d\eta}\hat{e}_z\right] =$$

$$C_x\hat{e}_x + C_z\hat{e}_z$$

Thus

$$y^+\frac{df_x}{dy^+} = -\eta\frac{dF_x}{d\eta} = C_x \rightarrow \begin{cases} f_x = C_x \ln y^+ + B_x \\ F_x = -C_x \ln \eta + A_x' \end{cases} \qquad (D6)$$

$$y^+\frac{df_z}{dy^+} = -\eta\frac{dF_z}{d\eta} = C_z \rightarrow \begin{cases} f_z = C_z \ln y^+ + B_z \\ F_z = -C_z \ln \eta + A_z' \end{cases} \qquad (D7)$$

comparing these results with Eqns. (B10) and (B11) yields

$$u_x^+ = f_x = \hat{u}_2,\ C_x = b_2,\ B_x = \hat{C}_2,\ y^+ = \hat{y} \qquad (D8)$$

$$F_x = -u_2, \qquad A_x' = -C_2,\ \eta = y$$

with similar expressions for the z-components. Note that $\eta = y$ dictates the scale of the outer flow as $l = \lambda\delta$.

Since the Law-of-the-Wall is 2D (in τ_w-direction), it follows that

$$u^+ \sim \kappa^{-1}\ln y^+ + B;\ y^+ \rightarrow \infty \qquad (D9)$$

whence

$$\begin{bmatrix} u_x^+ \\ u_z^+ \end{bmatrix} = u^+ \begin{bmatrix} \cos\phi_w \\ \sin\phi_w \end{bmatrix} - \kappa^{-1} \begin{bmatrix} \cos\phi_w \\ \sin\phi_w \end{bmatrix} \ln y^+ +$$

$$\begin{bmatrix} \cos\phi_w \\ \sin\phi_w \end{bmatrix} B ; \; y^+ \to \infty$$

comparing this with Eqn. (D8) and its z- counterpart, one gets

$$\begin{bmatrix} b_2 \\ d_2 \end{bmatrix} = \begin{bmatrix} C_x \\ C_z \end{bmatrix} = \begin{bmatrix} \cos\phi_w \\ \sin\phi_w \end{bmatrix} \kappa^{-1}$$

$$\begin{bmatrix} \hat{C}_2 \\ \hat{e}_2 \end{bmatrix} = \begin{bmatrix} B_x \\ B_z \end{bmatrix} = \begin{bmatrix} \cos\phi_w \\ \sin\phi_w \end{bmatrix} B$$

Eqns. (D6) and (D7) then imply that

$$F \cos\gamma \equiv F_x \tilde{} - \kappa^{-1} \cos\phi_w \ln \eta + A_x' \quad ; \eta \to 0 \quad \text{(D10)}$$

$$- F \sin\gamma \equiv F_z \tilde{} - \kappa^{-1} \sin\phi_w \ln \eta + A_z'$$

If one now assumes that

$$\begin{bmatrix} A_x' \\ A_z' \end{bmatrix} = A' \begin{bmatrix} \cos\phi_w \\ \sin\phi_w \end{bmatrix} = \begin{bmatrix} \cos\phi_w \\ \sin\phi_w \end{bmatrix} 2 \frac{\Pi}{\kappa}$$

then it follows from Eqn. (D10) that

$$F = \sqrt{F_x^2 + F_z^2} \sim -\kappa^{-1}\left[\ln \eta - 2\,\Pi\right]: \eta \to 0$$

which establishes, together with (D9), the logarithmic overlap for the 3D case. This was also established by the matched asymptotic analysis, Eqns. (B10), (B11) and their crosswise counterparts.

Appendix E: Details Pertaining to Profile Relations

E1: *Determination of the Wake Parameter, Π*

Since F_{2D} is the defect function of the streamwise component of the skewed boundary layer, the following log. friction law applies to it:

$$\kappa\lambda_x = \ln\left[Re_\delta/\lambda_x\right] + \kappa B + 2\Pi \qquad \text{(E1-1)}$$

where

$$\lambda_x = \lambda/\left[\cos\phi_w\right]^{1/2}$$

By using Coles' [1] formulation of the 2D Law-of-the-Wake, subject to his normalizing conditions, a further relationship involving Π is

$$\kappa\lambda_x Re_{\delta_x^*}/Re_\delta = 1 + \Pi \qquad \text{(E1-2)}$$

Combining Eqns. (E1-1) and (E1-2) then yields the equation for Π in the form

$$2\Pi - \ln\frac{1+\Pi}{\kappa Re_{\delta_x^*}} + \kappa\left[B - \lambda_x\right] = 0$$

from which Π is determinable, using a root finder algorithm [13].

E2: Determination of the function $\gamma(\eta)$

From the Law-of-the-Wall, Eq. (4), one gets

$$\frac{d\tilde{U}}{d\tilde{Y}} = \frac{u_\tau^2}{\nu}\frac{df}{dy^+}$$

From the Law-of-the-Wake, Eq. (7), one gets

$$\frac{d\tilde{U}}{d\tilde{Y}} = \frac{u_\tau^2}{\delta\tilde{U}}\left[F\frac{dF}{d\eta} - \lambda\left[\frac{dF}{d\eta}\cos\gamma - F\sin\gamma\frac{d\gamma}{d\eta}\right]\right]$$

Multiplying both expressions by $\frac{\tilde{Y}}{u_\tau}$ and equating, yields

$$y^+\frac{df}{dy^+} = \frac{\eta}{U}\left[\left[\frac{F}{\lambda} - \cos\gamma\right]\frac{dF}{d\eta} + F\sin\gamma\frac{d\gamma}{d\eta}\right] = \kappa^{-1} \qquad \text{(E2-1)}$$

Since the L.H.S. is a function of y^+ only and the R.H.S. of η only (these are independent variables in the context of asymptotic analysis), both are equal to the same constant, κ^{-1}. Integration of the L.H.S. yields

$$f = \kappa^{-1}\ln y^+ + B$$

which is the logarithmic overlap expressed in terms of wall variables. Substituting Eq. (6) into the R.H.S. of Eq. (E2-1) yields

$$\frac{\eta}{U}\left[\left[\frac{F_{2D}}{\lambda\cos^2\gamma} - 1\right]\frac{dF_{2D}}{d\eta} + \frac{F_{2D}^2\tan\gamma}{\lambda\cos^2\gamma}\frac{d\gamma}{d\eta}\right] = \kappa^{-1}$$

from which

$$\frac{d\gamma}{d\eta} = \frac{\lambda\cos^2\gamma}{F_{2D}^2\tan\gamma}\left[\frac{U}{\kappa\eta} - \left[\frac{F_{2D}}{\lambda\cos^2\gamma} - 1\right]\frac{dF_{2D}}{d\eta}\right] \tag{9}$$

where U is given by Eq. (7) and F_{2D} by Eq. (5). The initial condition required for the solution of Eq. (9) is determined as follows: according to the asymptotic analysis the hodograph (Fig. 7) starts deviating from the ϕ_w- direction at the point in the logarithmic overlap where the wall- and wake-velocity vectors are in the same direction. This point is designated as η_o.

From Fig. 7,

$$u^+ = \frac{\lambda}{\left[\cos\phi_w + \frac{\sin\phi_w}{\tan\gamma}\right]}$$

combining this with Eqs. (6) and (8) yields

$$\tan\phi(\eta) = \frac{\sin\phi_w}{\left[\frac{\lambda}{u^+\left[y^+\right]} - \cos\phi_w\right]\left[\frac{\lambda}{F_{2D}(\eta)} - 1\right]} \tag{E2-2}$$

in the logarithmic overlap. Here

$$y^+ \equiv \frac{Re_\delta}{\lambda}\,\eta$$

and u^+ and F_{2D} are given by Eqs. (4) and (5) respectively. Eq. (E2-2) is solved iteratively for η_o which is the largest η for which $\phi(\eta) = \phi_w$. γ_o is then found from Eq. (8) with $\eta = \eta_o$ and $\phi = \phi_w$. This determines the required initial conditions for Eq.

(9), the solution of which provides $\gamma(\eta)$ in the logarithmic overlap region, which is the lower portion of the $\gamma(\eta)$ curve.

At the upper portion of the defect layer, $\gamma = \gamma_m$ [Eq. (11)]. To complete the formulation of γ, it is necessary to devise a curve-fit which smoothly connects the lower and upper portions of the $\gamma(\eta)$ curve. To this end one defines the function

$$\Gamma \equiv \frac{\gamma}{\gamma_m} = 1 - \beta \left[1-\eta\right]^{\alpha} \qquad (10)$$

The following requirements are necessary to be met by this function:

1) $\Gamma(1) = 1$

2) $\frac{d\Gamma}{d\eta} > 0$

3) $\lim_{\eta \to 1} \frac{d\Gamma}{d\eta} = 0$

4) $\frac{d^2\Gamma}{d\eta^2} < 0$

5) $\lim_{\eta \to 1} \frac{d^2\Gamma}{d\eta^2} = 0$

(zero curvature as $\eta \to 1$).

These requirements are met provided that $\alpha > 2$ and $\beta > 0$. The latter two parameters are determined by matching Γ to the curve described by Eq. (9) at a matching point, η_1, where the velocity profile switches from the logarithmic overlap to the wake (see Fig. 8):

$$\begin{cases} \Gamma = \dfrac{\gamma_1}{\gamma_m} & @\ \eta = \eta_1 \\ \dfrac{d\Gamma}{d\eta} = \gamma_m^{-1}\dfrac{d\gamma}{d\eta} & @\eta=\eta_1 \end{cases}$$

where $\gamma(\eta)$ is the function at the logarithmic overlap region, and γ_1 is its value at $\eta = \eta_1$. From this one gets:

$$\alpha = \frac{1-\eta_1}{1-\Gamma_1}\frac{d\Gamma}{d\eta}\Bigg]_{\eta=\eta_1}$$

and

$$\beta = \frac{1-\Gamma_1}{\left[1-\eta_1\right]^{\alpha}}$$

η_1 is generally a function of Re_δ and pressure gradient. Based on experimental data, a typical value for it is 0.035. See Appendix E3 for an outline of an iterative procedure to determine η_1.

E3: Procedure to Determine η_1

η_1 is a function of both Re number and pressure gradient, for which a model does not seem to exist at the present time. In this work, η_1 is found by an iterative procedure such that the correct value produces a branch of $\Gamma(\eta)$ where Γ first becomes unity at the correct value of η for the particular case under investigation. In the example of Fig. 11, the first guess, labelled η_1', produces a branch such that Γ first becomes 1 at an η which is lower than the correct value for this particular case (which would

typically be taken from an actual experiment). The next guess, η_1'', leads to a branch in which Γ first attains unity at an η which is higher than the true value. Iterating between η_1' and η_1'' eventually produces the correct branch, shown in the figure as a solid line.

Appendix F: Detailed Analysis of a Juncture Flow

F1: Preliminary form of juncture equations

Introducing the normalized variables of Section 2.2.1. (2) into the 3D Navier-Stokes equations, the juncture region equations become

$$\frac{\partial U}{\partial x} + \frac{\tilde{x}_{ref}}{\lambda_w \Delta} \frac{\partial V}{\partial Y} + \frac{\lambda_w \Delta}{\lambda_b \delta} \frac{\tilde{x}_{ref}}{\lambda_w \Delta} \frac{\partial W}{\partial Z} = 0$$

$$U \frac{\partial U}{\partial x} + \frac{\tilde{x}_{ref}}{\lambda_w \Delta} V \frac{\partial U}{\partial Y} + \frac{\lambda_w \Delta}{\lambda_b \delta} \frac{\tilde{x}_{ref}}{\lambda_w \Delta} W \frac{\partial U}{\partial Z} = - \frac{\partial P}{\partial x} +$$

$$\frac{\partial}{\partial x}\left[\frac{\lambda_w \Delta}{\tilde{x}_{ref}} \frac{\nu}{\tilde{U}_e \lambda_w \Delta} \frac{\partial U}{\partial x} + \left[\frac{u_\tau w}{\tilde{U}_e}\right]^2 T_{xx}\right]$$

$$+ \frac{\tilde{x}_{ref}}{\lambda_w \Delta} \frac{\partial}{\partial Y}\left[\frac{\nu}{\tilde{U}_e \lambda_w \Delta} \frac{\partial U}{\partial Y} + \left[\frac{u_\tau w}{\tilde{U}_e}\right]^2 T_{yx}\right] +$$

---

(2) $U_i = \tilde{U}_i / \tilde{U}_e$. $P = \tilde{P} / \rho \tilde{U}_e^2$. $T_{ij} = - \overline{\tilde{u}_i' \tilde{u}_j'} / u_\tau^2 T_{ij}$

$x = \tilde{x} / \tilde{x}_{ref}$. $Y = \tilde{Y} / (\lambda_w \Delta)$. $Z = \tilde{Z} / (\lambda_b \delta)$

$$\frac{\lambda_w^{\Delta}}{\lambda_b^{\delta}} \frac{\tilde{x}_{ref}}{\lambda_w^{\Delta}} \frac{\partial}{\partial Z} \left[\frac{\lambda_w^{\Delta}}{\lambda_b^{\delta}} \frac{\nu}{\tilde{U}_e \lambda_w^{\Delta}} \frac{\partial U}{\partial Z} + \left[\frac{u_{\tau_w}}{\tilde{U}_e} \right]^2 T_{zx} \right]$$

$$U \frac{\partial V}{\partial x} + \frac{\tilde{x}_{ref}}{\lambda_w^{\Delta}} V \frac{\partial V}{\partial Y} + \frac{\lambda_w^{\Delta}}{\lambda_b^{\delta}} \frac{\tilde{x}_{ref}}{\lambda_w^{\Delta}} W \frac{\partial V}{\partial Z} =$$

$$- \frac{\tilde{x}_{ref}}{\lambda_w^{\Delta}} \frac{\partial P}{\partial Y} +$$

$$\frac{\partial}{\partial x} \left[\frac{\lambda_w^{\Delta}}{\tilde{x}_{ref}} \frac{\nu}{\tilde{U}_e \lambda_w^{\Delta}} \frac{\partial V}{\partial x} + \left[\frac{u_{\tau_w}}{\tilde{U}_e} \right]^2 T_{xy} \right] +$$

$$\frac{\tilde{x}_{ref}}{\lambda_w^{\Delta}} \frac{\partial}{\partial Y} \left[\frac{\nu}{\tilde{U}_e \lambda_w^{\Delta}} \frac{\partial V}{\partial Y} + \left[\frac{u_{\tau_w}}{\tilde{U}_e} \right]^2 T_{yy} \right] +$$

$$\frac{\lambda_w^{\Delta}}{\lambda_b^{\delta}} \frac{\tilde{x}_{ref}}{\lambda_w^{\Delta}} \frac{\partial}{\partial Z} \left[\frac{\lambda_w^{\Delta}}{\lambda_b^{\delta}} \frac{\nu}{\tilde{U}_e \lambda_w^{\Delta}} \frac{\partial V}{\partial Z} + \left[\frac{u_{\tau_w}}{\tilde{U}_e} \right]^2 T_{zy} \right]$$

$$U \frac{\partial W}{\partial x} + \frac{\tilde{x}_{ref}}{\lambda_w \Delta} V \frac{\partial W}{\partial Y} + \frac{\lambda_w \Delta}{\lambda_b \delta} \frac{\tilde{x}_{ref}}{\lambda_w \Delta} W \frac{\partial W}{\partial Z} =$$

$$- \frac{\lambda_w \Delta}{\lambda_b \delta} \frac{\tilde{x}_{ref}}{\lambda_w \Delta} \frac{\partial P}{\partial Z} +$$

$$\frac{\partial}{\partial Y} \left[\frac{\lambda_w \Delta}{\tilde{x}_{ref}} \frac{\nu}{\tilde{U}_e \lambda_w \Delta} \frac{\partial W}{\partial x} + \left[\frac{u_{\tau_b}}{u_{\tau_w}} \right]^2 \cdot \right.$$

$$\left. \left[\frac{u_{\tau_w}}{\tilde{U}_e} \right]^2 T_{xz} \right] +$$

$$\frac{\tilde{x}_{ref}}{\lambda_w \Delta} \frac{\partial}{\partial Y} \left[\frac{\nu}{\tilde{U}_e \lambda_w \Delta} \frac{\partial W}{\partial Y} + \left[\frac{u_{\tau_b}}{u_{\tau_w}} \right]^2 \cdot \right.$$

$$\left. \left[\frac{u_{\tau_w}}{\tilde{U}_e} \right]^2 T_{yz} \right] +$$

$$\frac{\lambda_w \Delta}{\lambda_b \delta} \frac{\tilde{x}_{ref}}{\lambda_w \Delta} \frac{\partial}{\partial Z} \left[\frac{\lambda_w \Delta}{\lambda_b \delta} \frac{\nu}{\tilde{U}_e \lambda_w \Delta} \frac{\partial W}{\partial Z} + \right.$$

$$\left. \left[\frac{u_{\tau_b}}{u_{\tau_w}} \right]^2 \cdot \left[\frac{u_{\tau_w}}{\tilde{U}_e} \right]^2 T_{zz} \right]$$

with the notation

$$\epsilon_w \equiv \frac{u_{\tau_w}}{\tilde{U}_e} \ , \quad \epsilon_w^2 \hat{\epsilon}_w \equiv \frac{\nu}{\tilde{U}_e \lambda_w \Delta} \ , \quad \zeta \equiv \frac{\lambda_b \delta}{\lambda_w \Delta} \ , \quad \xi \equiv \frac{\tilde{x}_{ref}}{\lambda_w \Delta} \ ,$$

$$\frac{u_{\tau_b}}{u_{\tau_w}} \equiv \frac{\epsilon_b}{\epsilon_w} \ ,$$

these equations become Eqns. (3) of Section 2.2.1.

Before treating these equations by an asymptotic analysis, it is of interest to relate ζ to the parameters ϵ_w and ϵ_b.

Both δ and Δ increase with x. At the blade leading edge, $\delta/\Delta \sim 0$, while at the trailing edge $\delta/\Delta \sim 1$. For the purpose of scaling, the (1/n)th power law growth for turbulent flat plate flow is used, according to which $\delta \sim x^{\frac{n-1}{n}}$. Thus, for any streamwise location along the blade,

$$\frac{\delta}{\Delta} = \left[\frac{x - x_{L.E.}}{x - x_\infty}\right]^{\frac{n-1}{n}}$$

This relation may be expressed in terms of λ's, using another relationship from the (1/n)th power law, namely

$$C_f = K \ Re_x^{-1/n} \qquad (K - \textit{a constant})$$

Thus

$$\frac{\delta}{\Delta} = \left[\frac{\frac{U_e}{\nu}\left[x - x_{L.E.}\right]}{\frac{U_e}{\nu}\left[x - x_{\infty}\right]}\right]^{\frac{n-1}{n}} =$$

$$\left[\frac{Re_{x-x_{L.E.}}}{Re_{x-x_{\infty}}}\right]^{\frac{n-1}{n}} =$$

$$\left[\frac{C_{f_b}}{C_{f_w}}\right]^{1-n} = \left[\frac{\lambda_w}{\lambda_b}\right]^{2(1-n)} = \left[\frac{\epsilon_b}{\epsilon_w}\right]^{2(1-n)}$$

and hence

$$\zeta = \left[\frac{\epsilon_b}{\epsilon_w}\right]^{1-2n} = \left[\frac{\delta}{\Delta}\right]^{\frac{2n-1}{2n-2}}$$

Thus ζ is a measure of the streamwise development of the corner-flow asymmetry. The case $\delta/\Delta = 1$ formally reduces Eqns. (3) to Eqns. (1) and (2), since then also $\xi \equiv \frac{\bar{x}_{ref}}{\lambda\Delta} = 1$. This case corresponds to the symmetric corner flow. In the present work, both this and the asymmetrical situtation, which occurs in large portions of turbomachinery blade/endwall juncture flows, are investigated.

The analysis is carried out for an arbitrary, but non-zero, δ/Δ ratio (or ζ), so that the leading edge region is excluded from the present discussion.

The following generalized expansions are defined:

Middle region

$$y = \frac{Y}{\phi} \ , \ z = \frac{Z}{\Psi}$$

$$U = f\left[u_1 \ (x,y,z) + \epsilon_c u_2 + \epsilon_c^2 u_3 + \cdots\right]$$

$$V = g\left[v_1 \ (x,y,z) + \epsilon_c v_2 + \epsilon_c^2 v_3 + \cdots\right]$$

$$W = h\left[w_1 \ (x,y,z) + \epsilon_c w_2 + \epsilon_c^2 w_3 + \cdots\right]$$

$$P = p_1 \ (x,y,z) + \epsilon_c p_2 + \epsilon_c^2 p_3 + \cdots$$

$$T_{ij} = \left[\left[\frac{\epsilon_c}{\epsilon_w}\right]^2 + q \ \delta_{jz}\right]\left[t_{1_{ij}} \ (x,y,z) + \epsilon_c t_{2_{ij}} + \epsilon_c^2 t_{3_{ij}} + \cdots\right]$$

Inner region

$$\hat{y} = \frac{Y}{\hat{\phi}} \ , \ \hat{z} = \frac{Z}{\hat{\Psi}}$$

$$U = \hat{f}\left[\hat{u}_1 + \epsilon_c \hat{u}_2 + \epsilon_c^2 \hat{u}_3 + \ldots\right]$$

$$V = \hat{g}\left[\hat{v}_1 + \epsilon_c \hat{v}_2 + \epsilon_c^2 \hat{v}_3 + \cdots\right]$$

$$W = \hat{h}\left[\hat{w}_1 + \epsilon_c \hat{w}_2 + \epsilon_c^2 \hat{w}_3 + \cdots\right]$$

$$P = \hat{p}_1 + \epsilon_c \hat{p}_2 + \epsilon_c^2 \hat{p}_3 + \cdots$$

$$T_{ij} = \left[\left[\frac{\epsilon_c}{\epsilon_w} \right]^2 + \hat{q}\ \delta_{jz} \right] \left[\hat{t}_{1_{ij}} + \epsilon_c \hat{t}_{2_{ij}} + \epsilon_c^2 \hat{t}_{3_{ij}} + \cdots \right]$$

Here the parameters f, g, h, q, $\hat{f}$, $\hat{g}$, $\hat{h}$, $\hat{q}$ are in general functions of ϵ_c, $\hat{\epsilon}_c$, ϵ_w, $\hat{\epsilon}_w$, ζ and ξ or of some of them: ϵ_c and $\hat{\epsilon}_c$ are small perturbation parameters appropriate to the juncture, to be determined later from matching conditions; and ϕ, $\hat{\phi}$, Ψ and $\hat{\Psi}$ are stretching parameters whose purpose is to create symmetric juncture equations regardless of whether the flow itself is symmetric or not. These stretching parameters are also functions of ϵ_c, $\hat{\epsilon}_c$, ϵ_w, $\hat{\epsilon}_w$, ζ and ξ. The above expansions are inserted into Eqns. (3), yielding:

Middle region

$$f \frac{\partial}{\partial x} (u_1 + \cdots) + \xi \frac{g}{\phi} \frac{\partial}{\partial y} (v_1 + \cdots) + \frac{\xi}{\zeta} \frac{h}{\Psi} \frac{\partial}{\partial z} (w_1 + \cdots) = 0$$

$$f^2 (u_1 + \cdots) \frac{\partial}{\partial x} (u_1 + \cdots) + \xi \frac{fg}{\phi} (v_1 + \cdots) \frac{\partial}{\partial y} (u_1 + \cdots) +$$

$$\frac{\xi f h}{\zeta \Psi} (w_1 + \cdots) \frac{\partial}{\partial z} (u_1 + \cdots) = - \frac{\partial}{\partial x} (p_1 + \cdots) +$$

$$+ \frac{\partial}{\partial x} \left[\frac{f}{\xi} \epsilon_w^2 \hat{\epsilon}_w \frac{\partial}{\partial x} (u_1 + \cdots) + \epsilon_c^2 \left[t_{1_{xx}} + \cdots \right] \right] +$$

$$\frac{\xi}{\phi}\frac{\partial}{\partial y}\left[\frac{f}{\phi}\epsilon_w^2\hat{\epsilon}_w\frac{\partial}{\partial y}(u_1+\cdots)+\epsilon_c^2\left[t_{1_{yx}}+\cdots\right]\right]+$$

$$+\frac{\xi}{\zeta\Psi}\frac{\partial}{\partial z}\left[\frac{f}{\zeta\Psi}\epsilon_w^2\hat{\epsilon}_w\frac{\partial}{\partial z}(u_1+\cdots)+\epsilon_c^2\left[t_{1_{zx}}+\cdots\right]\right]$$

$$fg(u_1+\cdots)\frac{\partial}{\partial x}(v_1+\cdots)+\xi\frac{g^2}{\phi}(v_1+\cdots)\frac{\partial}{\partial y}(v_1+\cdots)+$$

$$\frac{\xi gh}{\zeta\Psi}(w_1+\cdots)\frac{\partial}{\partial z}(v_1+\cdots)=-\frac{\xi}{\phi}\frac{\partial}{\partial y}(p_1+\cdots)+$$

$$+\frac{\partial}{\partial x}\left[\frac{g}{\xi}\epsilon_w^2\hat{\epsilon}_w\frac{\partial}{\partial x}(v_1+\cdots)+\epsilon_c^2\left[t_{1_{xy}}+\cdots\right]\right]+$$

$$\frac{\xi}{\phi}\frac{\partial}{\partial y}\left[\frac{g}{\phi}\epsilon_w^2\hat{\epsilon}_w\frac{\partial}{\partial y}(v_1+\cdots)+\epsilon_c^2\left[t_{1_{yy}}+\cdots\right]\right]+$$

$$+\frac{\xi}{\zeta\Psi}\frac{\partial}{\partial z}\left[\frac{g}{\zeta\Psi}\epsilon_w^2\hat{\epsilon}_w\frac{\partial}{\partial z}(v_1+\cdots)+\epsilon_c^2\left[t_{1_{zy}}+\cdots\right]\right]$$

$$fh(u_1+\cdots)\frac{\partial}{\partial x}(w_1+\cdots)+\xi\frac{gh}{\phi}(v_1+\cdots)\frac{\partial}{\partial y}(w_1+\cdots)+$$

$$\frac{\xi h^2}{\zeta\Psi}(w_1+\cdots)\frac{\partial}{\partial z}(w_1+\cdots)=-\frac{\xi}{\zeta\Psi}\frac{\partial}{\partial z}(p_1+\cdots)+$$

$$+\frac{\partial}{\partial x}\left\{\frac{h}{\xi}\epsilon_w^2\hat{\epsilon}_w\frac{\partial}{\partial x}(w_1+\cdots)+\zeta^{2\sigma}\epsilon_w^2\left[\left[\frac{\epsilon_c}{\epsilon_w}\right]^2+q\right]\right.$$

$$\left[t_1{}_{xz} + \cdots\right]\Big\} +$$

$$\frac{\xi}{\phi}\frac{\partial}{\partial y}\left\{\frac{h}{\phi}\,\epsilon_w^2\hat{\epsilon}_w\frac{\partial}{\partial y}(w_1 + \cdots) + \zeta^{2\sigma}\,\epsilon_w^2\left[\left[\frac{\epsilon_c}{\epsilon_w}\right]^2 + q\right]\cdot\right.$$

$$\left[t_1{}_{yz} + \cdots\right]\Big\} +$$

$$\frac{\xi}{\zeta\Psi}\frac{\partial}{\partial z}\left\{\frac{h}{\zeta\Psi} + \epsilon_w^2\hat{\epsilon}_w\frac{\partial}{\partial z}(w_1 + \cdots) + \zeta^{2\sigma}\epsilon_w^2\left[\left[\frac{\epsilon_c}{\epsilon_w}\right]^2 + q\right]\cdot\right.$$

$$\left[t_1{}_{zz} + \cdots\right]\Big\}$$

Imposing symmetry in Y and Z and in V and W on these equations results in the following relations:

$$q = \left[\frac{\epsilon_c}{\epsilon_w}\right]^2\left[\zeta^{-2\sigma} - 1\right]$$

$$f = 1,\ g = h = \epsilon_c$$

$$\phi = \zeta\Psi = \xi\epsilon_c$$

and

$$\xi = \frac{\epsilon_w^2 \hat{\epsilon}_w}{\epsilon_c^2 \hat{\epsilon}_c}$$

Inner region

$$\hat{f}\,\frac{\partial}{\partial x}\,(\hat{u}_1 + \cdots) + \xi\,\frac{\hat{g}}{\hat{\phi}}\,\frac{\partial}{\partial \hat{y}}\,(\hat{v}_1 + \cdots) + \frac{\xi \hat{h}}{\zeta \hat{\Psi}}\,\frac{\partial}{\partial z}\,(\hat{w}_1 + \cdots) = 0$$

$$\hat{f}^2\,(\hat{u}_1 + \cdots)\,\frac{\partial}{\partial x}\,(\hat{u}_1 + \cdots) + \xi\,\frac{\hat{g}\hat{f}}{\hat{\phi}}\,(\hat{v}_1 + \cdots)\,\frac{\partial}{\partial \hat{y}}\,(\hat{u}_1 + \cdots) +$$

$$\frac{\xi \hat{h} \hat{f}}{\zeta \hat{\Psi}}\,(\hat{w}_1 + \cdots)\,\frac{\partial}{\partial \hat{z}}\,(\hat{u}_1 + \cdots) = -\frac{\partial}{\partial x}\,(\hat{p}_1 + \cdots) +$$

$$+ \frac{\partial}{\partial x}\left[\frac{\hat{f}}{\xi}\,\epsilon_w^2 \hat{\epsilon}_w\,\frac{\partial}{\partial x}\,(\hat{u}_1 + \cdots) + \epsilon_c^2\,\left[\hat{t}_{1_{xx}} + \cdots\right]\right] +$$

$$\frac{\xi}{\hat{\phi}}\,\frac{\partial}{\partial \hat{y}}\left[\frac{\hat{f}}{\hat{\phi}}\,\epsilon_w^2 \hat{\epsilon}_w\,\frac{\partial}{\partial \hat{y}}\,(\hat{u}_1 + \cdots) +\right.$$

$$\left.\epsilon_c^2\,\left[\hat{t}_{1_{yx}} + \cdots\right]\right] +$$

$$+ \frac{\xi}{\zeta \hat{\Psi}}\,\frac{\partial}{\partial \hat{z}}\left[\frac{\hat{f}}{\zeta \hat{\Psi}}\,\epsilon_w^2 \hat{\epsilon}_w\,\frac{\partial}{\partial \hat{z}}\,(\hat{u}_1 + \cdots) + \epsilon_c^2\,(\hat{t}_{1_{zx}} + \cdots)\right]$$

$$\hat{f}\hat{g}\,(\hat{u}_1 + \cdots)\,\frac{\partial}{\partial x}\,(\hat{v}_1 + \cdots) + \xi\,\frac{\hat{g}^2}{\hat{\phi}}\,(\hat{v}_1 + \cdots)\,\frac{\partial}{\partial \hat{y}}\,(\hat{v}_1 + \cdots) +$$

$$\frac{\xi\hat{g}\hat{h}}{\zeta\hat{\Psi}}\,(\hat{w}_1+\cdots)\,\frac{\partial}{\partial\hat{z}}\,(\hat{v}_1+\cdots)=-\frac{\xi}{\hat{\phi}}\,\frac{\partial}{\partial\hat{y}}\,(\hat{p}_1+\cdots)+$$

$$+\frac{\partial}{\partial x}\left[\frac{\hat{g}}{\xi}\,\epsilon_w^2\hat{\epsilon}_w\,\frac{\partial}{\partial x}\,(\hat{v}_1+\cdots)+\epsilon_c^2\left[\hat{t}_1{}_{xy}+\cdots\right]\right]+$$

$$\frac{\xi}{\hat{\phi}}\,\frac{\partial}{\partial\hat{y}}\left[\frac{\hat{g}}{\hat{\phi}}\,\epsilon_w^2\hat{\epsilon}_w\,\frac{\partial}{\partial\hat{y}}\,(\hat{v}_1+\cdots)+\right.$$

$$\left.\epsilon_c^2\left[\hat{t}_1{}_{yy}+\cdots\right]\right]+$$

$$+\frac{\xi}{\zeta\hat{\Psi}}\,\frac{\partial}{\partial\hat{z}}\left[\frac{\hat{g}}{\zeta\hat{\Psi}}\,\epsilon_w^2\hat{\epsilon}_w\,\frac{\partial}{\partial\hat{z}}\,(\hat{v}_1+\cdots)+\right.$$

$$\left.\epsilon_c^2\left[\hat{t}_1{}_{zy}+\cdots\right]\right]$$

$$\hat{f}\hat{h}\,(\hat{u}_1+\cdots)\,\frac{\partial}{\partial x}\,(\hat{w}_1+\cdots)+\xi\,\frac{\hat{g}\hat{h}}{\hat{\phi}}\,(\hat{v}_1+\cdots)\,\frac{\partial}{\partial\hat{y}}\,(\hat{w}_1+\cdots)+$$

$$\frac{\xi\hat{h}^2}{\zeta\hat{\Psi}}\,(\hat{w}_1+\cdots)\frac{\partial}{\partial\hat{z}}\,(\hat{w}_1+\cdots)=-\frac{\xi}{\zeta\hat{\Psi}}\,\frac{\partial}{\partial z}\,(\hat{p}_1+\cdots)+$$

$$+\frac{\partial}{\partial x}\left\{\frac{\hat{h}}{\xi}\,\epsilon_w^2\hat{\epsilon}_w\,\frac{\partial}{\partial x}\,(\hat{w}_1+\cdots)+\zeta^{2\sigma}\,\epsilon_w^2\left[\left[\frac{\epsilon_c}{\epsilon_w}\right]^2+\hat{q}\right]\cdot\right.$$

$$\left.\left[\hat{t}_1{}_{xz}+\cdots\right]\right\}+$$

$$\frac{\xi}{\hat{\phi}}\frac{\partial}{\partial\hat{y}}\left\{\frac{\hat{h}}{\hat{\phi}}\,\epsilon_w^2\hat{\epsilon}_w\frac{\partial}{\partial\hat{y}}\,(\hat{w}_1+\cdots)+\zeta^{2\sigma}\,\epsilon_w^2\cdot\right.$$

$$\left.\left[\left[\frac{\epsilon_c}{\epsilon_w}\right]^2+\hat{q}\right]\left[\hat{f}_{1_{yz}}+\cdots\right]\right\}+$$

$$\frac{\xi}{\zeta\hat{\Psi}}\frac{\partial}{\partial\hat{z}}\left\{\frac{\hat{h}}{\zeta\hat{\Psi}}\,\epsilon_w^2\hat{\epsilon}_w\frac{\partial}{\partial\hat{z}}\,(\hat{w}_1+\cdots)+\zeta^{2\sigma}\,\epsilon_w^2\cdot\right.$$

$$\left.\left[\left[\frac{\epsilon_c}{\epsilon_w}\right]^2+\hat{q}\right]\left[\hat{f}_{1_{zz}}+\cdots\right]\right\}$$

Imposing symmetry again, one obtains

$$\hat{q}=q,\quad \hat{f}=1,\quad \hat{g}=\hat{h}=\epsilon_c\hat{\epsilon}_c,\quad \hat{\phi}=\zeta\hat{\Psi}=\xi\epsilon_c\hat{\epsilon}_c$$

With the scales thus determined, the equations are rewritten as follows:

Middle region

$$\frac{\partial}{\partial x}\left[u_1+\epsilon_c u_2+\cdots\right]+\frac{\partial}{\partial y}\left[v_1+\epsilon_c v_2+\cdots\right]+$$

$$\frac{\partial}{\partial z}\left[w_1+\epsilon_c w_2+\cdots\right]=0$$

$$\left[u_1+\epsilon_c u_2+\cdots\right]\frac{\partial}{\partial x}\left[u_1+\epsilon_c u_2+\cdots\right]+$$

$$\left[v_1 + \epsilon_c\, v_2 + \cdots\right] \frac{\partial}{\partial y}\left[u_1 + \epsilon_c\, u_2 + \cdots\right] + \left[w_1 + \epsilon_c\, w_2 + \cdots\right] \cdot$$

$$\frac{\partial}{\partial z}\left[u_1 + \epsilon_c\, u_2 + \cdots\right] = -\frac{\partial}{\partial x}\left[p_1 + \epsilon_c\, p_2 + \cdots\right] +$$

$$\frac{\partial}{\partial x}\left[\epsilon_c^2 \hat{\epsilon}_c \frac{\partial}{\partial x}\left[u_1 + \epsilon_c u_2 + \cdots\right] + \epsilon_c^2\left[t_{1_{xx}} + \epsilon_c t_{2_{xx}} + \cdots\right]\right]$$

$$+ \frac{\partial}{\partial y}\left[\hat{\epsilon}_c \frac{\partial}{\partial y}\left[u_1 + \epsilon_c\, u_2 + \cdots\right] + \epsilon_c\left[t_{1_{yx}} + \epsilon_c t_{2_{yx}} + \right]\right] +$$

$$+ \frac{\partial}{\partial z}\left[\hat{\epsilon}_c \frac{\partial}{\partial z}\left[u_1 + \epsilon_c u_2 + \cdots\right] + \epsilon_c\left[t_{1_{zx}} + \epsilon_c t_{2_{zx}} + \cdots\right]\right]$$

$$\epsilon_c^2\left[\left[u_1 + \epsilon_c u_2 + \cdots\right] \frac{\partial}{\partial x}\left[v_1 + \epsilon_c v_2 + \cdots\right] + \left[v_1 + \epsilon_c v_2 + \cdots\right] \cdot\right.$$

$$\frac{\partial}{\partial y}\left(v_1 + \epsilon_c v_2 + \cdots\right) +$$

$$\left.\left[w_1 + \epsilon_c w_2 + \cdots\right] \frac{\partial}{\partial z}\left[v_1 + \epsilon_c v_2 + \cdots\right]\right] =$$

$$= -\frac{\partial}{\partial y}\left[p_1 + \epsilon_c p_2 + \cdots\right] + \frac{\partial}{\partial x}\left[\epsilon_c^4 \hat{\epsilon}_c \frac{\partial}{\partial x}\left[v_1 + \epsilon_c v_2 + \cdots\right] +\right.$$

$$\left.\epsilon_c^3\left[t_{1_{xy}} + \cdots\right]\right] +$$

$$+ \frac{\partial}{\partial y}\left[\epsilon_c^2 \hat{\epsilon}_c \frac{\partial}{\partial y}(v_1 + \cdots) + \epsilon_c^2\left[t_{1_{yy}} + \cdots\right]\right] +$$

$$\frac{\partial}{\partial z}\left[\epsilon_c^2\hat{\epsilon}_c\frac{\partial}{\partial z}(v_1+\cdots)+\epsilon_c^2\left[t_{1_{zy}}+\cdots\right]\right]$$

$$\epsilon_c^2\left[\left[u_1+\cdots\right]\frac{\partial}{\partial x}(w_1+\cdots)+(v_1+\cdots)\frac{\partial}{\partial y}(w_1+\cdots)+\right.$$

$$\left.(w_1+\cdots)\frac{\partial}{\partial z}(w_1+\cdots)\right]=$$

$$-\frac{\partial}{\partial z}\left[p_1+\epsilon_c p_2+\epsilon_c^2 p_3+\cdots\right]+\frac{\partial}{\partial x}\left[\epsilon_c^4\hat{\epsilon}_c\frac{\partial}{\partial x}(w_1+\cdots)+\right.$$

$$\left.\epsilon_c^3\left[t_{1_{xz}}+\cdots\right]\right]+$$

$$+\frac{\partial}{\partial y}\left[\epsilon_c^2\hat{\epsilon}_c\frac{\partial}{\partial y}(w_1+\cdots)+\epsilon_c^2\left[t_{1_{yz}}+\cdots\right]\right]+$$

$$+\frac{\partial}{\partial z}\left[\epsilon_c^2\hat{\epsilon}_c\frac{\partial}{\partial z}(w_1+\cdots)+\epsilon_c^2\left[t_{1_{zz}}+\cdots\right]\right]$$

Inner region

$$\frac{\partial}{\partial x}\left[\hat{u}_1+\epsilon_c\hat{u}_2+\cdots\right]+\frac{\partial}{\partial\hat{y}}\left[\hat{v}_1+\epsilon_c\hat{v}_2+\cdots\right]+$$

$$\frac{\partial}{\partial\hat{z}}\left[\hat{w}_1+\epsilon_c\hat{w}_2+\cdots\right]=0$$

$$\hat{\epsilon}_c\left[(\hat{u}_1+\cdots)\frac{\partial}{\partial x}(\hat{u}_1+\cdots)+(\hat{v}_1+\cdots)\frac{\partial}{\partial\hat{y}}(\hat{u}_1+\cdots)+\right.$$

$$\left.(\hat{w}_1+\cdots)\frac{\partial}{\partial\hat{z}}(\hat{u}_1+\cdots)\right]=$$

$$- \hat{\epsilon}_c \frac{\partial}{\partial x} (\hat{p}_1 + \cdots) + \frac{\partial}{\partial x} \left[\epsilon_c^2 \hat{\epsilon}_c^2 \frac{\partial}{\partial x} (\hat{u}_1 + \cdots) + \right.$$

$$\left. \epsilon_c^2 \hat{\epsilon}_c \left[\hat{t}_{1_{xx}} + \cdots \right] \right] +$$

$$\frac{\partial}{\partial \hat{y}} \left[\frac{\partial}{\partial \hat{y}} (\hat{u}_1 + \cdots) + \epsilon_c \left[\hat{t}_{1_{yx}} + \cdots \right] \right] +$$

$$+ \frac{\partial}{\partial \hat{z}} \left[\frac{\partial}{\partial \hat{z}} \left[\hat{u}_1 + \epsilon_c \hat{u}_2 + \epsilon_c^2 \hat{u}_3 + \cdots \right] + \epsilon_c \left[\hat{t}_{1_{zx}} + \right. \right.$$

$$\left. \left. \epsilon_c \hat{t}_{2_{zx}} + \cdots \right] \right]$$

$$\left[\epsilon_c \hat{\epsilon}_c \right]^2 \left[\left[\hat{u}_1 + \cdots \right] \frac{\partial}{\partial x} (\hat{v}_1 + \cdots) + (\hat{v}_1 + \cdots) \frac{\partial}{\partial \hat{y}} (\hat{v}_1 + \cdots) + \right.$$

$$\left. (\hat{w}_1 + \cdots) \frac{\partial}{\partial \hat{z}} (\hat{v}_1 + \cdots) \right] =$$

$$- \frac{\partial}{\partial \hat{y}} \left[\hat{p}_1 + \epsilon_c \hat{p}_2 + \epsilon_c^2 \hat{p}_3 + \cdots \right] + \frac{\partial}{\partial x} \left[\epsilon_c^4 \hat{\epsilon}_c^3 \frac{\partial}{\partial x} (\hat{v}_1 + \cdots) + \right.$$

$$\left. \epsilon_c^3 \hat{\epsilon}_c \left[\hat{t}_{1_{xy}} + \cdots \right] \right] +$$

$$\frac{\partial}{\partial \hat{y}} \left[\epsilon_c^2 \hat{\epsilon}_c \frac{\partial}{\partial \hat{y}} (\hat{v}_1 + \cdots) + \epsilon_c^2 \left[\hat{t}_{1_{yy}} + \cdots \right] \right] +$$

$$\frac{\partial}{\partial \hat{z}}\left[\epsilon_c^2 \hat{\epsilon}_c \frac{\partial}{\partial \hat{z}} (\hat{v}_1 + \cdots) + \epsilon_c^2 \left[\hat{t}_1{}_{zy} + \cdots\right]\right]$$

$$\left[\epsilon_c \hat{\epsilon}_c\right]^2 \left[(\hat{u}_1 + \cdots) \frac{\partial}{\partial x} (\hat{w}_1 + \cdots) + (\hat{v}_1 + \cdots) \frac{\partial}{\partial \hat{y}} (\hat{w}_1 + \cdots) + \right.$$

$$\left. (\hat{w}_1 + \cdots) \frac{\partial}{\partial \hat{z}} (\hat{w}_1 + \cdots)\right] =$$

$$- \frac{\partial}{\partial \hat{z}}\left[\hat{p}_1 + \epsilon_c \hat{p}_2 + \epsilon_c^2 \hat{p}_3 + \cdots\right] + \frac{\partial}{\partial x}\left[\epsilon_c^4 \hat{\epsilon}_c^3 \frac{\partial}{\partial x} (\hat{w}_1 + \cdots) + \right.$$

$$\left. \epsilon_c^3 \hat{\epsilon}_c \left[\hat{t}_1{}_{xz} + \cdots\right]\right] +$$

$$\frac{\partial}{\partial \hat{y}}\left[\epsilon_c^2 \hat{\epsilon}_c \frac{\partial}{\partial \hat{y}} (\hat{w}_1 + \cdots) + \epsilon_c^2 \left[\hat{t}_1{}_{yz} + \cdots\right]\right] +$$

$$\frac{\partial}{\partial \hat{z}}\left[\epsilon_c^2 \hat{\epsilon}_c \frac{\partial}{\partial \hat{z}} (\hat{w}_1 + \cdots) + \epsilon_c^2 \left[\hat{t}_1{}_{zz} + \cdots\right]\right]$$

Sorting the above equations according to orders of magnitude results in the following equations:

Middle region

$O(1)$

$$\frac{\partial u_1}{\partial x} + \frac{\partial v_1}{\partial y} + \frac{\partial w_1}{\partial z} = 0$$

$$u_1 \frac{\partial u_1}{\partial x} + v_1 \frac{\partial u_1}{\partial y} + w_1 \frac{\partial u_1}{\partial z} = - \frac{\partial p_1}{\partial x}$$

$$0 = \frac{\partial p_1}{\partial y}$$

$$0 = \frac{\partial p_1}{\partial z}$$

$O(\epsilon_c)$

$$\frac{\partial u_2}{\partial x} + \frac{\partial v_2}{\partial y} + \frac{\partial w_2}{\partial z} = 0$$

$$\frac{\partial}{\partial x}(u_1 u_2) + v_1 \frac{\partial u_2}{\partial y} + v_2 \frac{\partial u_1}{\partial y} + w_1 \frac{\partial u_2}{\partial z} + w_2 \frac{\partial u_1}{\partial z} =$$

$$- \frac{\partial p_2}{\partial x} + \frac{\partial t_{1_{yx}}}{\partial y} + \frac{\partial t_{1_{zx}}}{\partial z}$$

$$0 = \frac{\partial p_2}{\partial y}$$

$$0 = \frac{\partial p_2}{\partial z}$$

$O(\epsilon_c^2)$

$$\frac{\partial u_3}{\partial x} + \frac{\partial v_3}{\partial y} + \frac{\partial w_3}{\partial z} = 0$$

$$\frac{\partial}{\partial x}(u_1 u_3) + u_2 \frac{\partial u_2}{\partial x} + v_1 \frac{\partial u_3}{\partial y} + v_2 \frac{\partial u_2}{\partial y} + v_3 \frac{\partial u_1}{\partial y} +$$

$$w_1 \frac{\partial u_3}{\partial z} + w_2 \frac{\partial u_2}{\partial z} + w_3 \frac{\partial u_1}{\partial z} =$$

$$- \frac{\partial p_3}{\partial x} + \frac{\partial t_{1_{xx}}}{\partial x} + \frac{\partial t_{2_{yx}}}{\partial y} + \frac{\partial t_{2_{zx}}}{\partial z}$$

$$u_1 \frac{\partial v_1}{\partial x} + v_1 \frac{\partial v_1}{\partial y} + w_1 \frac{\partial v_1}{\partial z} = - \frac{\partial p_3}{\partial y} + \frac{\partial t_{1_{yy}}}{\partial y} + \frac{\partial t_{1_{zy}}}{\partial z}$$

$$u_1 \frac{\partial w_1}{\partial x} + v_1 \frac{\partial w_1}{\partial y} + w_1 \frac{\partial w_1}{\partial z} = - \frac{\partial p_3}{\partial z} + \frac{\partial t_{1_{yz}}}{\partial y} + \frac{\partial t_{1_{zz}}}{\partial z}$$

Inner region

$O(1)$

$$\frac{\partial \hat{u}_1}{\partial x} + \frac{\partial \hat{v}_1}{\partial \hat{y}} + \frac{\partial \hat{w}_1}{\partial \hat{z}} = 0$$

$$0 = \frac{\partial^2 \hat{u}_1}{\partial \hat{y}^2} + \frac{\partial^2 \hat{u}_1}{\partial \hat{z}^2} \qquad \text{(F1)}$$

$$0 = \frac{\partial \hat{p}_1}{\partial \hat{y}}$$

$$0 = \frac{\partial \hat{p}_1}{\partial \hat{z}}$$

$O(\epsilon_c)$

$$\frac{\partial \hat{u}_2}{\partial x} + \frac{\partial \hat{v}_2}{\partial \hat{y}} + \frac{\partial \hat{w}_2}{\partial \hat{z}} = 0$$

$$0 = \frac{\partial}{\partial \hat{y}}\left[\frac{\partial \hat{u}_2}{\partial \hat{y}} + \hat{t}_{1_{yx}}\right] + \frac{\partial}{\partial \hat{z}}\left[\frac{\partial \hat{u}_2}{\partial \hat{z}} + \hat{t}_{1_{zx}}\right] *$$

$$0 = \frac{\partial \hat{p}_2}{\partial \hat{y}}$$

$$0 = \frac{\partial \hat{p}_2}{\partial \hat{z}}$$

$O\left[\epsilon_c^2\right]$

$$\frac{\partial \hat{u}_3}{\partial x} + \frac{\partial \hat{v}_3}{\partial \hat{y}} + \frac{\partial \hat{w}_3}{\partial \hat{z}} = 0$$

$$0 = \frac{\partial}{\partial \hat{y}}\left[\frac{\partial \hat{u}_3}{\partial \hat{y}} + \hat{t}_{2_{yx}}\right] + \frac{\partial}{\partial \hat{z}}\left[\frac{\partial \hat{u}_3}{\partial \hat{z}} + \hat{t}_{2_{zx}}\right] *$$

$$0 = -\frac{\partial \hat{p}_3}{\partial \hat{y}} + \frac{\partial \hat{t}_{1_{yy}}}{\partial \hat{y}} + \frac{\partial \hat{t}_{1_{zy}}}{\partial \hat{z}}$$

$$0 = -\frac{\partial \hat{p}_3}{\partial \hat{z}} + \frac{\partial \hat{t}_{1_{yz}}}{\partial \hat{y}} + \frac{\partial \hat{t}_{1_{zz}}}{\partial \hat{z}}$$

F2: Matching procedure

The following relationships exist between the juncture coordinates and those of the endwall and blade:

$$y_c = \frac{Y_c}{\xi \epsilon_c} = \frac{\tilde{Y}}{\lambda_w \Delta \xi \epsilon_c} = \frac{Y_b \lambda_b \delta}{\xi \epsilon_c \lambda_w \Delta} = \frac{\zeta}{\xi} \frac{Y_b}{\epsilon_c}$$

$$z_c = \frac{Z_c \zeta}{\epsilon_c \xi} = \frac{\zeta}{\xi} \frac{\tilde{Z}}{\lambda_b \delta \epsilon_c} = \frac{\zeta}{\xi} \frac{\lambda_b \delta \epsilon_b \hat{\epsilon}_b \hat{z}_b}{\lambda_b \delta \epsilon_c} =$$

$$\frac{\zeta}{\xi} \frac{\epsilon_b \hat{\epsilon}_b}{\epsilon_c} \hat{z}_b$$

$$y_c = \frac{\lambda_w \Delta \epsilon_w \hat{\epsilon}_w \hat{y}_w}{\lambda_w \Delta \xi \epsilon_c} = \frac{\epsilon_w \hat{\epsilon}_w}{\xi \epsilon_c} \hat{y}_w$$

$$z_c = \frac{\zeta}{\xi} \frac{\lambda_w \Delta Z_w}{\lambda_b \delta \epsilon_c} = \frac{Z_w}{\xi \epsilon_c}$$

The first pair of relations indicates that for smooth matching between the juncture and the blade,

$$\left.\begin{aligned} \lim_{y \to \infty} y_c &= \frac{Y_b}{\epsilon_b} \\ \lim_{z \to 0} z_c &= \hat{\epsilon}_b \hat{z}_b \end{aligned}\right\} \therefore \epsilon_c \to \frac{\zeta}{\xi} \epsilon_b \quad \textit{(blade matching)} \qquad \text{(F2-A)}$$

The second pair indicates the requirement for smooth matching between juncture and endwall:

$$\left.\begin{aligned} \lim_{y\to 0} y_c &= \hat{\epsilon}_w \hat{y}_w \\ \lim_{z\to\infty} z_c &= \frac{Z_w}{\epsilon_w} \end{aligned}\right\} \therefore \epsilon_c \to \frac{\epsilon_w}{\xi} \text{ (endwall matching)} \qquad \text{(F2-B)}$$

Since $\xi \equiv \frac{x_{ref}}{\lambda_w \Delta}$ and from Eqns. (F2) it follows that

$$\lim_{z_c\to\infty} \xi = 1 \to \lim_{z_c\to\infty} \epsilon_c = \epsilon_w$$

(F3)

$$\lim_{y_c\to\infty} \xi = \zeta \to \lim_{y_c\to\infty} \epsilon_c = \epsilon_b$$

In a similar manner

$$\lim_{\hat{z}_c\to\infty} \hat{\epsilon}_c = \hat{\epsilon}_w, \quad \lim_{\hat{y}_c\to\infty} \hat{\epsilon}_c = \hat{\epsilon}_b$$

Eqns. (F3) are in agreement with the previously obtained result $\xi = \frac{\epsilon_w^2 \hat{\epsilon}_w}{\epsilon_c^2 \hat{\epsilon}_c}$.

Thus ϵ_c and $\hat{\epsilon}_c$ have the correct limiting values to guarantee smooth matching with Regions I on both endwall and blade. Hence, one may define ϵ_c and $\hat{\epsilon}_c$ in a similar manner to the corresponding definitions of ϵ_w, $\hat{\epsilon}_w$, ϵ_b and $\hat{\epsilon}_b$, namely

$$\epsilon_c \equiv \frac{u_{\tau_c}}{\bar{U}_e} \; , \quad \hat{\epsilon}_c \equiv \frac{\nu}{u_{\tau_c} \Delta_c}$$

where u_{τ_c} and Δ_c are, respectively, friction velocity and length scale characteristic of the juncture region.

Since the equations of motion derived earlier are symmetric, it suffices to perform the matching procedure for one half of the juncture region. The matching will be done with the endwall, along the following limiting lines:

1. Juncture middle region and endwall middle layer;
2. Juncture inner region and endwall inner layer;
3. Juncture middle region and endwall inner layer.

These lines are denoted by the numerals 1, 2 and 3 in Fig. 4. A completely analogous procedure applies for the blade-matching, denoted by the numerals 4, 5 and 6 in the figure.

In the following, the subscript w is dropped from ϵ_w, since both juncture- and endwall- expansions are using this same perturbation parameter, as demonstrated earlier [Eqns. (F4)]. The expansions for the endwall layers incorporate the results found earlier for the case of pressure-driven boundary layer (see Appendix C).

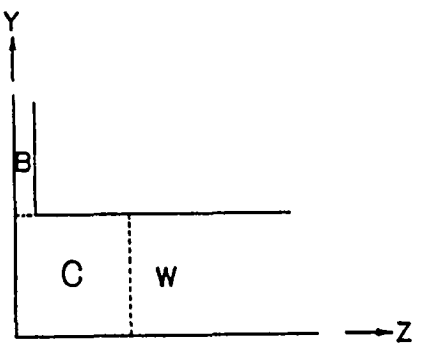

1. $\begin{cases} Z_w \to 0 \\ z_c \to \infty \end{cases}$

$$U_w = u_{w_1}(x,y,Z_w) + \epsilon u_{w_2} + \epsilon^2 u_{w_3} + \cdots = u_{w_1}(x,y,0) +$$

$$\epsilon z_c \frac{\partial u_{w_1}}{\partial Z_w}(x,y,0) + \epsilon^2 \frac{z_c^2}{2} \frac{\partial^2 u_{w_1}}{\partial Z_w^2}(x,y,0) + \cdots + \epsilon u_{w_2}(x,y,0) +$$

$$\epsilon^2 z_c \frac{\partial u_{w_2}}{\partial Z_w}(x,y,0) + \cdots + \epsilon^2 u_{w_3}(x,y,0) + \cdots - u_{c_1}(x,y,z_c) +$$

$$\epsilon u_{c_2}(x,y,z_c) + \epsilon^2 u_{c_3}(x,y,z_c) + \cdots ; \; z_c \to \infty$$

$$u_{c_1}(x,y,z_c) - u_{w_1}(x,y,0) : \; z_c \to \infty$$

$$u_{c_2}(x,y,z_c) - z_c \frac{\partial u_{w_1}}{\partial Z_w}(x,y,0) + u_{w_2}(x,y,0) : \; z_c \to \infty$$

$$u_{c_3}(x,y,z_c) - \frac{z_c^2}{2} \frac{\partial^2 u_{w_1}}{\partial Z_w^2}(x,y,0) + z_c \frac{\partial u_{w_2}}{\partial Z_w}(x,y,0) +$$

$$u_{w_3}(x,y,0) : \; z_c \to \infty$$

$\vdots$

$$V_w = \epsilon v_{w_1} + \epsilon^2 v_{w_2} + \cdots = \epsilon v_{w_1}(x,y,0) + \epsilon^2 z_c \frac{\partial v_{w_1}}{\partial Z_w}(x,y,0) + \cdots$$

$$+ \epsilon^2 v_{w_2} + \cdots \sim \epsilon v_{c_1}(x,y,z_c) + \epsilon^2 v_{c_2}(x,y,z_c) + \cdots ; \; z_c \to \infty$$

$$v_{c_1}(x,y,z_c) \sim v_{w_1}(x,y,0) ; \; z_c \to \infty$$

$$v_{c_2}(x,y,z_c) \sim z_c \frac{\partial v_{w_1}}{\partial Z_w}(x,y,0) + v_{w_2} ; \; z_c \to \infty$$

$$\vdots$$

$$W_w = w_{w_1} + \epsilon w_{w_2} + \epsilon^2 w_{w_3} + \cdots \sim \epsilon w_{c_1} + \epsilon^2 w_{c_2} + \cdots ; \quad \begin{cases} Z_w \to 0 \\ z_c \to \infty \end{cases}$$

Differentiate w.r.t. Z_w:

$$\frac{\partial w_{w_1}}{\partial Z_w}(x,y,0) + \epsilon z_c \frac{\partial^2 w_{w_1}}{\partial Z_w^2}(x,y,0) + \frac{\epsilon^2 z_c^2}{2} \frac{\partial^3 w_{w_1}}{\partial Z_w^3}(x,y,0) + \cdots +$$

$$+ \epsilon \frac{\partial w_{w_2}}{\partial Z_w}(x,y,0) + \epsilon^2 z_c \frac{\partial^2 w_{w_2}}{\partial Z_w^2}(x,y,0) + \cdots + \epsilon^2 \frac{\partial w_{w_3}}{\partial Z_w}(x,y,0) + \cdots$$

$$\sim \frac{\partial w_{c_1}}{\partial z_c}(x,y,z_c) + \epsilon \frac{\partial w_{c_2}}{\partial z_c}(x,y,z_c) + \epsilon^2 \frac{\partial w_{c_3}}{\partial z_c}(x,y,0) + \cdots z_c \to \infty$$

$$\frac{\partial w_{c_1}}{\partial z_c}(x,y,z_c) \sim \frac{\partial w_{w_1}}{\partial z_w}(x,y,0);\ z_c \to \infty$$

$$\frac{\partial w_{c_2}}{\partial z_c}(x,y,z_c) \sim z_c \frac{\partial^2 w_{w_1}}{\partial z_w^2}(x,y,0) + \frac{\partial w_{w_2}}{\partial z_w}(x,y,0);\ z_c \to \infty$$

$$\frac{\partial w_{c_3}}{\partial z_c}(x,y,z_c) \sim \frac{z_c^2}{2}\frac{\partial^3 w_{w_1}}{\partial z_w^3}(x,y,0) + z_c \frac{\partial^2 w_{w_2}}{\partial z_w^2}(x,y,0) +$$

$$\frac{\partial w_{w_3}}{\partial z_w}(x,y,0);\ z_c \to \infty$$

$$P_w = P_1(x,0,0) + \epsilon z_c \frac{\partial P_1}{\partial z_w}(x,0,0) +$$

$$\epsilon^2 \frac{z_c^2}{2}\frac{\partial^2 P_1}{\partial z_w^2}(x,0,0) + \cdots +$$

$$+ \epsilon^2 p_{w_3}(x,y,0) + \cdots \sim p_{c_1}(x) + \epsilon p_{c_2}(x) +$$

$$\epsilon^2 p_{c_3}(x,y,z_c) + \cdots;\ z_c \to \infty$$

$$p_{c_1}(x,y,z_c) = P_1(x,0,0) \qquad \text{(F4)}$$

$$p_{c_2}(x,y,z_c) \sim z_c \frac{\partial P_1}{\partial Z_w}(x,0,0);\ z_c \to \infty \qquad \text{(F5)}$$

$$p_{c_3}(x,y,z_c) \sim \frac{z_c^2}{2}\frac{\partial^2 P_1}{\partial Z_w^2}(x,0,0) + p_{w_3}(x,y,0);\ z_c \to \infty$$

$$T_{w_{ij}} = t_{w_{ij}}(x,y,0) + \epsilon z_c \frac{\partial t_{w_1}{}_{ij}}{\partial Z_w}(x,y,0) + \epsilon^2 \frac{z_c^2}{2}\frac{\partial^2 t_{w_1}{}_{ij}}{\partial Z_w^2}(x,y,0) +$$

$$+ \cdots + \epsilon t_{w_2}{}_{ij}(x,y,0) + \epsilon^2 z_c \frac{\partial t_{w_2}{}_{ij}}{\partial Z_w}(x,y,0) + \cdots +$$

$$\epsilon^2 t_{w_3}{}_{ij}(x,y,0) + \cdots \sim t_{c_1}{}_{ij}(x,y,z_c) + \epsilon t_{c_2}{}_{ij}(x,y,z_c) +$$

$$\epsilon^2 t_{c_3}{}_{ij}(x,y,z_c) + \cdots;\ z_c \to \infty$$

$$t_{c_1}{}_{ij}(x,y,z_c) \sim t_{w_1}{}_{ij}(x,y,0);\ z_c \to \infty$$

$$t_{c_2}{}_{ij}(x,y,z_c) \sim z_c \frac{\partial t_{w_1}{}_{ij}}{\partial Z_w}(x,y,0) + t_{w_2}{}_{ij}(x,y,0);\ z_c \to \infty$$

$$t_{c_3}{}_{ij}(x,y,z_c) \sim \frac{z_c^2}{2}\frac{\partial^2 t_{w_1}{}_{ij}}{\partial Z_w^2}(x,y,0) + z_c \frac{\partial t_{w_2}{}_{ij}}{\partial Z_w}(x,y,0) + t_{w_3}{}_{ij}(x,y,0);\ z_c \to \infty$$

$$\vdots$$

2. $\begin{cases} z_w \to 0 \\ \hat{z}_c \to \infty \end{cases}$

$$U_w = \epsilon \hat{u}_{w_2}(x, \hat{y}, 0) + O(\hat{\epsilon}) + \epsilon^2 \hat{u}_{w_3}(x, \hat{y}, 0) + \cdots - \hat{u}_{c_1}(x, \hat{y}, \hat{z}_c) +$$

$$+ \epsilon \hat{u}_{c_2}(x, \hat{y}, \hat{z}_c) + \epsilon^2 \hat{u}_{c_3}(x, \hat{y}, \hat{z}_c) + \cdots; \ \hat{z}_c \to \infty$$

$$\hat{u}_{c_1}(x, \hat{y}, \hat{z}_c) \sim 0; \ \hat{z}_c \to \infty \qquad \text{(F6)}$$

$$\hat{u}_{c_2}(x, \hat{y}, \hat{z}_c) \sim \hat{u}_{w_2}(x, \hat{y}, 0); \ \hat{z}_c \to \infty$$

$$\hat{u}_{c_3}(x, \hat{y}, \hat{z}_c) \sim \hat{u}_{w_3}(x, \hat{y}, 0); \ \hat{z}_c \to \infty$$

$$\vdots$$

$$V_w = \epsilon^2 \hat{\epsilon} \hat{v}_{w_2}(x, \hat{y}, 0) + O(\hat{\epsilon}^2) + \epsilon^3 \hat{\epsilon} \hat{v}_{w_3}(x, \hat{y}, 0) + \cdots$$

$$- \epsilon \hat{\epsilon} \hat{v}_{c_1}(x, \hat{y}, \hat{z}_c) + \epsilon^2 \hat{\epsilon} \hat{v}_{c_2}(x, \hat{y}, \hat{z}_c) + \epsilon^3 \hat{\epsilon} \hat{v}_{c_3}(x, \hat{y}, \hat{z}_c) +$$

$$\cdots; \ \hat{z}_c \to \infty$$

$$\hat{v}_{c_1}(x,\hat{y},\hat{z}_c) \sim 0;\ \hat{z}_c \to \infty \qquad \text{(F7)}$$

$$\hat{v}_{c_2}(x,\hat{y},\hat{z}_c) \sim \hat{v}_{w_2}(x,\hat{y},0);\ \hat{z}_c \to \infty$$

$$\hat{v}_{c_3}(x,\hat{y},\hat{z}_c) \sim \hat{v}_{w_3}(x,\hat{y},0);\ \hat{z}_c \to \infty$$

$$\vdots$$

$$W_w = \epsilon\,\hat{w}_{w_2}(x,\hat{y},Z_w) + \epsilon^2\,\hat{w}_{w_3}(x,\hat{y},Z_w) + \cdots$$

$$\sim \epsilon\hat{\epsilon}\hat{w}_{c_1}(x,\hat{y},\hat{z}_c) + \epsilon^2\hat{\epsilon}\,\hat{w}_{c_2}(x,\hat{y},\hat{z}_c) + \epsilon^3\hat{\epsilon}\hat{w}_{c_3}(x,\hat{y},\hat{z}_c) +$$

$$\cdots \begin{cases} Z_w \to 0 \\ z_c \to \infty \end{cases}$$

Differentiate w.r.t. Z_w:

$$\epsilon\,\frac{\partial\hat{w}_{w_2}}{\partial Z_w}(x,\hat{y},0) + O(\hat{\epsilon}) + \epsilon^2\,\frac{\partial\hat{w}_{w_3}}{\partial Z_w}(x,\hat{y},0) + \cdots$$

$$\sim -\frac{\partial\hat{w}_{c_1}}{\partial\hat{z}_c}(x,\hat{y},\hat{z}_c) + \epsilon\,\frac{\partial\hat{w}_{c_2}}{\partial\hat{z}_c}(x,\hat{y},\hat{z}_c) +$$

$$\epsilon^2 \frac{\partial \hat{w}_{c_3}}{\partial \hat{z}_c}(x,\hat{y},\hat{z}_c): \hat{z}_c \to \infty$$

$$\frac{\partial \hat{w}_{c_1}}{\partial \hat{z}_c}(x,\hat{y},\hat{z}_c) \sim 0: \hat{z}_c \to \infty \qquad \text{(F8)}$$

$$\frac{\partial \hat{w}_{c_2}}{\partial \hat{z}_c}(x,\hat{y},\hat{z}_c) \sim \frac{\partial \hat{w}_{w_2}}{\partial Z_w}(x,\hat{y},0): \hat{z}_c \to \infty$$

$$\frac{\partial \hat{w}_{c_3}}{\partial \hat{z}_c}(x,\hat{y},\hat{z}_c) \sim \frac{\partial \hat{w}_{w_3}}{\partial Z_w}(x,\hat{y},0): \hat{z}_c \to \infty$$

$$\vdots$$

$$P_w = P_1(x,0,0) + O(\hat{\epsilon}) + \epsilon^2 \hat{p}_{w_3}(x,\hat{y},0) + \cdots \sim \hat{p}_{c_1}(x) +$$

$$\epsilon \hat{p}_{c_2}(x) +$$

$$+ \epsilon^2 \hat{p}_{c_3}(x,\hat{y},\hat{z}_c) + \cdots: \hat{z}_c \to \infty$$

$$\hat{p}_{c_1}(x,\hat{y},\hat{z}_c) = P_1(x,0,0) \qquad \text{(F9)}$$

$$\hat{p}_{c_2} = 0 \qquad \text{(F10)}$$

$$\hat{p}_{c_3}(x, \hat{y}, \hat{z}_c) \sim \hat{p}_{w_3}(x, \hat{y}, 0); \ \hat{z}_c \to \infty$$

$$\vdots$$

$$T_{w_{ij}} = \hat{t}_{w_{1_{ij}}}(x, \hat{y}, 0) + O(\hat{\epsilon}) + \epsilon \hat{t}_{w_{2_{ij}}}(x, \hat{y}, 0) + \cdots +$$

$$\epsilon^2 \hat{t}_{w_{3_{ij}}}(x, \hat{y}, 0) +$$

$$+ \cdots \sim \hat{t}_{c_{1_{ij}}}(x, \hat{y}, \hat{z}_c) + \epsilon \hat{t}_{c_{2_{ij}}}(x, \hat{y}, \hat{z}_c) +$$

$$\epsilon^2 \hat{t}_{c_{3_{ij}}}(x, \hat{y}, \hat{z}_c) + \cdots; \ z_c \to \infty$$

$$\hat{t}_{c_{1_{ij}}}(x, \hat{y}, \hat{z}_c) \sim \hat{t}_{w_{1_{ij}}}(x, \hat{y}, 0); \ \hat{z}_c \to \infty$$

$$\hat{t}_{c_{2_{ij}}}(x, \hat{y}, \hat{z}_c) \sim \hat{t}_{w_{2_{ij}}}(x, \hat{y}, 0); \ \hat{z}_c \to \infty$$

$$\hat{t}_{c_{3_{ij}}}(x, \hat{y}, \hat{z}_c) \sim \hat{t}_{w_{3_{ij}}}(x, \hat{y}, 0); \ \hat{z}_c \to \infty$$

$$\vdots$$

3. $\begin{cases} y_c \to 0 \\ \hat{y}_w \to \infty \end{cases}$

$$U_c = u_{c_1}(x, y, z_c) + \epsilon u_{c_2}(x, y, z_c) + \epsilon^2 u_{c_3}(x, y, z_c) + \cdots$$

$$- \epsilon\, \hat{u}_{w_2}(x, \hat{y}, Z_w) + \epsilon^2\, \hat{u}_{w_3}(x, \hat{y}, Z_w) + \cdots : \begin{cases} y \to 0 \\ \hat{y} \to \infty \end{cases}$$

Differentiate w.r.t. y:

$$\frac{\partial u_{c_1}}{\partial y}(x, y, z_c) + \epsilon \frac{\partial u_{c_2}}{\partial y}(x, y, z_c) + \epsilon^2 \frac{\partial u_{c_3}}{\partial y}(x, y, z_c) + \cdots$$

$$- \frac{\epsilon}{\hat{\epsilon}} \left[\frac{\partial \hat{u}_{w_2}}{\partial \hat{y}}(x, \hat{y}, Z_w) + \epsilon \frac{\partial \hat{u}_{w_3}}{\partial \hat{y}}(x, \hat{y}, Z_w) + \right.$$

$$\left. \epsilon^2 \frac{\partial \hat{u}_{w_4}}{\partial \hat{y}}(x, \hat{y}, Z_w) + \cdots \right] : \begin{cases} y \to 0 \\ \hat{y} \to \infty \end{cases}$$

In analogy with the discussion in Appendix B,

$$\frac{\partial u_{c_1}}{\partial y}(x, 0, z_c) = 0$$

$$\frac{\partial u_{c_2}}{\partial y} - \frac{\phi_2(x, z_c)}{y}, \quad \frac{\partial u_{c_3}}{\partial y} - \frac{\phi_3(x, z_c)}{y}, \quad \cdots ; \quad y \to 0$$

$$\frac{\partial \hat{u}_{w_2}}{\partial \hat{y}} \sim \frac{\phi_2(x, Z_w)}{\hat{y}}, \quad \frac{\partial \hat{u}_{w_3}}{\partial \hat{y}} \sim \frac{\phi_3(x, Z_w)}{\hat{y}}, \quad \cdots; \quad \hat{y} \to \infty$$

or

$$\left.\begin{aligned} u_{c_l} &\sim \phi_l(x, z_c) \ln y + \Psi_l(x, z_c), \quad l = 2, 3, \cdots; \quad y \to 0 \\ \hat{u}_{w_l} &\sim \phi_l(x, Z_w) \ln \hat{y} + \hat{\Psi}_l(x, Z_w), \quad l = 2, 3, \cdots; \quad \hat{y} \to \infty \end{aligned}\right\} \qquad (F11)$$

$$V_c = \epsilon v_{c_1}(x, y, z_c) + \epsilon^2 v_{c_2}(x, y, z_c) + \cdots \sim \epsilon^2 \hat{\epsilon} \hat{v}_{w_2}(x, \hat{y}, Z_w) +$$

$$+ \epsilon^3 \hat{\epsilon}\, \hat{v}_{w_3}(x, \hat{y}, Z_w) + \cdots; \quad \begin{cases} y \to 0 \\ \hat{y} \to \infty \end{cases}$$

Differentiate w.r.t. y:

$$\epsilon \frac{\partial v_{c_1}}{\partial y}(x, y, z_c) + \epsilon^2 \frac{\partial v_{c_2}}{\partial y}(x, y, z_c) + \cdots \sim \epsilon^2 \frac{\partial \hat{v}_{w_2}}{\partial \hat{y}}(x, \hat{y}, Z_w) +$$

$$+ \epsilon^3 \frac{\partial \hat{v}_{w_3}}{\partial \hat{y}}(x, \hat{y}, Z_w) + \cdots; \quad \begin{cases} y \to 0 \\ \hat{y} \to \infty \end{cases}$$

$$\frac{\partial v_{c_1}}{\partial y}(x, 0, z_c) = 0$$

$$\frac{\partial v_{c_2}}{\partial y}(x, 0, z_c) \sim \frac{\partial \hat{v}_{w_2}}{\partial \hat{y}}(x, \hat{y}, Z_w); \quad \hat{y} \to \infty$$

$$\vdots$$

$$W_c = \epsilon\, w_{c_1}(x,y,z_c) + \epsilon^2 w_{c_2}(x,y,z_c) + \cdots - \epsilon\, \hat{w}_{w_2}(x,\hat{y},Z_w) +$$

$$+ \epsilon^2\, \hat{w}_{w_3}(x,\hat{y},Z_w) + \cdots; \quad \begin{cases} y \to 0 \\ \hat{y} \to \infty \end{cases}$$

$$w_{c_l}(x,0,z_c) - \hat{w}_{w_{l+1}}(x,\hat{y},Z_w);\ \hat{y} \to \infty,\ l = 1,2,\cdots$$

$$P_c = P_1(x,0,0) + \epsilon p_{c_2}(x) + \epsilon^2 p_{c_3}(x,y,z_c) + \cdots$$

$$- P_1(x,0,Z_w) + \epsilon^2 \hat{p}_{w_3}(x,\hat{y},Z_w) + \cdots; \quad \begin{cases} y \to 0 \\ \hat{y} \to \infty \end{cases}$$

$$p_{c_2} = 0 \qquad \text{(F12)}$$

$$p_{c_3}(x,0,z_c) - \hat{p}_{w_3}(x,\hat{y},Z_w);\ \hat{y} \to \infty$$

$$\vdots$$

$$T_{c_{ll}} = t_{c_{1_{ll}}}(x,y,z_c) + \epsilon\, t_{c_{2_{ll}}}(x,y,z_c) + \epsilon^2 t_{c_{3_{ll}}}(x,y,z_c) + \cdots$$

$$- \hat{t}_{w_{1_{ll}}}(x,\hat{y},Z_w) + \epsilon\, \hat{t}_{w_{2_{ll}}}(x,\hat{y},Z_w) + \epsilon^2 \hat{t}_{w_{3_{ll}}}(x,\hat{y},Z_w) + \cdots; \quad \begin{cases} y \to 0 \\ \hat{y} \to \infty \end{cases}$$

$$t_{c_{n_{ij}}}(x,0,z_c) \sim \hat{t}_{w_{n_{ij}}}(x,\hat{y},Z_w): \hat{y} \to \infty,\ n = 1,2,\cdots$$

Important results from matching procedure:

1. From Eqns. (F1), (F6) and the one equivalent to (F6) for $\hat{y}_c \to \infty$ plus the boundary conditions $\hat{u}_{c_1} = 0$ @

$$\begin{cases} \hat{z}_c = 0 \\ or \\ \hat{y}_c = 0 \end{cases}$$

it follows that $\hat{u}_{c_1}$ is described by Laplace's equation with homogeneous boundary conditions. By the Maximum and Minimum Theoren, $\hat{u}_{c_1} \equiv 0$.

2. From Eqns. (F4) and (F9), both p_{c_1} and $\hat{p}_{c_1}$ are given by the external pressure evaluated at the corner. Moreover, since both p_{c_2} and $\hat{p}_{c_2}$ vanish [Eqns. (F10) and (F12)], the above conclusion carries through order ϵ.

3. By Eqns. (F5) and (F12), $\partial P_1/\partial Z_w$ vanishes along the corner. From symmetry, $\partial P_1/\partial Y_b$ also vanishes along the corner.

4. From Eqns. (F11) and their equivalents on the blade, the streamwise velocity has a common logarithmic overlap between the corner middle region and the inner layers on both endwall and blade.

Appendix G. Effects of Rotation

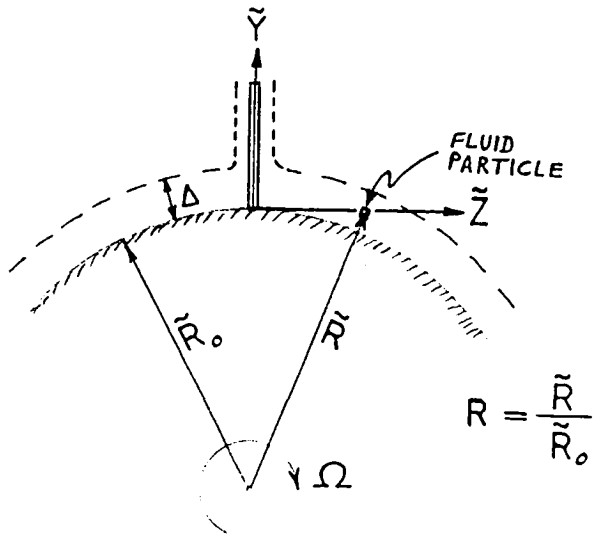

If the $(\tilde{x}, \tilde{Y}, \tilde{Z})$ coordinate system is rigidly attached to a rotor, rotating at a constant angular velocity Ω around the $\tilde{x}$-axis, the inertia terms of the N-S equation will include centrifugal and Coriolis accelerations and will assume the following form [14]:

$$\tilde{U}\frac{\partial \tilde{U}}{\partial \tilde{x}} + \tilde{V}\frac{\partial \tilde{U}}{\partial \tilde{Y}} + \tilde{W}\frac{\partial \tilde{U}}{\partial \tilde{Z}} - \Omega^2 \tilde{R}\frac{\partial \tilde{R}}{\partial \tilde{X}}$$

$$\tilde{U}\frac{\partial \tilde{V}}{\partial \tilde{x}} + \tilde{V}\frac{\partial \tilde{V}}{\partial \tilde{Y}} + \tilde{W}\frac{\partial \tilde{V}}{\partial \tilde{Z}} - 2\,\Omega\,\tilde{W} - \Omega^2 \tilde{R}\frac{\partial \tilde{R}}{\partial \tilde{Y}}$$

$$\tilde{U}\frac{\partial \tilde{W}}{\partial \tilde{x}} + \tilde{V}\frac{\partial \tilde{W}}{\partial \tilde{Y}} + \tilde{W}\frac{\partial \tilde{W}}{\partial \tilde{Z}} + 2\Omega\tilde{V} - \Omega^2\tilde{R}\frac{\partial \tilde{R}}{\partial \tilde{Z}}$$

After the usual normalization, these become

$$\frac{\tilde{U}_e^2}{\lambda\Delta}\left[U\frac{\partial U}{\partial x} + V\frac{\partial U}{\partial Y} + W\frac{\partial U}{\partial Z}\right] - \frac{\left[\Omega\tilde{R}_0\right]^2}{\lambda\Delta}R\frac{\partial R}{\partial x}$$

$$\frac{\tilde{U}_e^2}{\lambda\Delta}\left[U\frac{\partial V}{\partial x} + V\frac{\partial V}{\partial Y} + W\frac{\partial V}{\partial Z}\right] - 2\Omega\tilde{U}_e W -$$

$$\frac{\left[\Omega\tilde{R}_0\right]^2}{\lambda\Delta}R\frac{\partial R}{\partial Y}$$

$$\frac{\tilde{U}_e^2}{\lambda\Delta}\left[U\frac{\partial W}{\partial x} + V\frac{\partial W}{\partial Y} + W\frac{\partial W}{\partial Z}\right] + 2\Omega\tilde{U}_e V -$$

$$\frac{\left[\Omega\tilde{R}_0\right]^2}{\lambda\Delta}R\frac{\partial R}{\partial Z}$$

Multiplying through by $\lambda\delta/\tilde{U}_e^2$, as done before for the non-rotating case, yields:

$$U\frac{\partial U}{\partial x} + V\frac{\partial U}{\partial Y} + W\frac{\partial U}{\partial Z} - \left[\frac{\Omega\,\tilde{R}_0}{\tilde{U}_e}\right]^2 R\frac{\partial R}{\partial x}$$

$$U\frac{\partial V}{\partial x} + V\frac{\partial V}{\partial Y} + W\frac{\partial V}{\partial Z} - 2\frac{\Omega\lambda\Delta}{\tilde{U}_e}W - \left[\frac{\Omega\tilde{R}_o}{\tilde{U}_e}\right]^2 R\frac{\partial R}{\partial Y}$$

$$U \frac{\partial W}{\partial x} + V \frac{\partial W}{\partial Y} + W \frac{\partial W}{\partial Z} + 2 \frac{\Omega \lambda \Delta}{\tilde{U}_e} V - \left[\frac{\Omega \tilde{R}_0}{\tilde{U}_e}\right]^2 R \frac{\partial R}{\partial Z}$$

In turbomachinery components,

$$\frac{\Omega \tilde{R}_0}{\tilde{U}_e} = O(1)$$

Also, $\tilde{R}_o \gg \Delta$ and hence $\tilde{R}_o$ scales with the outer, inviscid scale:

$$\tilde{R}_o = O(\lambda\Delta) \rightarrow \frac{\Omega \lambda \Delta}{\tilde{U}_e} = O(1)$$

With these non-dimensional parameters thus established, it is now possible to determine the effect of rotation on the various sub-layers and sub-regions found earlier. This is done by the usual sorting out of terms in each sub-region to orders 1, ϵ and ϵ^2.

The following momentum equations are thus found for the case of a rotor, rotating at constant angular velocity about the x-coordinate:

1. Outer flow

$$U \frac{\partial U}{\partial x} + V \frac{\partial V}{\partial Y} + W \frac{\partial U}{\partial Z} - R \frac{\partial R}{\partial x} = - \frac{\partial P}{\partial x} ,$$

$$U \frac{\partial V}{\partial x} + V \frac{\partial V}{\partial Y} + W \frac{\partial V}{\partial Z} - 2 W - R \frac{\partial R}{\partial Y} = - \frac{\partial P}{\partial Y}$$

$$U \frac{\partial W}{\partial x} + V \frac{\partial W}{\partial Y} + W \frac{\partial W}{\partial Z} + 2 V - R \frac{\partial R}{\partial Z} = - \frac{\partial P}{\partial Z}$$

2. Middle layer (Region I):

$O(1)$

$$u_1 \frac{\partial u_1}{\partial x} + v_1 \frac{\partial u_1}{\partial y} + w_1 \frac{\partial u_1}{\partial Z} - R \frac{\partial R}{\partial x} = - \frac{\partial p_1}{\partial x}$$

$$R \frac{\partial R}{\partial y} = \frac{\partial p_1}{\partial y}$$

$$u_1 \frac{\partial w_1}{\partial x} + v_1 \frac{\partial w_1}{\partial y} + w_1 \frac{\partial w_1}{\partial Z} - R \frac{\partial R}{\partial Z} = - \frac{\partial p_1}{\partial Z}$$

$O(\epsilon)$

$$\frac{\partial}{\partial x} (u_1 u_2) + v_1 \frac{\partial u_2}{\partial y} + v_2 \frac{\partial u_1}{\partial y} + w_1 \frac{\partial u_2}{\partial Z} + w_2 \frac{\partial u_1}{\partial Z} =$$

$$- \frac{\partial p_2}{\partial x} + \frac{\partial t_{1_{yx}}}{\partial y}$$

$$2 w_1 = \frac{\partial p_2}{\partial y}$$

$$u_1 \frac{\partial w_2}{\partial x} + u_2 \frac{\partial w_1}{\partial x} + v_1 \frac{\partial w_2}{\partial y} + v_2 \frac{\partial w_1}{\partial y} + \frac{\partial}{\partial Z} (w_1 w_2) + 2 v_1 =$$

$$- \frac{\partial p_2}{\partial Z} + \frac{\partial t_{1_{yz}}}{\partial y}$$

$O(\epsilon^2)$

$$\frac{\partial}{\partial x}(u_1 u_3) + u_2 \frac{\partial u_2}{\partial x} + v_1 \frac{\partial u_3}{\partial y} + v_2 \frac{\partial u_2}{\partial y} + v_3 \frac{\partial u_1}{\partial y} + w_1 \frac{\partial u_3}{\partial Z} +$$

$$w_2 \frac{\partial u_2}{\partial Z} + w_3 \frac{\partial u_1}{\partial Z} =$$

$$- \frac{\partial p_3}{\partial x} + \frac{\partial t_{1_{xx}}}{\partial x} + \frac{\partial t_{2_{yx}}}{\partial y} + \frac{\partial t_{1_{zx}}}{\partial Z}$$

$$u_1 \frac{\partial v_1}{\partial x} + v_1 \frac{\partial v_1}{\partial y} + w_1 \frac{\partial v_1}{\partial Z} - 2 w_2 = - \frac{\partial p_3}{\partial y} + \frac{\partial t_{1_{yy}}}{\partial y}$$

$$u_1 \frac{\partial w_3}{\partial x} + u_2 \frac{\partial w_2}{\partial x} + u_3 \frac{\partial w_1}{\partial x} + v_1 \frac{\partial w_3}{\partial y} + v_2 \frac{\partial w_2}{\partial y} + v_3 \frac{\partial w_1}{\partial y} +$$

$$w_2 \frac{\partial w_2}{\partial Z} + \frac{\partial}{\partial Z}(w_1 w_3) +$$

$$2 v_2 = - \frac{\partial p_3}{\partial Z} + \frac{\partial t_{1_{xz}}}{\partial x} + \frac{\partial t_{2_{yz}}}{\partial y} + \frac{\partial t_{1_{zz}}}{\partial Z}$$

3. Inner layer (Region I):

O(1)

$$0 = \frac{\partial^2 \hat{u}_1}{\partial \hat{y}^2}$$

$$R \frac{\partial R}{\partial \hat{y}} = \frac{\partial \hat{p}_1}{\partial \hat{y}}$$

$$0 = \frac{\partial^2 \hat{w}_1}{\partial \hat{y}^2}$$

$O(\epsilon)$

$$0 = \frac{\partial}{\partial \hat{y}}\left[\hat{t}_{1_{yx}} + \frac{\partial \hat{u}_2}{\partial \hat{y}}\right]$$

$$0 = \frac{\partial \hat{p}_2}{\partial \hat{y}}$$

$$0 = \frac{\partial}{\partial \hat{y}}\left[\hat{t}_{1_{yz}} + \frac{\partial \hat{w}_2}{\partial \hat{y}}\right]$$

$O(\epsilon^2)$

$$0 = \frac{\partial}{\partial \hat{y}}\left[\hat{t}_{2_{yx}} + \frac{\partial \hat{u}_3}{\partial \hat{y}}\right]$$

$$0 = \frac{\partial}{\partial \hat{y}}\left[- \hat{p}_3 + \hat{t}_{1_{yy}}\right]$$

$$0 = \frac{\partial}{\partial \hat{y}}\left[\hat{t}_{2_{yz}} + \frac{\partial \hat{w}_3}{\partial \hat{y}}\right]$$

4. Middle region (Region II)

$O(1)$

$$u_1 \frac{\partial u_1}{\partial x} + v_1 \frac{\partial u_1}{\partial y} + w_1 \frac{\partial u_1}{\partial z} - R \frac{\partial R}{\partial x} = - \frac{\partial p_1}{\partial x}$$

$$R \frac{\partial R}{\partial y} = \frac{\partial p_1}{\partial y}$$

$$R \frac{\partial R}{\partial z} = \frac{\partial p_1}{\partial z}$$

$O(\epsilon)$

$$\frac{\partial}{\partial x} (u_1 u_2) + v_1 \frac{\partial u_2}{\partial y} + v_2 \frac{\partial u_1}{\partial y} + w_1 \frac{\partial u_2}{\partial z} + w_2 \frac{\partial u_1}{\partial z} =$$

$$- \frac{\partial p_2}{\partial x} + \frac{\partial t_{1_{yx}}}{\partial y} + \frac{\partial t_{1_{zx}}}{\partial z}$$

$$0 = \frac{\partial p_2}{\partial y}$$

$$0 = \frac{\partial p_2}{\partial z}$$

$O(\epsilon^2)$

$$\frac{\partial}{\partial x} (u_1 u_3) + u_2 \frac{\partial u_2}{\partial x} + v_1 \frac{\partial u_3}{\partial y} + v_2 \frac{\partial u_2}{\partial y} + v_3 \frac{\partial u_1}{\partial y} + w_1 \frac{\partial u_3}{\partial z} +$$

$$w_2 \frac{\partial u_2}{\partial z} + w_3 \frac{\partial u_1}{\partial z} = - \frac{\partial p_3}{\partial x} + \frac{\partial t_{1_{xx}}}{\partial x} + \frac{\partial t_{2_{yx}}}{\partial y} + \frac{\partial t_{2_{zx}}}{\partial z}$$

$$u_1 \frac{\partial v_1}{\partial x} + v_1 \frac{\partial v_1}{\partial y} + w_1 \frac{\partial v_1}{\partial z} - 2 w_1 =$$

$$- \frac{\partial p_3}{\partial y} + \frac{\partial t_{1_{yy}}}{\partial y} + \frac{\partial t_{1_{zy}}}{\partial z}$$

$$u_1 \frac{\partial w_1}{\partial x} + v_1 \frac{\partial w_1}{\partial y} + w_1 \frac{\partial w_1}{\partial z} + 2 v_1 =$$

$$- \frac{\partial p_3}{\partial z} + \frac{\partial t_{1_{yz}}}{\partial y} + \frac{\partial t_{1_{zz}}}{\partial z}$$

5. Inner region (Region II)

$O(1)$

$$0 = \frac{\partial^2 \hat{u}_1}{\partial \hat{y}^2} + \frac{\partial^2 \hat{u}_1}{\partial \hat{z}^2}$$

$$R \frac{\partial R}{\partial \hat{y}} = \frac{\partial \hat{p}_1}{\partial \hat{y}}$$

$$R \frac{\partial R}{\partial \hat{z}} = \frac{\partial \hat{p}_1}{\partial \hat{z}}$$

$O(\epsilon)$

$$0 = \frac{\partial}{\partial \hat{y}} \left[\frac{\partial \hat{u}_2}{\partial \hat{y}} + \hat{t}_{1_{yx}} \right] + \frac{\partial}{\partial \hat{z}} \left[\frac{\partial \hat{u}_2}{\partial \hat{z}} + \hat{t}_{1_{zx}} \right] *$$

$$0 = \partial \hat{p}_2 / \partial \hat{y}$$

$$0 = \partial \hat{p}_2 / \partial \hat{z}$$

$O(\epsilon^2)$

$$0 = \frac{\partial}{\partial \hat{y}}\left[\frac{\partial \hat{u}_3}{\partial \hat{y}} + \hat{t}_{2_{yx}}\right] + \frac{\partial}{\partial \hat{z}}\left[\frac{\partial \hat{u}_3}{\partial \hat{z}} + \hat{t}_{2_{zx}}\right]^*$$

$$0 = -\frac{\partial \hat{p}_3}{\partial \hat{y}} + \frac{\partial t_{1_{yy}}}{\partial \hat{y}} + \frac{\partial \hat{t}_{1_{zy}}}{\partial \hat{z}}$$

$$0 = -\frac{\partial \hat{p}_3}{\partial \hat{z}} + \frac{\partial \hat{t}_{1_{yz}}}{\partial \hat{y}} + \frac{\partial \hat{t}_{1_{zz}}}{\partial \hat{z}}$$

From these equations, the following effects of rotation are observed:

1. In the outer flow, there is a centrifugal term in the streamwise component of momentum and both Coriolis and centrifugal terms in the crosswise and normal components.
2. In the middle layer of Region I, there are centrifugal terms to $O(1)$ in all three momentum components, and Coriolis terms in the normal- and crosswise- components to orders ϵ and ϵ^2. The streamwise momentum component is not affected by rotation to these orders.
3. The inner layer of Region I is unaffected by rotation except for the $O(1)$ normal momentum, where the pressure gradient is balanced by a centrifugal acceleration.
4. In the middle region of Region II, there are centrifugal terms in all three momentum components to $O(1)$. In particular, crosswise pressure gradients are balanced by centrifugal accelerations. There are no rotational effects

on the $O(\epsilon)$ equations, while Coriolis terms reappear in the two crosswise momentum components of $O(\epsilon^2)$.

5. The only effect of rotation on the inner region of Region II is in the $O(1)$ crosswise momentum components, where pressure gradients and centrifugal accelerations balance each other.

1. Report No.	2. Government Accession No.	3. Recipient's Catalog No.
NASA CR-3792		

4. Title and Subtitle	5. Report Date
Scaling and Modeling of Three-Dimensional, End-Wall, Turbulent Boundary Layers	June 1984
	6. Performing Organization Code

7. Author(s)	8. Performing Organization Report No.
Uriel C. Goldberg and Eli Reshotko	None
	10. Work Unit No.

9. Performing Organization Name and Address	11. Contract or Grant No.
Case Western Reserve University Dept. of Mechanical and Aerospace Engineering Cleveland, Ohio 44106	NAG3-270
	13. Type of Report and Period Covered
12. Sponsoring Agency Name and Address	Contractor Report
National Aeronautics and Space Administration Washington, D.C. 20546	14. Sponsoring Agency Code 505-31-0A (E-2024)

15. Supplementary Notes

Final report. Project Manager, Peter M. Sockol, Fluid Mechanics and Instrumentation Division, NASA Lewis Research Center, Cleveland, Ohio 44135. This report was submitted by Uriel C. Goldberg as a dissertation in partial fulfillment of the requirements for the degree Doctor of Philosophy to Case Western Reserve University, Cleveland, Ohio.

16. Abstract

The method of matched asymptotic expansions is employed to identify the various sub-regions in three-dimensional, turbomachinery end-wall turbulent boundary layers, and to determine the proper scaling of these regions. The two parts of the b.l. investigated are the 3D pressure-driven part over the endwall, and the 3D part located at the blade/end-wall juncture. Based on the results of the analysis for the pressure-driven part, models are proposed for the 3D Law-of-the-Wall and Law-of-the-Wake. Comparisons between these models and the data of van den Berg and Elsenaar and of Mueller show good agreement between models and experiments.

17. Key Words (Suggested by Author(s))	18. Distribution Statement
Boundary layers Turbulence Turbomachinery	Unclassified - unlimited STAR Category 34

19. Security Classif. (of this report)	20. Security Classif. (of this page)	21. No. of pages	22. Price*
Unclassified	Unclassified	134	A07

*For sale by the National Technical Information Service, Springfield, Virginia 22161

NASA-Langley, 1984

National Aeronautics and
Space Administration

Washington, D.C.
20546

Official Business
Penalty for Private Use, $300

THIRD-CLASS BULK RATE

Postage and Fees Paid
National Aeronautics and
Space Administration
NASA-451

NASA

POSTMASTER: If Undeliverable (Section 158
Postal Manual) Do Not Return